



# Photodegradation of organic pollutants induced by iron-carboxylate complexes in aqueous solutions

Changbo Zhang

## ► To cite this version:

Changbo Zhang. Photodegradation of organic pollutants induced by iron-carboxylate complexes in aqueous solutions. Organic chemistry. Université Blaise Pascal - Clermont-Ferrand II; Université de Wuhan (Chine), 2009. English. NNT : 2009CLF21925 . tel-00725597

**HAL Id: tel-00725597**

**<https://theses.hal.science/tel-00725597>**

Submitted on 27 Aug 2012

**HAL** is a multi-disciplinary open access archive for the deposit and dissemination of scientific research documents, whether they are published or not. The documents may come from teaching and research institutions in France or abroad, or from public or private research centers.

L'archive ouverte pluridisciplinaire **HAL**, est destinée au dépôt et à la diffusion de documents scientifiques de niveau recherche, publiés ou non, émanant des établissements d'enseignement et de recherche français ou étrangers, des laboratoires publics ou privés.

Numéro d'Ordre: D.U. 1925

**UNIVERSITE BLAISE PASCAL**

U. F. R. Sciences et Technologies

**ECOLE DOCTORALE DES SCIENCES FONDAMENTALES**

N°: 606

**THESE EN COTUTELLE**

Avec l'Université de Wuhan (Chine)

**Présentée pour obtenir le grade de**

**DOCTEUR D'UNIVERSITE**

**Spécialité: Chimie Physique et chimie de l'environnement**

**Par**

**Changbo ZHANG**

Diplômé de Master

**PHOTODEGRADATION OF ORGANIC POLLUTANTS**

**INDUCED BY IRON-CARBOXYLATE COMPLEXES IN**

**AQUEOUS SOLUTIONS**

Soutenue publiquement à Wuhan le 29 Mai 2009, devant la commission d'examen

Président

Dr. Feng WU

Rapporteurs:

Pr. Jean-Marc CHOVELON

Pr. Hui ZHANG

Examineurs:

Pr. Nansheng DENG

Dr. Khalil HANNA

Dr. Gilles MAILHOT



## **Acknowledgements**

It would be impossible to individually acknowledge all those who merit this thesis. However, I will try to express my gratitude to those who made this thesis possible and enriched my life in the past years.

This project has been carried out within the framework of the cooperation program, between Wuhan University and Blaise Pascal University. Part of my work was carried out in the Laboratory of Environmental Science directed by Pr. Nansheng DENG. The other part was carried out in Laboratoire de Photochimie Moléculaire et Macromoléculaire UMR CNRS 6505 from Blaise Pascal University led by Dr. Claire RICHARD. I would sincerely like to thank them for the confidence they placed in me in the laboratory.

I cordially express my thanks to Prof. Nansheng DENG and Dr. Feng WU, who give me a lot of help during my study in Wuhan University. Thanks a lot for their great support and helpful guide on my thesis.

I'm honored to express my deepest gratitude to Dr. Michèle BOLTE, Dr. Gilles MAILHOT, Dr. Hana MESTANKOVA, who provided the scientific responsibility of this thesis. They have offered me valuable ideas and suggestions to prepare my thesis. Their enthusiasm and availability throughout last year of research, their friendly and everlasting help and attention, their moral support have established an atmosphere conducive to work. I spend a very happy time in Clermont-Ferrand.

I want to sincerely thank Ms. Lei WNAG, Mr. Jie SUN, Ms. Jing LI, Mr. Yanxiang LIU, Mr. Xuwei WU, Mr. Lijie BAI, Mr. Li GUO, Ms. Zhang'E PENG, Ms. Beibei WANG, Mr. Xu ZHANG, Mr. Xiaofei XUE, Ms. Yixin LIN, Mr. Zhiping

WANG, Mr. Mingwu GUO, Ms. Yu HUANG, and Ms. Yanmei ZHANG who are my colleagues in the lab and friends of Wuhan University. I am very grateful to Mrs. Mei XIAO, Mrs. Lin ZHANG and Mrs. Chaozhen HU, who give me a lot of help in Wuhan University.

I also wish to express my thanks to all members of the laboratory Madam Benedicte MAILHOT, Mrs. Bernadette LAVEDRINE, Mr. Guillaume VOYARD, Mr. Jean-Philippe DEBOUT, Mr. Mohamed SARAKHA, Mr. Pascal WONG WAH CHUNG, Mrs. Alexandra TER HALLE, Mr. Vincent VERNEY, Mr. Ghislain GUYOT, Mr. Marius PARAZOLS, Mr. Christian COELHO, Ms. Marie SIAMPIRINGUE, Mr. Boris EYHERAGUIBEL, Ms. Delphine LAVIEILLE, Mr. Sebastien BELLINCK and Mr. Michal KOLAR, and to the people that I forgot the name and that I have not mentioned. Thanks for their friendship and help for me when I stay in Blaise Pascal University.

I would like to take the opportunity to thank my friends, who lived in France, for their kindly help. They are Mr. Wei ZHANG, Ms. Qian ZHOU, Mr. Biao LI, Ms. Jing MAI, Mr. Wei LIU, Ms. Wei ZHOU, Mr. Qingrui ZENG, Mr. Guisong XIA, Ms. Xianjing WU, Ms. Ruijuan CHAI, Ms. Jie LI, Mr. Yuan MA, Mr. Peng SHEN, Ms. Yun DENG, Ms. Airong FENG, Mr. Qiao ZHAO, Ms. Na ZHAN, Mr. Xiaoxu LI, Ms. Lijun YAO, Ms. Lingjun YAN, Ms. Liyue SHEN and Ms. Yuan WANG.

Thanks for the fund support of China Scholarship Council (CSC) affiliated with the Ministry of Education of the P. R. China. Thanks also go to the Education Service of China Embassy in Paris.

I am immensely grateful to my parents, who have always supported me and have been willing to make considerable sacrifices for giving to me all possible advantages in life.

# CONTENTS

I-Introduction .....	3
II-Bibliography study .....	9
A-Photochemical properties of iron and goethite in environment .....	9
A-1-Iron ions in the natural environment .....	9
A-2-reactions of $\text{Fe}^{2+}$ , $\text{Fe}^{3+}$ and $\text{H}_2\text{O}_2$ in aqueous solution .....	12
A-3-reactions of $\text{Fe}^{2+}$ / $\text{Fe}^{3+}$ / $\text{H}_2\text{O}_2$ in the presence of organic substances .....	14
A-4-Photochemical reactions .....	17
A-5-Application to wastewater treatment .....	19
B-Iron oxides in the natural environment .....	21
B-1-Chemical Properties of goethite .....	23
B-2-Pathway of $\text{FeOOH}$ -induced hydroxyl radical .....	26
C- $\text{Fe(III)}$ -EDDS complex .....	27
C-1-Aminopolycarboxylates: EDDS-a biodegradable strong metal chelant .....	27
C-2- Iron-carboxylate complexes .....	30
C-3-Photochemistry of Iron-Carboxylate .....	31
D- pesticide and herbicide .....	35
D-1- Atrazine .....	37
D-1-1- Atrazine degradation .....	38
D-2- 2, 4-Dichlorophenoxyacetic acid (2, 4-D) .....	42
III-EXPERIMENTAL MATERIALS AND METHODS .....	47
A-REAGENTS .....	47
B-PREPARATION OF SOLUTIONS .....	48
B-1-Preparation of stock solutions .....	48
B-2-Preparation of reaction solutions .....	50
C-IRRADIATION .....	51
C-1-Ferrioxalate actinometry .....	51
C-2-Irradiation with monochromator .....	53
C-3-Irradiation at 365nm .....	55
D-ANALYSIS METHODS .....	56
D-1-Spectroscopy methods .....	56
D-2-Chromatography methods .....	56
D-3-Dosage methods .....	57
D-4-Molar ratio method .....	60
RESULTS AND DISCUSSION .....	63
IV-study on photoactivity of $\text{Fe(III)}$ -EDDS complex .....	65
IV-A-physicochemical property of $\text{Fe(III)}$ -EDDS complex .....	65
A-1-Properties of $\text{Fe(III)}$ solutions .....	65
A-2-Property of the EDDS .....	66

A-3-Study of the stoichiometric composition of Fe(III) in complexes with EDDS .....	70
A-4-Property of Fe(III)-EDDS complex .....	71
A-4-1 Stability of Fe(III)-EDDS complex .....	72
A-4-2 pH effect .....	73
A-4-3 Irradiation effect .....	74
Conclusions .....	75
IV-B-Determination of hydroxyl radicals from photolysis of Fe(III)-EDDS complex in aqueous solutions .....	76
B-1-Generation of hydroxyl radicals in the irradiated aqueous solution containing Fe(III)-EDDS complex.....	77
B-2-Effect of pH on the generation of hydroxyl radicals in the irradiated aqueous solution containing Fe(III)-EDDS complex.....	78
B-3-Effect of Fe(III) and EDDS concentrations on the photogeneration of hydroxyl radicals in aqueous solution .....	79
Conclusions .....	81
V-Photodegradation of 2, 4-D photoinduced by the Fe(III)-EDDS complex and goethite-EDDS complex.....	83
A-Photodegradation of 2, 4-D induced by the Fe(III)-EDDS complexe.....	83
A-1-Properties of 2, 4-D in aqueous solution .....	83
A-2-Quantum yields of 2, 4-D degradation and Fe(II) formation.....	86
A-2-1-Influence of the irradiation wavelength on the quantum yields of Fe(II) and 2,4-D in Fe(III) -EDDS complex aqueous solution.....	87
A-2-2-influence of oxygen on the quantum yields of Fe(II) and 2, 4-D with Fe(III)-EDDS complex ( $\lambda_{irr}= 365nm$ ).....	88
A-2-3-Influence of pH on the quantum yields of Fe(II) and 2, 4-D in Fe(III)-EDDS complex ( $\lambda_{irr}= 365 nm$ ) .....	89
A-3- Degradation of 2, 4-D photoinduced by Fe(III)-EDDS complex at 365 nm under polychromatic irradiation.....	90
A-3-1-Effect of Fe(III)-EDDS concentration.....	90
A-3-2 Effect of oxygen on the 2, 4-D photodegradation.....	93
A-3-3-Effect of pH on photodegradation of 2, 4-D.....	96
A-3-4-study on the effect of isopropanol on photodegradation of 2, 4-D .....	97
Conclusions .....	99
B-Photodegradation of 2, 4-D induced by the Goethite in the presence of EDDS .....	100
B-1-Adsorption of 2, 4-D on goethite .....	100
B-2-Photodegradation of 2, 4-D at 365 nm in suspension of the goethite.....	103
B-2-1-Effect of goethite concentration in suspension .....	103
B-2-2- initial pH effect of suspension on photodegradation of 2, 4-D .....	105
B-2-3- Effect of isopropanol on photodegradation of 2, 4-D .....	106
B-2-4-comparation of 2, 4-D and 2, 4-DCP on photogdegradation .....	108
B-3- Photodegradation of 2, 4-D at 365 nm in suspension of goethite with EDDS.....	109
B-3-1- influence of [EDDS] on 2, 4-D photodegradation in the suspension of goethite .....	109

B-3-2- influence of goethite concentration on 2, 4-D photodegradation .....	111
B-3-3- influence of initial pH on 2, 4-D photodegradation in goethite suspension .....	113
Conclusions.....	114
VI-Photodegradation of atrazine photoinduced by the Fe(III)-EDDS complex and Fe(III)-pyruvate complex.....	117
A-1-atrazine in aqueous solution .....	118
A-2-Degradation of atrazine photoinduced by Fe(III)-EDDS complex at 365 nm.....	119
A-2-1- Effect of initial Fe(III), EDDS concentrations on the degradation of atrazine..	119
A-2-2- Effect of initial pH on the degradation of atrazine .....	122
A-2-3- Effect of initial atrazine concentration on the degradation of atrazine.....	124
B-Photodegradation of atrazine in the aqueous solutions containing Fe(III)-Pyr complex ..	126
B-1-control experiment on photodegradation of atrazine .....	126
B-2-Effect of pH, initial Fe(III), Pyr and atrazine concentrations on the degradation of atrazine.....	127
B-3- Degradation products of atrazine .....	132
Conclusions.....	136
VII-General conclusions .....	141
APPENDIX.....	145
VIII-1-List of tables .....	147
VIII-2-List of Figures.....	148
VIII-REFERENCES .....	157





# **I**

## **Introduction**



## **I-Introduction**

Iron is an element of great biological and geochemical importance. The transformation of Fe(III) in water occurs in many geochemical environments: at the oxic/anoxic boundary in marine and freshwater basins; at the oxycline, which exists in sediments; at the sediment-water interfaces; and in surface waters by photochemical processes. The Fe(III) in marine aerosols and rainwater can be reduced to Fe(II) by photochemical processes. The presence of Fe(II) could cause an increase in the dissolved iron fraction making more iron available for use by biota. The oxidation of Fe(II) with  $\text{H}_2\text{O}_2$  has been studied in seawater by a number of authors. Results represent a significant thermal source of hydroxyl radicals ( $\bullet\text{OH}$ ).  $\bullet\text{OH}$  radicals can oxidize a wide variety of natural and anthropogenic organic and inorganic substances. Iron oxides are widely spread in soils, sediments, rocks and aquatic systems. Iron oxides, hydroxides, and oxy-hydroxides are efficient sorbents for inorganic and organic species. Many oxide iron compounds not only play an important role in a variety of disciplines and also serve as a model system of reduction and catalytic reactions. They are also of substantial interest in environmental sciences since some of them are frequently occurring in soil minerals having significant impact on the behavior of pollutants in soils. Goethite,  $\alpha\text{-FeO(OH)}$ , is one of the most widespread forms of iron oxy-hydroxides in terrestrial soils, sediments, and ore deposits as well as a common weathering product in rocks of all types. Goethite particles have high specific surface areas in excess of  $200 \text{ m}^2 \text{ g}^{-1}$  and strong affinities for oxyanions and heavy metals. The basic charge properties of oxide surfaces are of crucial importance for their chemical behavior in aqueous systems, driving sorption, dissolution and precipitation processes as well as redox reactions.

Low molecular weight organic acids have been identified and measured in a wide variety of environments, such as marine and continental air, rural and remote atmospheres and tropical and temperate zones. The [S, S']-stereoisomer of ethylenediaminedisuccinic acid (EDDS), a biodegradable strong metal ligand, has

substituted traditional ligands in a number of consumer products. It like its structural isomer EDTA, forms stable hexadentate chelates with transition metals. The ability of aminopolycarboxylates and aminopolyphosphonates to form stable metal complexes has been widely utilized in analytical chemistry and industrial applications. Because EDTA is very recalcitrant to microbial degradation, it is quite mobile in soils and readily transported to the groundwater together with the mobilized metals. The persistence of EDTA and its metal complexes in the nature may, however, cause environmental harm. The extraction of heavy metals from soils using ligands has been studied extensively. S, S'-Ethylenediaminedisuccinic acid (EDDS) has received much attention in the past few years as a potential replacement for EDTA.

The formation of iron-carboxylate complexes can undergo rapid photochemical reactions under solar irradiation. The photolysis of Fe(III)-polycarboxylates could represent an important source of  $\text{H}_2\text{O}_2$  to some atmospheric and surface waters. Fe(III)-NTA, Fe-EDTA, Fe-Oxalate and Fe(III)-Citrate have been used to degrade organic and inorganic pollutants. However, there are little published studies on the photochemical reactivity of Fe(III)-EDDS complexes.

2, 4-dichlorophenoxyacetic acid (2, 4-D) is an organic acid with pKa of 2.6 and high water solubility ( $45 \text{ g L}^{-1}$ ). 2, 4-D is classified by both ANVISA (Brazilian National Agency for Sanitarian Vigilance) and WHO (World Health Organization) as a hormonal herbicide of level II toxicity. It is considered as a carcinogenic agent, affecting liver, heart and central nervous system, leading to convulsions. It presents a systemic mode of action and has been widely employed in wheat, rice, corn, sorghum and sugar cane cultures to control harmful wide-leaf weeds. Particularly in Brazil, this herbicide is extensively used in many crops. Because it is highly selective and systemic, this herbicide is transported through the plant, being accumulated in the growing roots, inhibiting the growth of weeds. This herbicide is usually commercialized as salt, amine and ester formulations, and has post-emergence action. After its application in field, the excess of the herbicide is easily transferred to the groundwater, due to its high solubility in water. Even after a long period of disuse, considerable amounts of either 2, 4-D or its main product of degradation might be

found in surface waters and groundwater as well. Therefore, the development of an efficient degradation process for this herbicide is extremely relevant and necessary.

For decades, the atrazine (2-chloro-4-(ethylamino)-6-(isopropylamino)-1, 3, 5-triazine) has been widely used all over the world to control a variety of broadleaf and grass weeds in agriculture and forestry. Atrazine has a high mobility in soils, which results in the contamination of soil, surface and groundwater, rainwater and tile drain water; thus frequently, atrazine levels in water exceed the maximum level for drinking water which is  $0.1 \mu\text{g L}^{-1}$  in Europe and  $3 \mu\text{g L}^{-1}$  in USA. The presence of this chemical compound on the environment and its toxicological properties are being taken into account by regulatory bodies in EU countries, leading to increased restrictions on its use or to its banning.

Many kinds of methods are used to degrade them. Advanced oxidation technologies is thought to be the preferable means for the degradation of 2, 4-D and atrazine. However, little references reported using iron complexes to degrade them under irradiation. The objective of this work is to understand the fate of pollutants in the aquatic environment in the presence of light and Fe(III)-EDDS complex or goethite and EDDS.

In the present work, we studied the physicochemical properties of Fe(III)-EDDS complex. It should be indicated that until now no published reports about the stoichiometry of Fe(III)-EDDS complex were found. The photogeneration of  $\cdot\text{OH}$  and peroxy radicals have been determined in aqueous solutions with Fe(III)-EDDS complex.

2, 4-D and atrazine were used as model compounds to certify the photochemical properties of iron-carboxylate complexes. Irradiation experiments were carried out separately under monochromatic irradiation in a short time and irradiation at 365 nm (93% of all the radiation) in a longer time. Quantum yields of Fe(II) formation, 2, 4-D and atrazine disappearance were determined in the present study. Parameters affecting the photoreaction, including excitation wavelength, concentrations of iron-carboxylate complex and pollutants, oxygen and pH were all studied in this thesis.



## **II**

### **Bibliography Study**





## **II-Bibliography study**

### **A-Photochemical properties of iron and goethite in environment**

#### **A-1-Iron ions in the natural environment**

Behind oxygen, silicon and aluminium, iron is the fourth most abundant element in the earth's crust. It occurs in oxidation numbers from  $-II$  to  $+VI$  with coordination numbers of 3 to 8 (Hawker and Twigg, 1994). Desert sands, dust and ash make iron omnipresent in the environment and practical all natural water contains iron at least in traces. In clouds, fog, lakes and rivers the iron concentration is around  $10^{-5}$  M (Faust and Hoigné 1990). Iron is as well a vital element for life present in the whole biosphere. It is also an essential nutrient in aerobic biological wastewater treatment (Henze et al., 2000).

In aqueous solution the most abundant iron species have an oxidation number of  $+II$  (ferrous iron) and  $+III$  (ferric iron). Dissolved ferrous and ferric iron species are present in octahedral complexes with six ligands of water. Iron is complexed by water and hydroxyl ligands provided that no other complexing substances are present. How many of these ligands are hydroxyl ions, depends on the solution's pH, which influences directly the acid/base equilibrium of the aquacomplexes. Ferric iron is the more critical iron species in the photo-Fenton process, because its hydroxides precipitate at lower pH than those of ferrous iron. Consequently, only the acid/base equilibrium for the ferric iron aquo complex is described here, Eq. (1) - (3). For simplification, coordinated water molecules in the coordinate sphere will not be included in the chemical formulae. Eq. (4), dimers and oligomers were the most important species at pH below 3.0 (Flynn C. M. Jr., 1984).

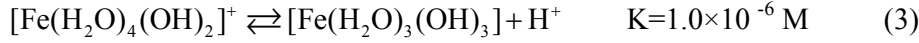
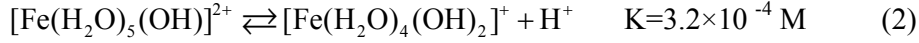
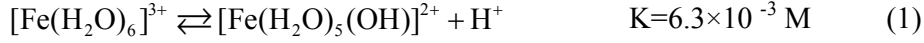
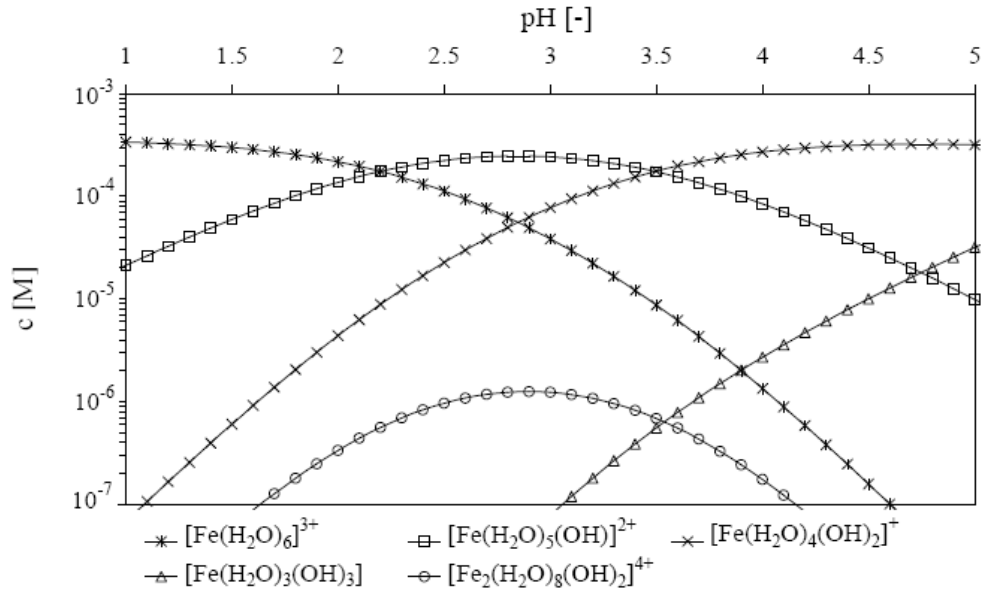


Figure II-A-1 shows the equilibrium concentrations of the most important ferric iron aquacomplexes in the absence of further complexing substances at different pH for a ferric iron concentration of  $0.36 \text{ mmol L}^{-1}$ . The dimer concentration is rather low at this ferric iron concentration. As the formation of the dimer is a process of second order, the relative amount of this species increases at higher iron concentrations. It is evident that between pH 2.5 and 3.0  $[\text{Fe}(\text{H}_2\text{O})_5(\text{OH})]^{2+}$  is the dominant species.



**Figure II-A-1 Ferric iron species present in aqueous solution at different pH and at a concentration of  $20 \text{ mg L}^{-1}$ , calculated with equilibrium constants from (Flynn C. M. Jr. 1984),  $T = 20 \text{ }^\circ\text{C}$ .**

Fe(III) is generally believed to be the dominant form of dissolved iron in surface seawater, because the oxidation of Fe(II) by hydrogen peroxide and oxygen is rapid

(Byrne et al., 1988; Millero et al., 1987; Millero and Sotolongo, 1989; Moffett and Zika, 1987). The speciation of Fe(III) in seawater as a function of pH is shown in Figure II-A-2 (Millero et al., 1995).

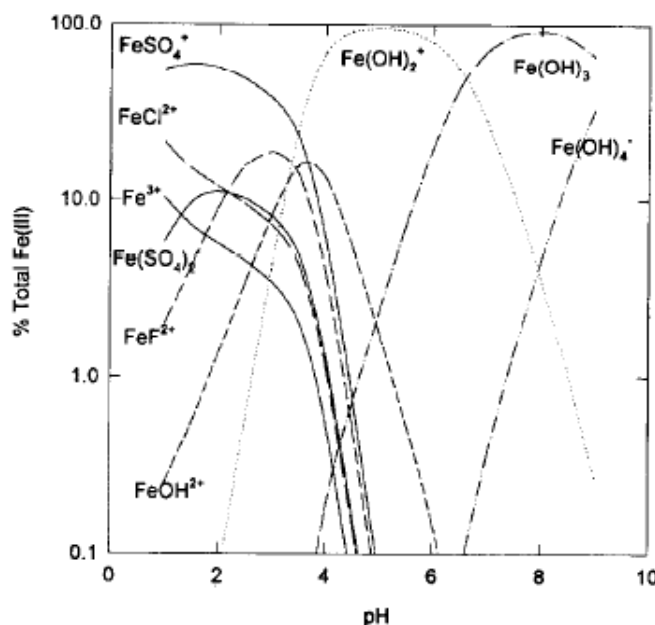


**Figure II-A-2 Speciation of Fe(III) in seawater as a function of pH (Millero et al., 1995).**

The total concentrations of iron in freshwater systems are generally higher than in the oceans, due to larger particulate inputs (Davison, 1993; Sigg et al., 1991), and therefore limitation of phytoplankton growth by this element is not likely. Its speciation and biological availability as essential element is an important and puzzling issue. The thermodynamically stable form of iron in oxic natural waters, Fe(III), has an extremely low solubility, while Fe(II) is much more soluble under most natural water conditions. It has been shown that light-induced reduction of Fe(III) is a process of major importance for the formation of dissolved iron in marine surface waters (King et al., 1993; Miller et al., 1995; Voelker and Sedlak, 1995; Voelker et al., 1997; Wells and Mayer, 1991) and in acidic surface waters (Mcknight et al., 1988; Sulzberger et al., 1990). Emmenegger et al., (1998) studied the oxidation of Fe(II) in the euphotic Swiss lake. In oxic environmental systems, the reduced iron species are rapidly oxidized by  $\text{O}_2$  at near-neutral pH, yielding Fe(III) and reactive oxygen

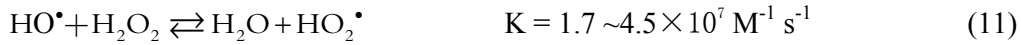
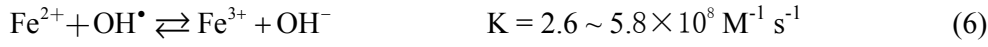
species.

### **A-2-reactions of $\text{Fe}^{2+}$ , $\text{Fe}^{3+}$ and $\text{H}_2\text{O}_2$ in aqueous solution**

The oxidation of Fe(II) with  $\text{H}_2\text{O}_2$  has been studied in seawater by a number of authors.  $\text{H}_2\text{O}_2$  is an intermediate in the reduction of oxygen to water and can act as an oxidant in the reaction with Fe(II) (Moffett and Zika, 1987). The  $\text{H}_2\text{O}_2$  in surface water is also generated by photochemical processes, due to the presence of organic compounds (Moffet and Zika, 1983). The  $\text{H}_2\text{O}_2$  is present at a concentration of  $10^{-7}$  M in surface seawater (Moore et al., 1993; Zika et al., 1985a, 1985b).

Hydrogen peroxide is decomposed to water and oxygen in the presence of iron ions in aqueous solution. Two reaction pathways have been proposed in literature (Sychev A. Y., Isaak V. G., 1995), the first formulating a radical chain reaction (Haber-Weiss mechanism) (Barb W. G. et al., 1951a, 1951b; Haber F. and Weiss J., 1934; Walling C., 1975), the other an ionic mechanism (Kremer-Stein mechanism) (Kremer M. L., 1962; Kremer M. L. and Stein G., 1959; Kremer M. L. and Stein G., 1977). After the work of Walling (Walling C., 1975), the radical mechanism has been broadly accepted for reactions in acidic medium. Yet, it should be mentioned that discussion is still on-going and the occurrence of ferrate and ferryl iron (+IV and +V), at least in intermediate complexes, has been proposed (Bossmann S. H. et al., 1998; Pignatello J. J. et al., 1999).

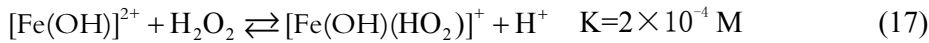
Mixtures of ferrous iron and hydrogen peroxide are called Fenton reagent. If ferrous is replaced by ferric iron it is called Fenton-like reagent. The Fenton reaction, Eq. (5), was first reported by H. J. H. Fenton in 1894 (Fenton H. J. H., 1894). Eq. (5) to Eq. (11) show the reactions of ferrous iron, ferric iron and hydrogen peroxide in the absence of other interfering ions and organic substances. The regeneration of ferrous iron from ferric iron by Eq. (8) to Eq. (10), is the rate limiting step in the catalytic iron cycle, if iron is added in small amounts. The listed rate and equilibrium constants for Eq. (5) to Eq. (14) were reported in (Sychev A. Y., Isaak V. G., 1995).



Furthermore, radical-radical reactions have to be taken into account:



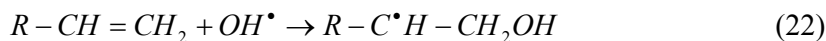
Finally, the following equilibriums have to be taken into account (Gallard et al., 1999; Bielski et al., 1985):



### **A-3-reactions of Fe<sup>2+</sup>/ Fe<sup>3+</sup>/ H<sub>2</sub>O<sub>2</sub> in the presence of organic substances**

If organic substances (in the case of wastewater) are present in the system Fe<sup>2+</sup>/ Fe<sup>3+</sup>/ H<sub>2</sub>O<sub>2</sub>, they react in many ways with the generated hydroxyl radicals. Yet, in all cases the oxidative attack is electrophilic and the rate constants are close to the diffusion-controlled limit (Buxton G. U. et al., 1988; Haag W. R., Yao C. D., 1992; Malato et al., 2002). The following reactions with organic substrates have been reported (Haag W. R., Yao C. D., 1992; Legrini O. et al., 1993).

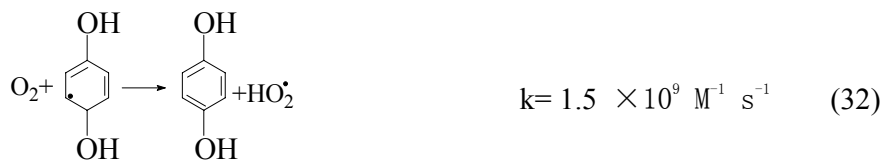
- Hydrogen abstraction from aliphatic carbon atoms, Eq. (21).
- Electrophilic addition to double bonds or aromatic rings, Eq. (22).
- Electron transfer reactions, Eq. (23).



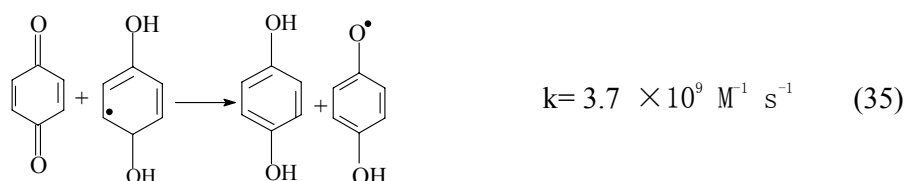
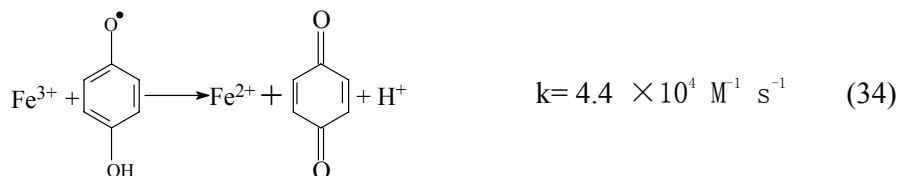
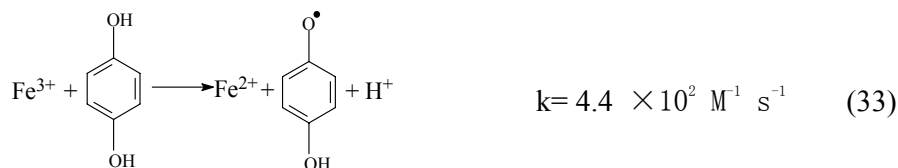
The generated organic radicals continue reacting prolonging the chain reaction. Depending on the oxidation-reduction potential of the organic radical generated, reactions (25) to (27) can take place. The organic peroxide generated in reaction (27) can further react with ferrous iron similar to the Fenton reaction (28) (Huyser S., Hawkins G., 1983). Of special interest is the reaction with dissolved oxygen (Dorfman-mechanism), Eq. (29) and (30) (Dorfman L. M. et al., 1962; Von Sonntag C. et al., 1997), because the peroxy radical can regenerate hydrogen peroxide by reaction (7) and thereby contribute to reduce the consumption of oxidant in wastewater treatment by Fenton and photo-Fenton method.



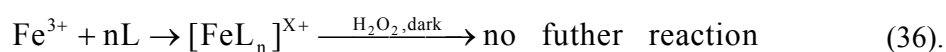
In the case of aromatic pollutants the ring usually is hydroxylated before it is broken up during the oxidation process. Substances containing quinone and hydroquinone structures are typical intermediate degradation products, e.g. produced by reactions equivalent to Eq. (31) and (32). These are especially worth mentioning because they provide an alternative, quicker pathway for ferrous iron regeneration through Eq. (33) and (34) accelerating thereby the process. Resulting benzoquinone structures can also be reduced as in Eq. (35). Thereby, each molecule can reduce several ferric iron ions in a catalytic cycle. Anyway, sooner or later this catalytic cycle is interrupted, because in competition with reactions (31) - (35) also ring opening reactions occur, which further carry on the mineralisation of the molecule (Chen R., Pignatello J. J., 1997).







There is one great set back of the Fenton method. Especially when the treatment goal is the total mineralisation of organic pollutants, carboxylic intermediates cannot be further degraded. Carboxylic and dicarboxylic acids are known to form stable iron complexes, which inhibit the reaction with peroxide (Kavitha and Palanivelu, 2004). Hence, the catalytic iron cycle reaches a standstill before total mineralisation is accomplished, Eq. (36).

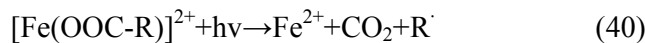
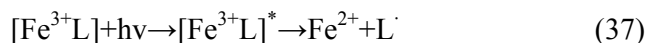


L: Mono- or Dicarboxylic acid

Due to the high oxidation potential of the hydroxyl radical, it can also react with inorganic ions present in the solution. Several authors have described the strong negative effect of the presence of carbonate and phosphate in the Fenton reaction, while the effect of other ions such as chloride or sulphate is not as strong (De Laat J. et al., 2004; Kiwi J. et al., 2000; Lipczynska-Kochany E. et al., 1995; Maciel R. et al., 2004; Pignatello J. J., 1992; Von Sonntag C., 1997).

#### **A-4-Photochemical reactions**

Irradiation with light up to 580 nm leads to photoreduction of dissolved ferric iron to ferrous iron (Bauer R. et al., 1999). The primary step is a ligand-to-metal charge-transfer (LMCT) reaction. Subsequently, intermediate complexes dissociate as shown in reaction (37) (Zepp et al., 1992). The ligand can be any Lewis base able to form a complex with ferric iron ( $\text{OH}^-$ ,  $\text{H}_2\text{O}$ ,  $\text{HO}_2^-$ ,  $\text{Cl}^-$ ,  $\text{R-COO}^-$ ,  $\text{R-OH}$ ,  $\text{R-NH}_2$  etc.). Depending on the reacting ligand, the product may be a hydroxyl radical such as in Eq. (38) and (39) or another radical derivated from the ligand. The direct oxidation of an organic ligand is possible as well as shown for carboxylic acids in Eq. (40). The omnipresence of iron makes the Photo- Fenton reaction an important factor for the autopurification capacity of lakes, rivers (Sulzberger et al., 1994) and atmospheric water droplets (Faust and Hoigné, 1990).



Depending on the ligand the ferric iron complex has different light absorption properties and reaction (37) takes place with different quantum yields and also at different wavelengths. Consequently, the pH plays a crucial role in the efficiency of the photo-Fenton reaction, because it strongly influences which complexes are formed (Figure II-A-1). Thus, pH 2.8 was frequently postulated as an optimum pH for photo-Fenton treatment (Pignatello, 1992; Safarzadeh-Amiri et al., 1996b), because at this pH precipitation does not take place yet and the dominant iron species in solution is  $[\text{Fe}(\text{OH})]^{2+}$ , the most photoactive ferric iron aquacomplex.

In fact, as shown in its general form in Eq. (37), ferric iron can form complexes with many substances and undergo photoreduction. Carboxylic acids are important because they are frequent intermediate products in an oxidative treatment. Such ferric iron – carboxylate complexes can have much higher quantum yields than ferric iron – water complexes. It is therefore a typical observation that a reaction shows an initial lag phase, until intermediates are formed, which can regenerate more efficiently ferrous iron from ferric iron accelerating the process. This can either happen through a photochemical pathway, Eq. (40), a thermal pathway, or a combination of both.

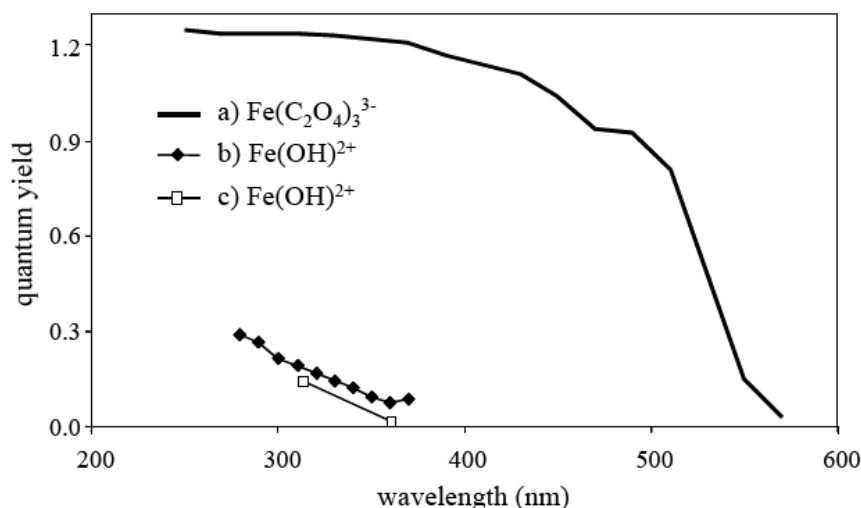


**Figure II-A-3 Quantum yields from literature. a) (Braun A. M., Maurette M. T. and Oliveros E. 1991) is for the reaction in Eq. (41) and (42). b) (David F., David P.G. 1976) and c) (Faust B. and Hoigné J., 1990) are for the reaction in Eq. (39)**

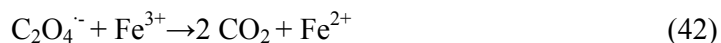
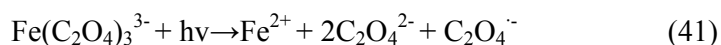
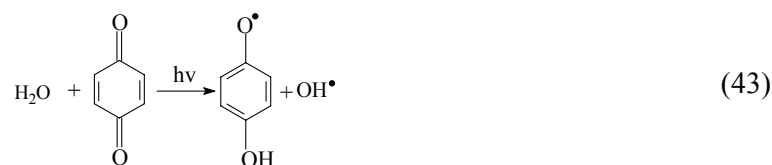


Figure II-A-3 illustrates the quantum yield of several complexes at different wavelengths by some examples from literature. Consequently, the addition of oxalate has been proposed to overcome the initial lag phase (Nogueira et al., 2002; Safarzadeh-Amiri et al., 1996a; Paterlini and Nogueira, 2005). Thereby, the wastewater throughput in a photo-Fenton plant can be raised, but these gains have to

be compared to the increased reagent cost due to the addition of oxalate, because oxalate is not acting as a catalyst, as it is as well degraded during this photochemical reaction. Other chelating agents have been proposed as well with the additional aim of working at neutral pH (Sun and Pignatello 1992, 1993a). The photolysis of ferric iron–oxalate complexes has been known for a long time and is used in actinometry for its high quantum yield (Braun et al., 1991; Cooper and DeGraff, 1971; Hatchard and Parker, 1956).

Finally, another photochemical reaction should be mentioned, which is the photoreduction of quinones to semiquinones, Eq. (43) (Ononye A. I. et al., 1986). By this reaction intermediate quinonic reaction products can be reduced and can further contribute to accelerate the reduction of ferric iron by Eq. (34). Moreover, as a side product even a hydroxyl radical is generated.



#### **A-5-Application to wastewater treatment**

While the Fenton reaction has been known for more than a hundred years (Fenton H. J. H., 1894), it has only been in 1968 that it has been first suggested as means for wastewater treatment (Bishop D. F. et al., 1968). The photo-Fenton reaction was at first investigated by atmospheric researchers to clarify natural mechanisms of hydrogen peroxide production and oxidation of several pollutants in atmospheric water droplets (Faust B. C., Hoigné J., 1990). At the beginning of the 1990s it was introduced in wastewater technology (Lipczynska-Kochany E., 1991; Lipczynska-Kochany E., 1992; Pignatello J. J., 1992; Ruppert G. et al., 1993; Sun Y. and Pignatello J. J., 1993).

Later on it was applied to waste water containing many different pollutants, such as pesticides (Fallmann H. et al., 1999; Hincapié M. et al., 2005; Huston P. and

Pignatello J. J., 1999; Malato S. et al., 2003), chlorophenols (Krutzler T. et al., 1999; Pera-Titus M. et al., 2004), natural phenolic pollutants (Gernjak W. et al., 2003; Herrera F. et al., 1998), pharmaceuticals (Arslan-Alaton I. and Gurses F., 2004; Pérez-Estrada L. et al., 2005), etc. It was also successfully applied to waste water with high organic load in the order of  $10 \text{ g L}^{-1}$  to  $20 \text{ g L}^{-1}$  total organic carbon (Sigman et al., 2004). Originally toxic waste water has been proven to lose its toxicity upon treatment by photo-Fenton process before total mineralisation has been achieved (Hincapié et al., 2005; Malato et al., 2003). Loss of toxicity usually is accompanied by an enhancement of biodegradability of the treated waste water (Sarria et al., 2002; Sarria et al., 2003). Consequently, photo-Fenton process and AOPs in general have been proposed as a pre-treatment to biological treatment (Esplugas S. and Ollis D. F., 1997; Scott J. P. and Ollis D. F., 1995).

Several studies have discussed the influence of iron concentration and its catalytic behaviour (Gob et al., 2001; Krutzler et al., 1999; Oliveros et al., 1997) and temperature effect (Krutzler et al., 1999; Sagawe et al., 2001; Sarria et al., 2003; Torrades et al., 2003;). Within the investigated limits (maximal iron concentration  $2.6 \text{ mM}$ , maximal temperature  $70^\circ\text{C}$ ) an increase of the respective parameter meant also an increase in reaction rate. Only one study examines the result of alternating time intervals with and without illumination (Herrera F., Pulgarin C., et al., 1998). It suggests the formation of pre-cursors in the dark prone to rapid photolysis upon irradiation. Consequently, by alternating dark and illumination periods a decrease of necessary number of photons can be achieved compared to permanent illumination.

Other studies deal with the application of iron as a heterogeneous catalyst, e.g. in the form of suspended oxides (Wu F. and Deng N. S., 2000), fixed on a support structure (Bozzi et al., 2005; Maletzky et al., 1999) or even a combination of both (Martínez F et al., 2005). While an easy separation and the possibility of working without pH adjustments are advantages of this approach, the drawback are generally diminished reaction rates compared to the homogeneous photo-Fenton process. This is mainly related with mass transfer limitations of the heterogeneous process and

worsened light penetration into the photoreactor (Pérez-Estrada et al., 2005). Whereas, industrial applications of the Photo-Fenton process are still very scarce.

## **B-Iron oxides in the natural environment**

Iron oxides (a group name for iron oxyhydroxides and oxides) are widely spread in soils, sediments, rocks and aquatic systems. Synthetic iron oxides are utilized in both traditional and advanced technologies. Hematite ( $\alpha\text{-Fe}_2\text{O}_3$ ) and goethite ( $\alpha\text{-FeOOH}$ ) are specifically important materials due to their diverse applications. These compounds are also scientifically important, because their particles often serve as model systems in colloid and surface chemistry.  $\alpha\text{-Fe}_2\text{O}_3$  and  $\alpha\text{-FeOOH}$  particles are characterized by specific acid/base surface properties and they can be produced in different geometrical shapes and sizes. The reactions of  $\text{Fe}^{3+}$  hydrolysis in aqueous media may be utilized in the synthesis of a specific form of iron oxides (Cornell and Schwertmann, 1996). Iron oxides, hydroxides, and oxy-hydroxides are efficient sorbents for inorganic and organic species and have a great potential in industrial applications. They are also of substantial interest in environmental sciences since some of them are frequently occurring in soil minerals (e.g., goethite and ferrihydrite) having significant impact on the behavior of pollutants in soils.

Many oxidic iron compounds not only play an important role in a variety of disciplines and also serve as a model system of reduction and catalytic reactions (Cornell and Schwertmann, 1996). Hematite  $\alpha\text{-Fe}_2\text{O}_3$  being a major and thermodynamically most stable oxide among the 16 identified iron oxide compounds it is commonly used as an adsorbent, a catalyst precursor and an active component of catalytic material (Bukur et al., 2004; Hua et al., 2004; Provendier et al., 1999; Spitzer et al., 1966).

The mineral solid – water interface plays a central role in regulating the concentrations of a large number of reactive elements in natural aqueous systems by influencing their biogeochemical cycles, and also in engineered aqueous systems such

as those in water treatment technologies (Dzombak and Morel, 1990; Hochella and White, 1990; Stumm, 1992). Goethite is the most abundant iron oxide in nature (Bigam et al., 2002), whose surface reactivity has been extensively studied. Particularly, multisite complexation (MUSIC) models (T. Hiemstra, et al., 1989; T. Hiemstra, 1996) have identified the participation to varying degrees of three differently coordinated oxygen-terminated groups at the surface of this mineral, namely singly, doubly, and triply coordinated oxygens to central Fe atoms, as well as specific distributions of different crystalline phases (Hiemstra et al., 1989; Hiemstra, 1996).

As we know, iron is an element that is dynamically present on the boundary between the oxidized and reduced world. Only a tiny shell of the geosphere is oxidized due to photosynthesis. On the long-term geo-historic record, it is a relatively recent phenomenon. Reduced conditions are maintained in water-logged soils and sediments due to back-consumption of oxygen and organic carbon by chemotrophic microorganisms. The rate of Fe(II) production by micro-organisms depends on the surface area of the ferric (hydr)oxide that is in contact with micro-organisms (Bonneville et al., 2006). Under intermediate redox conditions and neutral pH values, iron can be present as aqueous Fe(II) in combination with Fe(III) (hydr)oxides. Under these conditions, dissolved Fe(II) may interact with these ferric oxides and also with other minerals as well as organic matter.

Iron oxides are relatively abundant in soils and sediments, and therefore it is essential to understand their roles in sorption of metals and organic chemicals. The chemical nature and high specific surface area of iron oxides as discrete particles and coatings on other minerals make these oxides efficient sinks for many contaminants including both cations and anions. Adsorption of metals to oxides in soils and sediments is important because it affects their mobility and bioavailability. Wang et al. (2008) studied cosorption and adsorption of Zn and glyphosate (GPS) in soils, and found that Zn and GPS affected their adsorption on the soil surface by each other. The presence of GPS affected the adsorption of Zn on the goethite through altering solution pH and formation of complexes with Zn. GPS increased Zn adsorption on

goethite at low pH values ( $< 4.5$ ), while decreasing the adsorption at high pH. The former decreases the mobility of Zn from soil to underground water, which minimizes the potential risk to water quality. But in alkaline soil, application of GPS increases metal mobility resulting in increasing metal bioavailability. In addition to that, Zn adsorption takes place on sites where GPS is previously adsorbed and GPS acts as a bridge between the goethite and Zn when goethite possesses positive charged surface (Wang, et al., 2008).

### **B-1-Chemical Properties of goethite**

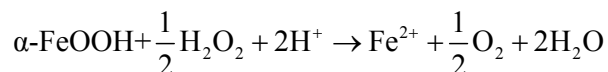
Goethite ( $\alpha$ -FeOOH) is one of the most widespread forms of iron oxy-hydroxides in terrestrial soils, sediments, and ore deposits (Cornell and Schwertmann, 2003) as well as a common weathering product in rocks of all types (Ozdemir and Dunlop, 2000). Goethite particles have high specific surface areas in excess of  $200 \text{ m}^2/\text{g}$  (Schwertmann and Cornell, 1991) and strong affinities for oxyanions and heavy metals (Hayes et al., 1987). The basic charge properties of oxide surfaces are of crucial importance for their chemical behavior in aqueous systems, driving sorption, dissolution and precipitation processes as well as redox reactions (Sposito, 2004).

Studies have shown that Fe oxides can effectively oxidize a range of pollutants including phenols (McBride, 1987; Pizzigallo et al., 1995), hydroquinone (e.g. Kung and McBride, 1988), and chloroanilines (Pizzigallo et al., 1998), in addition to strong adsorptive interactions. Fe oxides generally have lower oxidizing power than Mn oxides (e.g., reduction potentials of 0.67 V and 1.23 V for FeOOH and  $\text{MnO}_2$ , respectively) (Stone, 1987), but have greater abundance in soils and sediments. For example, in recognition of more amine loss than the amount of Mn(III/IV) being reduced to Mn(II) in whole soils, Li et al. (2003) proposed that Fe reduction did contribute to the further oxidation of the more reactive amines when all readily reducible Mn was consumed.



Adsorbed Fe(II) is known to be very reactive (Stumm and Sulzberger, 1992), acting as a reductant for elements like Hg(II), As(V) (Charlet et al., 2002), U(VI) (Liger et al., 1999), Cr(VI) (Buerge and Hug, 1999) or Cu(II) (Maithreepala and Doong, 2004) and for the transformation or natural attenuation of organic components (Amonette et al., 2000; Klausen et al., 1995; Klupinski et al., 2004; Liger et al., 1999; Maithreepala and Doong, 2004; Pecher et al., 2002; Strathmann and Stone, 2003; Vikesland and Valentine, 2002a,b). In addition, adsorbed Fe(II) may strongly affect the Fe(III) dissolution rate of iron oxide minerals in the presence of organic anions (Ballesteros et al., 1998; Stumm and Sulzberger, 1992), and may catalyze the transformation of Fe(III) minerals (Hansel et al., 2005; Pedersen et al., 2005; Zhang et al., 1992). In addition, adsorbed  $\text{Fe}^{2+}$  is far more easily oxidized if bound by mineral surfaces (Wehrli and Stumm, 1989; Wehrli et al., 1989).

In the goethite/ $\text{H}_2\text{O}_2$  process, ferrous ions are generated by the reductive dissolution of goethite shown as below (Sorensen and Frimmel, 1997):

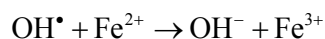


Advanced oxidation processes are commonly used for the treatment of wastewater containing recalcitrant organic pollutants (Pignatello, et al., 2006; Watts, et al., 1990; Varghese, et al., 2006) and can be used to destroy a variety of explosive ammunition residues in the environment (Bier et al., 1999). These methods are so attractive because of the possibility of the mineralization of the target compounds.

The required agents for the Fenton process are hydrogen peroxide ( $\text{H}_2\text{O}_2$ ) and iron oxide, where  $\text{H}_2\text{O}_2$  is a safe and economic oxidant. However, hydrogen peroxide is not an excellent oxidant for most organic substance of interest. In general, hydrogen peroxide is combined with UV-light, iron salts or ozone to produce a high concentration of hydroxyl radicals. Recently, the use of goethite ( $\alpha\text{-FeOOH}$ ) with hydrogen peroxide was found to effectively oxidize organic compounds due to the catalysis on goethite surface and ferrous ion generation (Lu, 2000; Zinder, et al.,

1986). Khan and Watts (1996) reported that adding appropriate amount of H<sub>2</sub>O<sub>2</sub> into the contaminated soils in the presence of goethite produced the reactive OH radicals, degrading most organic pollutants. Lu (2000) also indicated that 2-chlorophenol can be decomposed with H<sub>2</sub>O<sub>2</sub> catalyzed by goethite. Moreover, the capability of degradation can be greatly improved by the combination of goethite and UV/H<sub>2</sub>O<sub>2</sub> (M.A. Khan, J. R. Watts, 1996). This advantage is mainly due to the generation of more hydroxyl radicals from H<sub>2</sub>O<sub>2</sub> when exposed to UV-light (M. Arienzo, 1999).

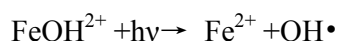
Ferrous ions are dissolved into the solution and then mixed with hydrogen peroxide to produce hydroxyl radicals ( $\bullet$ OH), commonly described as Fenton reaction (Lu et al., 1999):



The Fenton reaction is recognized as one of the most powerful oxidizing reactions that can be used to decompose a wide range of refractory synthetics or natural organic compounds, including nitroaromatic explosives, such as 2, 4, 6-trinitrophenol (PA) and ammonium picrate (AP) (Tanaka et al., 1997). This research describes the heterogeneous catalytic reactions of H<sub>2</sub>O<sub>2</sub> with granular size goethite ( $\alpha$ -FeOOH) particles in aqueous solution under various experimental conditions. PA and AP solutions at various initial concentrations were prepared under acidic condition (pH 2.8) to perform Fenton-like oxidation reaction. The objective of this study was to investigate the oxidation of explosives, namely AP and PA, by goethite/H<sub>2</sub>O<sub>2</sub> process. A kinetic model was proposed to successfully predict nitroaromatic decomposition half-lives. In addition, the inhibition and adsorption effect of intermediates on the parent compound oxidation can be quantified through this kinetic model.

Catalytic ozonation with the prepared FeOOH substantially improved the degradation of nitrobenzene in water through enhanced generation of hydroxyl

radicals. The activity of the FeOOH in this case is due to its highly hydroxylated surfaces in water. The surface hydroxyl groups on the FeOOH in water play an important role in the catalytic ozonation. It seems that the uncharged surface hydroxyl groups are more active in the catalytic ozonation than the protonated or deprotonated ones. Results indicate that the uncharged surface hydroxyl groups of FeOOH in water can induce aqueous ozone decomposition to generate hydroxyl radicals during the catalytic ozonation of nitrobenzene. Further researches are still needed to find out the relationship between the acidity as well as the coordination states of the surface hydroxyl groups and their activity in inducing hydroxyl radical generation from aqueous ozone. Organic products degradation efficiency was further increased by the exposure to 40W UV-light for 120 min. This is because the  $\text{Fe}^{3+}$  was reduced in acidic solution thus more active ferrous ions ( $\text{Fe}^{2+}$ ) were generated (Perez, et al., 2002).



### **B-2-Pathway of FeOOH-induced hydroxyl radical**

The surface hydroxyl groups at the water/oxide interface will interact with  $\text{O}_3$  and the substrate in catalytic ozonation.

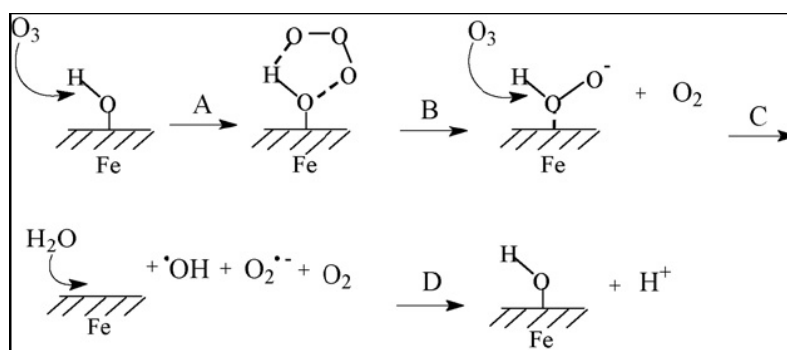


**Figure II-B-1 Scheme of the proposed pathway of hydroxyl radical generation when aqueous ozone interacts with surface hydroxyl group of FeOOH in water.**

Figure II-B-1 illustrates the possible pathway of hydroxyl radical generation

induced by the surface hydroxyl groups of the FeOOH. Since ozone has both nucleophilic site and electrophilic site as a dipole agent (Langlais, et al., 1991), the ozone molecule can be combined with the surface hydroxyl group as its H and O are electrophilic and nucleophilic respectively (step A). The combined species further decomposes into surface  $\text{HO}^{2-}$  (step B). The surface  $\text{HO}^{2-}$  reacts with another  $\text{O}_3$  forming  $\bullet\text{OH}$  and  $\text{O}_2^{\bullet-}$  (step C). The  $\text{O}_2^{\bullet-}$  can further reacts with  $\text{O}_3$ , which finally will yield another  $\bullet\text{OH}$  (von Gunten, 2003). The vacant surface Fe(III) site adsorbs another water molecule, which subsequently dissociates into surface hydroxyl group (step D). As far as the protonated surface hydroxyl group is concerned, its O is weaker in nucleophilicity than the O of neutral state hydroxyl group. Therefore, the protonation of the surface hydroxyl group will disadvantage the surface binding of ozone (step A). On the other hand, the deprotonated surface hydroxyl group cannot provide the electrophilic H, which would also handicap the proposed process.

### **C-Fe(III)-EDDS complex**

#### **C-1-Aminopolycarboxylates: EDDS-a biodegradable strong metal chelant**

Over the centuries, human activities have contaminated large areas in both developed and developing countries. The European Environment Agency has estimated the total costs for the clean-up of contaminated sites in Europe to be between 59 and 109 billion euros (Commission of the European Communities, 2002). At present not even highly industrial countries can afford to clean up contaminated sites. In Germany, for instance, only 30% of the soils from contaminated areas are cleaned up in soil remediation facilities, while the rest is stored untreated in waste disposal facilities. Heavy metals are a major factor of this pollution due to their atmospheric deposition, (Martley et al., 2004; Romo-Kroger et al., 1994; Steinnes et al., 1997; Tong and Lam, 2000), their leaching tendency, and the fact that they are undegradable.

Chelants or chelating agents are compounds that form coordinate covalent bonds with metal ions to form complexes. Transition metal chelators are broadly used in a variety of consumer products and processes, eg in the pulp and paper, textile, metal, photographic, leather, cosmetic and detergent industry. Their primary purpose is to control trace amounts of iron, manganese, copper, etc., that would otherwise be deleterious to product performance or commercial process. The molecular design requirements for an effective chelator (i.e., hexadentate ligand derived from a diamine with carboxylate or phosphonate moieties) are well known and exemplified in current commercially available materials, such as, aminopolycarboxylates (EDTA, DTPA, etc.) or aminopolyphosphonates (EDTMP, DETPMP, etc.). These chelators are, however, essentially nonbiodegradable or require special environmental conditions for degradation to occur (Schowanek and Verstraete, 1989).

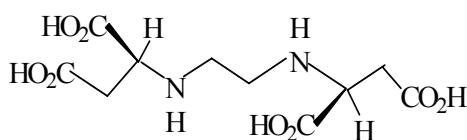
Chelating agents are potent agents for solubilizing heavy metals from polluted soils. Two different remediation methods using chelating agents are now being investigated: chelant assisted ex-situ soil washing and chelant assisted phytoextraction. In ex-situ soil washing two methods are possible, batch washing (Tandy et al., 2004; Vandevivere et al., 2001a) and heap leaching (Hauser et al., 2005). In chelant-assisted phytoextraction chelating agents are added to the soil to increase the solubilized metals and correspondingly uptake into plants (Garbisu and Alkorta, 2001). The enormous drawback of this method is the inevitable leaching of chelants and its metal-complexes into the deeper soil layers and eventually to groundwater. The ex-situ methods attract a lesser risk of leaching than phytoremediation as most of the chelating agent is removed from the soil before returning to the field. However some chelating agent is always left in the soil and the formation of metal complexes with this residual complexing agent is possible and in turn leaching of these metal complexes must be taken into consideration.

Previously the most used complexing agent for these methods was EDTA (Abumaizar and Khan, 1996; Peters, 1999; Thayalakumaran et al., 2003; Van Benschoten et al., 1997; Wenzel et al., 2003; Wu F. et al., 1999). It is however recalcitrant in the environment and leaching of metal-complexes over a long time

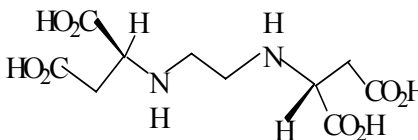
period was possible (Bucheli-Witschel and Egli, 2001; Wenzel et al., 2003; Wu et al., 2004).

S, S-ethylenediaminedisuccinic acid (EDDS) is a biodegradable chelating agent that is a structural isomer of EDTA (Schowanek et al., 1997; Vandevivere et al., 2001b). Studies have produced convincing evidence that EDDS is a viable replacement ligand for EDTA as used in the nuclear industry. In many respects, EDDS is as powerful as EDTA and can replace it directly as a readily biodegradable alternative. It is now starting to replace EDTA in soil washing and phytoextraction (Kos and Lestan, 2003; Tandy et al., 2004). It should not be confused with the other stereo-isomers of EDDS however (R, R-, R, S-, S, R-), which are partly or wholly non-biodegradable (Schowanek et al., 1997; Takahashi et al., 1997). Several authors recently have carried out work on EDDS assisted phytoextraction, mainly on Pb but also Zn, Cu, Cd and Ni (Grcman et al., 2003; Kos et al., 2003; Kos and Lestan, 2003, 2004a, b; Luo et al., 2005; Meers et al., 2005). An immediate leaching risk is possible during this method until the EDDS has degraded (Kos and Lestan, 2004a). Three studies have also used EDDS for soil washing or heap leaching (Hauser et al., 2005; Tandy et al., 2004; Vandevivere et al., 2001a).

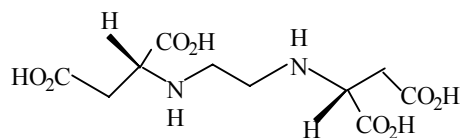
EDDS can be made from ethylene diamine and maleic anhydride (Ramsey-Downey and Kerzerian, 1963). This route yields a mixture of stereoisomers consisting of 25%[S, S], 50%[R, S]/[S, R], and 25%[R, R]- form (Figure II-B-1). Alternatively, single stereoisomers of EDDS can be prepared using 1,2-dibromoethane and a selected form of aspartic acid, i. e. [S, S]-EDDS from L-aspartic acid, [R, R]-EDDS from D-aspartic acid (Neal and Rose, 1968).



[S, S]-EDDS



[R, S]-EDDS or [S, R]-EDDS



[R, R]-EDDS

**Figure II-C-1. Chemical structure of the different stereoisomers of EDDS.**

Biodegradation work was done on the most degradable form, i.e. [S, S]-EDDS, in a variety of environmental compartments. Interestingly, the [S, S]-isomer of EDDS was also reported to be produced naturally by a number of microorganisms (Nishikiori et al., 1984), such as *Amycolatopsis japonicum sp. nov.* (Goodfellow et al., 1997).

### **C-2- Iron-carboxylate complexes**

Iron is the most abundant transition metal in the natural environment and it exists widely in the soil, fresh waters, ocean and atmosphere. It plays an important role in environmental and biochemical systems. Polycarboxylate can form strong complex with Fe(III) that undergo rapid photochemical reactions in sunlight (Faust and Hoigne, 1990; Thurman, 1985). For their high photoreactivity, Fe(III)-carboxylate complexes are important sources of H<sub>2</sub>O<sub>2</sub> for some atmospheric and surface waters. Therefore, the photochemistry of iron complexes in natural aquatic environments has received considerable attention over the past fifty years. Fe(II) is oxidized by molecular oxygen, whereas Fe(III) is photoreduced by sunlight at the expense of its ligands or other sacrificial donors present in the medium. These reactions are integral parts of the Fe(III)/Fe(II) photocatalytic cycle, in which organic pollutants undergo degradation (Ciesla et al., 2004).

ECOSAT software (Keizer and Van Riemsdijk, 1999) was used to model EDDS and metal speciation in soil solution. The binding of metals to dissolved organic matter was modelled using the consistent NICA-Donnan model (Kinniburgh et al.,

1999). It was assumed that all dissolved organic matter was in the form of fulvic acids (FA) as the soil solution had been filtered through 0.05 mm filter and FA-binding constants for generic fulvic acid were taken from Milne et al. (2003). Input parameters were the measured soil solution pH, dissolved organic matter, the major anions ( $\text{Cl}^-$ ,  $\text{NO}_3^-$ ,  $\text{SO}_4^{2-}$ ,  $\text{PO}_4^{3+}$ ), major cations ( $\text{Ca}^{2+}$ ,  $\text{Mg}^{2+}$ ) and the metals (Cu, Zn, Cd, Pb, Ni, Fe, Mn). Table II-B-1 shows the values and the sources of stability constants for EDDS complexes (Susan Tandy et al., 2006).

**Table II-C-1. EDDS complex stability constants. Calculated using source values and given at 0 M ionic strength as overall formation constant  $\beta$**

Complex	Log K	Source
$\text{CaEDDS}^{2-}$	6.34	(Orama et al., 2002)
$\text{CdEDDS}^{2-}$	12.70	(Martell et al., 2001)
$\text{CuEDDS}^{2-}$	20.46	(Orama et al., 2002)
$\text{CuHEDDS}^-$	24.39	(Orama et al., 2002)
$\text{CuH}_2\text{EDDS}$	26.80	(Orama et al., 2002)
$\text{Cu(OH)EDDS}^{3-}$	8.81	(Orama et al., 2002)
$\text{Fe(III)EDDS}^-$	23.68	(Orama et al., 2002)
$\text{HEDDS}^{3-}$	10.87	(Orama et al., 2002)
$\text{H}_2\text{EDDS}^{2-}$	18.33	(Orama et al., 2002)
$\text{H}_3\text{EDDS}^-$	22.5	(Orama et al., 2002)
$\text{H}_4\text{EDDS}$	25.66	(Orama et al., 2002)
$\text{H}_5\text{EDDS}^+$	26.95	(Orama et al., 2002)
$\text{H}_6\text{EDDS}^{2+}$	28.72	(Orama et al., 2002)
$\text{MgEDDS}^{2-}$	7.77	(Martell et al., 2001)
$\text{MnEDDS}^{2-}$	10.77	(Orama et al., 2002)
$\text{NiEDDS}^{2-}$	18.50	(Martell et al., 2001)
$\text{NiHEDDS}^-$	21.78	(Martell et al., 2001)
$\text{PbEDDS}^{2-}$	14.46	(Martell et al., 2001)
$\text{ZnEDDS}^{2-}$	15.34	(Martell et al., 2001)
$\text{ZnHEDDS}^-$	19.34	(Martell et al., 2001)

### **C-3-Photochemistry of Iron-Carboxylate**

Iron is the most abundant transition metal in the environment, typically found in



concentrations of several  $\mu\text{M}$ . Therefore, the photochemistry of the iron complexes in natural aquatic environments has received considerable attention over the past fifty years. Graedel et al. (Graedel, T. E., et al., 1986; Weschler C. J., et al., 1986) first attempted to explain the complicated redox chemistry of transition metals in atmospheric waters. They predicted the photolysis of Fe(III) complexes as important sources of  $\bullet\text{OH}$  in cloud, and they also predicted transition metals as the most important sink for  $\text{O}_2^{\bullet-}/\text{HO}_2^{\bullet}$  radicals in clouds.

In the presence of dissolved organic ligands of iron, the photoreactivity of iron is significantly altered (Figure II-C-2). Oxalic, citric, malic, glyceric, salicylic, tartaric, glutaric, gluconic, and p-hydroxybenzoic acids have all been shown to increase photoproduction of Fe(II) in solution (Cunningham et al., 1988; Kuma et al., 1992; Zuo and Zhan, 2005) by as much as three orders of magnitude depending on the nature and concentration of the ligand. Evidence has been presented for the extensive organic complexation of iron in oceanic waters (Gledhill and van den Berg, 1994; Rue and Bruland, 1995; Wells et al., 1995) which should make homogenous mechanisms for Fe(II) photoproduction (Faust B. C., 1994) also relevant to any explanation of observed Fe(II) distributions in natural waters.

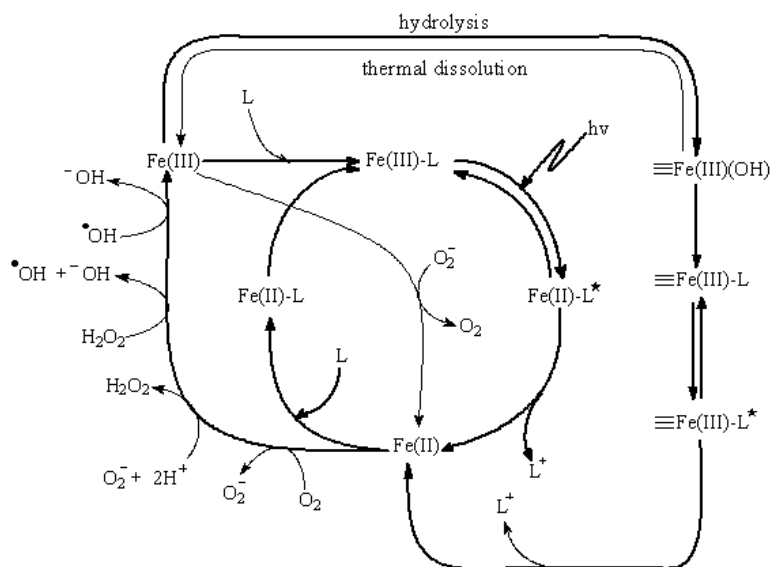
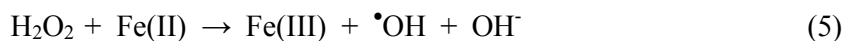
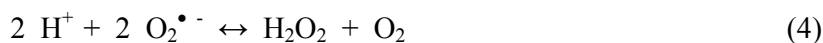
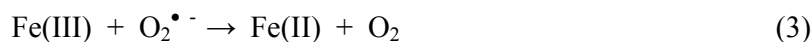
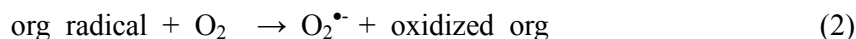
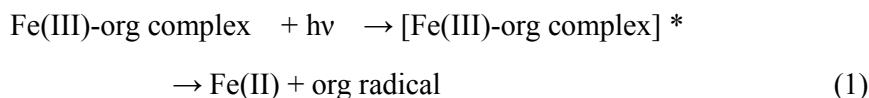


**Figure II-C-2. The mechanism of photochemical redox cycling of iron in the aqueous**

**solution. Fe(II)-L and Fe(III)-L represent Fe(II) and Fe(III) complexed with Ligand. (Abida, 2005)**

Carboxylic acids are considered to be one of the dominant classes of organic compounds found in the atmosphere in a variety of phases (Chebbi and Carlier, 1996; Talbot, 1997; Talbot et al., 1995). They have been found in rainwater, snow and ice, on aerosol particles and in the gas phase. Low molecular weight organic acids have been identified and measured in a wide variety of environments, such as marine and continental air, urban, rural and remote atmospheres and tropical and temperate zones. The presence of carboxylic acids, in the forms of oxalate, citrate and so on, has a significant effect on the speciation and photoactivity of Fe(III) ions in acidic conditions, because they may form stable complexes with Fe(III). Free Fe(III) cations absorb weakly in the solar UV region (290 nm - 400 nm), but the absorption spectra of hydrated or otherwise complexed iron species are shifted toward the visible, which might make their use in sunlight possible (Lente and Fábián, 2001). In natural waters, photochemically induced electron transfer from the complexing organic ligand to Fe(III) in the excited Fe(III)-org complexes can take place, and electron deficient Fe(III)-org complexes further reduce  $O_2$  to  $O_2^{\bullet -}$ .  $O_2^{\bullet -}$  rapidly reacts to yield the hydroxyl radical (Joseph et al., 2001; Zepp, et al, 1987; Zuo and Hoigné., 1992), as represented in the following reactions:



Deng and Wu (Deng, et al., 1998; Wu et al., 1999; Wu and Deng, 2000) studied Fe(III)-carboxylate complexes used to promote the degradation and decolorization of

dyes in aqueous solution under UV light and sunlight. Carboxylic acids can promote the photodegradation efficiency. Available data indicate that pyruvic acid is lost in the gas phase mainly through photolysis. Mellouki and Mu (Mellouki, Mu, 2003) measured the rate constant for the gas phase reaction of  $\bullet\text{OH}$  with pyruvic acid ( $\text{CH}_3\text{C}(\text{O})\text{C}(\text{O})\text{OH}$ ). The value obtained was found to be slow ( $k_{\text{PA}} = (1.2 \pm 0.4) \times 10^{-13} \text{ cm}^3 \text{ molecule}^{-1} \text{ s}^{-1}$  at 298 K). They also detected  $\bullet\text{OH}$  with a relative quantum yield of  $5 \pm 3 \%$  by the photolysis of pyruvic acid (Pyr). Pyruvic acid forms complexes with Fe(III) in the form of  $\text{Fe(III)(Pyr)}_x$  ( $x=1, 2$ ), but the equilibrium constants are unavailable from literature. And in our previous works (Wang et al., 2006), we investigated the photochemical reactivity of Fe(III)-Pyr complexes and determined the amount of  $\bullet\text{OH}$  produced by the photolysis of the Fe(III)-Pyr complexes in the aqueous solution. It was found that the Fe(III)-Pyr system is not catalytic. In the aqueous solution containing  $10.0 \mu\text{M}$  of Fe(III) and  $60.0 \mu\text{M}$  of Pyr at  $\text{pH} = 3.0$ ,  $\bullet\text{OH}$  was produced after 160 min of irradiation in amount of  $34 \mu\text{M}$ . The generation rate constant of  $\bullet\text{OH}$  was  $0.21 \mu\text{M L}^{-1} \text{ min}^{-1}$  and the quantum yield of  $\bullet\text{OH}$  was  $2 \times 10^{-2}$ . The study confirms that pH, temperature, concentration of the Fe(III) and Pyr, all have a great effect on the  $\bullet\text{OH}$  yield. Pyr and many other carboxylates can form complexes with Fe(III) and other metal ions in aqueous solutions.

Research results shows that the presence of Fe(III)-carboxylate complexes could have a considerable impact on the fate of organic pollutant in aquatic environment. Figure II-C-3 (Wang, 2008) presents the reaction scheme for the photolysis of Fe(III) complexes of polycarboxylates (oxalate, malonate, citrate). Under irradiation, many kinds of active radicals ( $\text{ROO}\bullet$ ,  $\text{O}_2\bullet$ ,  $\text{HO}_2\bullet$ ,  $\bullet\text{OH}$ ) are generated in the solution. From the scheme, iron concentration, pH and oxygen are all important parameters.

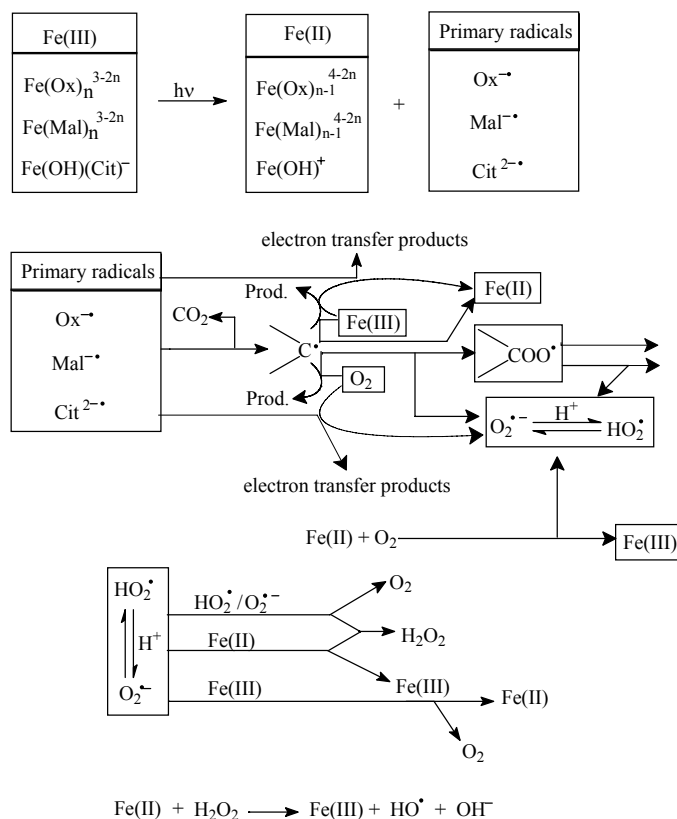


**Figure II-C-3. Reaction scheme for the photolysis of Fe(III)-polycarboxylate complexes.**

In natural waters, the Iron-complexes can potentially use sunlight as the irradiation source to produce reactive species, such as  $\cdot\text{OH}$ , which would play an important role in the oxidation of organic materials.

## **D- pesticide and herbicide**

The intensive use of pesticides all over the world has led to a ubiquitous contamination of exposed as well as remote areas. The environmental problem caused by pesticides has induced some contamination measurements in water (Albanis et al., 1986; Charreteur et al., 1996; Di Corcia and Marchetti, 1992; Ferrando et al., 1992), in soils (Coburn et al., 1976; Durand and Barcelo, 1991) and in the atmosphere (Aston and Seiber, 1997; Bidleman and Leonard, 1982; Chevreuil et al., 1989, 1996; Haragushi et al., 1994, 1995; McConnel et al., 1998; Millet et al., 1996, 1997; Oehme,

1991; Richartz et al., 1990; Sanusi et al., 1997; Seiber et al., 1993; Watanabe, 1998). The determination of atmospheric contamination by pesticides is of strong importance since it is known that atmosphere is the good pathway for the contamination of remote areas and aquatic ecosystems. It has been demonstrated that 98% of dichlorodiphenyltrichloroethane (DDT) measured in Canadian Great Lakes comes from atmospheric deposition (Chan et al., 1994). Pesticides enter the atmosphere through many processes: drift during spraying operations (Payne and Thompson, 1992; Watanabe, 1998), wind erosion of soil or by volatilisation (Foster et al., 1995; Glotfelty et al., 1984, 1989; Haenel and Siebers, 1994; Koppell and Kordel, 1997; Nash, 1989). Atmospheric concentrations of pesticides are an important problem for human health and forest ecosystems (Aston and Seiber, 1997; Eriksson et al., 1989; Richartz et al., 1990)

Physical-chemical properties of pesticides were presented in Table II-D-1.

**Table II-D-1. Physical-chemical properties of some pesticides (Tomlin, 1997; Mackay et al., 1997)**

Pesticide	PM (g mol <sup>-1</sup> )	Melting point (°C)	Boiling point (°C)	Solubility in water at 25°C (mg l <sup>-1</sup> )	Vapour pressure (25°C) (Pa)	Henry law constant (Pa m <sup>3</sup> mol <sup>-1</sup> )
Alachlor	269.77	39.5–41.5	100–135	242	2.9×10 <sup>-3</sup>	2.2×10 <sup>-3</sup>
Atrazine	215.68	175–177		33.0	3.9×10 <sup>-5</sup>	2.88×10 <sup>-4</sup>
Captan	300.6	160–170		3.3	1.0×10 <sup>-3</sup> – 1.1×10 <sup>-5</sup>	0.60
Formothion	257.3	25–26		2600	1.13×10 <sup>-4</sup>	1.1×10 <sup>-5</sup>
Lindane	290.85	112.5–113.5	323.4	7.3	4.0×10 <sup>-3</sup>	0.149
Phosalone	367.8	42–48		3.05	<6.67×10 <sup>-5</sup>	8.0×10 <sup>-3</sup>

The main sources for emission of pesticides in the atmosphere and rainfall are volatilization during application, volatilization from crops and soil, and wind erosion from soil. Once pesticides are emitted to the atmosphere, they can be transported long distances from the application site. How far a compound is transported depends on its half-life in the atmosphere, which in turn depends on the compounds reactivity (e. g.

with OH radicals) and its rate of removal by wet deposition.

#### **D-1- Atrazine**

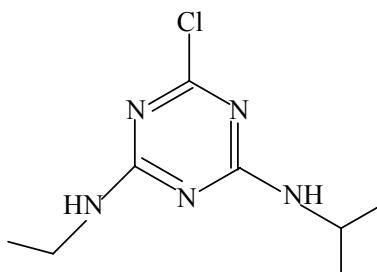


**Figure II-D-1 chemical structure of Atrazine**

Atrazine (2-chloro-4-ethylamino-6-isopropylamino-1, 3, 5-triazine), one of the most widely used herbicides, is registered in more than 70 countries worldwide (Kauffmann et al., 2000; Hayes et al., 2002; Zhang et al., 2004). Figure II-D-1 presents the chemical structure of Atrazine. Atrazine is a selective triazine herbicide used to control broadleaf and grassy weeds in corn, sorghum, sugarcane, pineapple and other crops, and in conifer reforestation plantings. It is also used as a nonselective herbicide on non-cropped industrial lands and on fallow lands. Atrazine is quite persistent in neutral environment and is toxic to various living organisms (Tomlin C. 1994).

Since 1958, it has been used as a pre- and postemergent herbicide to control broad-leaved weeds in the production of corn and grain sorghum. The widespread use of atrazine, however, is associated with an increasing incidence of contamination of drinking water supplies, with atrazine concentrations above the maximum contaminant level (MCL) of  $0.1 \mu\text{g L}^{-1}$  (Commission of the European Communities, 2001) reported in some regions (Cai et al., 2004; Lambropoulou et al., 2002; Thurman et al., 1992;). The behavior of atrazine in the environment depends upon several factors, including adsorption to soil components, uptake by plants, transport via runoff

and leaching, biodegradation, photodegradation, volatilization, and chemical degradation. Efforts have been made to study the adsorption mechanisms of atrazine to soil humic substances and clay minerals (Herwig et al., 2001; Piccolo et al., 1998).

Atrazine is the most commonly detected pesticide in the groundwater of USA (US Environmental Protection Agency, 1990; Blanchard and Donald, 1997; Gish, et al., 1998; Senseman, et al., 1997) and it was also detected in Germany (Dorfler et al., 1997; Guzzella et al., 1996), France (Garmouma et al., 1997), Canada (Masse et al., 1998), and Australia (Kookana et al., 1998).

#### **D-1-1- Atrazine degradation**

Earlier studies showed that atrazine was better degraded in anaerobic conditions than in aerobic one (Kearney et al., 1967). Many chlorinated aliphatic and aromatic compounds like Benzene Hexachloride (BHC) and DDT, which were earlier considered as recalcitrant in aerobic process, were successfully degraded in anaerobic condition (Burge, 1971; Sidderamappa et al., 1975). Literature showed that the aromatic structure of lignin, benzoate and other aromatic acids were metabolized to gaseous end products in mixed cultures, under methanogenic conditions (Young and Haggblom, 1990). However, degradation rate of such compounds by anaerobic mixed microbial culture was slow, as the energy required for bacterial growth was not adequate from such toxic compounds. In such cases, addition of easily biodegradable organic compounds stimulated the growth of anaerobic bacteria, and thereby enhanced the degradation rate by utilizing recalcitrant compound as secondary substrate in co-metabolic process. Enhanced degradation rate of atrazine was observed in both aerobic and anaerobic conditions, when external carbon sources were supplied to pure and mixed bacterial culture. Struther et al. (1998) used citrate and sucrose as external carbon source whereas Chung et al. (1996) used four different external carbon sources, methanol, sodium acetate, acetic acid and glucose.

Atrazine has recently been a compound of interest for a variety of chemical oxidation techniques. Nelieu et al. (2000) degraded atrazine to ammeline using a

combined ozone/hydrogen peroxide treatment. Acero et al. (2000) used conventional ozonation and the combined ozone/peroxide treatment to degrade low concentrations of atrazine. Balmer and Sulzberger (1999) applied an irradiated iron/oxalate treatment system to low concentrations of atrazine. Huston and Pignatello (1999) studied a photo-Fenton degradation of atrazine, while Arnold et al. (Arnold et al. 1995, 1998) applied a classic Fenton approach and combined chemical and biological degradation.

Advanced oxidation processes (AOPs) have been widely used in wastewater treatment (Stafford et al., 1994; Lunar et al., 2000; Kurbus et al., 2003; Brillas et al., 2003; Trojanowicz et al., 2002), the main feature of them is producing  $\cdot\text{OH}$  radicals to oxidize various organic contaminants (Figure II-D-2).

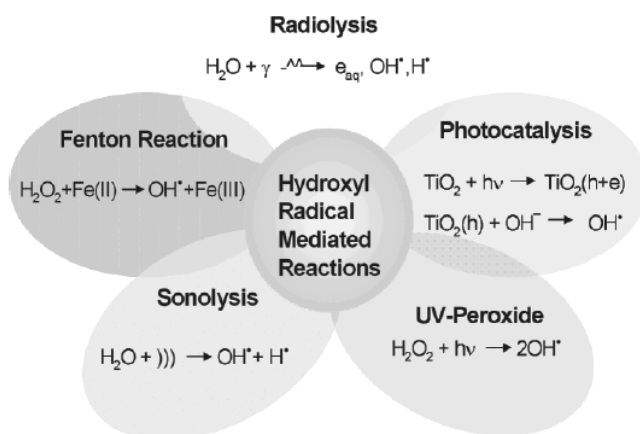


**Figure II-D-2. Advanced oxidation technologies**

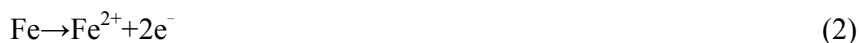
Electrochemical Fenton treatment (Pratap and Lemley, 1994; Roe and Lemley, 1996) is a radical oxidation process that was developed as an innovative application of the Fenton reaction Eq. (1) (Walling, 1975).



The method employs an electrochemical cell with iron electrodes (cathode and



anode). The anode is a sacrificial electrode that delivers iron to the solution, and the cathode functions as an inert electrode for the reduction of water as illustrated by the half reactions as follows:



This method has the disadvantage of requiring the Fenton reaction to occur at a non-optimal pH close to neutral, due to the formation of hydroxide ion at the cathode. Solids are also formed in solution from the precipitation of iron hydroxides.

AFT (Anodic Fenton treatment) method was applied to atrazine and determine its ability to degrade this pesticide and its degradation products (Saltmiras and Lemley, 2002). Figure II-D-3 is Anodic Fenton treatment apparatus. Seven degradation products of Atrazine (Table II-D-2) were quantified for measurement during AFT.

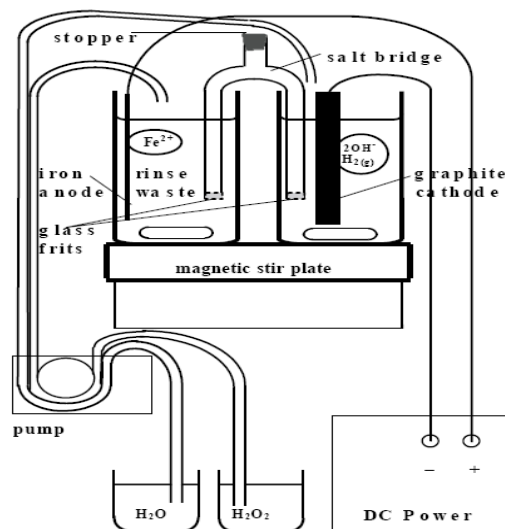
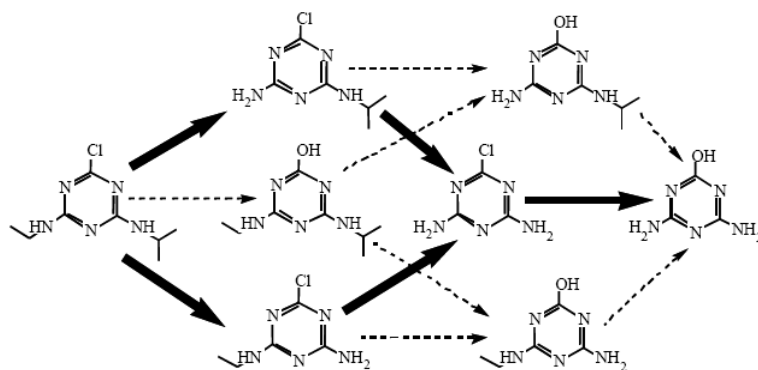


Figure II-D-3 Anodic Fenton treatment apparatus. (Saltmiras and Lemley, 2002)

**Table II-D-2. Seven degradation products of Atrazine (Saltmiras and Lemley, 2002)**




**Figure II-D-4. Proposed degradation pathways for the AFT of atrazine (Saltmiras and Lemley, 2002).**

A proposed degradation pathway for atrazine during AFT is shown in Fig. II-D-4. It shows preferred pathways with bold arrows and minor pathways with broken arrows. Dealkylation is the preferred pathway, but dechlorination does take place during AFT. The terminal degradation product is ammeline. The detoxifying step of dechlorination during AFT is important for atrazine rinse water remediation. The presence of chlorine, a xenophore, often inhibits degradation pathways of microorganisms, and if AFT were to be used for a prebioremediation technique, chlorine removal is important for biodegradation (Alexander, 1994).

### **D-2- 2, 4-Dichlorophenoxyacetic acid (2, 4-D)**

The herbicide 2, 4-dichlorophenoxyacetic acid (2, 4-D) is a herbicide widely used in the world to control broadleaf weeds in cereals and other crops. Persistence of 2, 4-D in soil is low because a wide range of soil microorganisms are capable of transforming the herbicide (Audus, 1949; Soulas, 1993; Getenga et al., 2004).

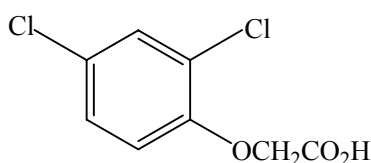


**Figure II-D-5 Chemical Structures of 2, 4-D**

Figure II-D-5 presents the Chemical Structures of 2, 4-D. 2, 4-D is an organic acid with pKa of 2.6 and high water solubility (45 g L<sup>-1</sup>). It presents a systemic mode of action and has been widely employed in wheat, rice, corn, sorghum and sugar cane cultures to control harmful wide-leaf weeds (Thill, 2003). Particularly in Brazil, this herbicide is extensively used in many crops (Prado and Airoidi, 2001). Because it is highly selective and systemic, this herbicide is transported through the plant, being accumulated in the growing roots, inhibiting the growth of weeds. 2, 4-D is classified by both ANVISA (Brazilian National Agency for Sanitarian Vigilance) and WHO (World Health Organization) as a hormonal herbicide of level II toxicity. It is considered as carcinogenic agent, affecting liver, heart and central nervous system, leading to convulsions (Maloney and Waxman, 1999; Garcia et al., 2006). This herbicide is usually commercialized as salt, amine and ester formulations, and has post-emergence action. After its application in field, the excess of the herbicide is easily transferred to the groundwater, due to its high solubility in water (600 mg L<sup>-1</sup> at 25°C). Even after a long period of disuse, considerable amounts of either 2, 4-D or its main product of degradation, 2,4-dichlorophenol (Amarante Junior et al., 2003),

might be found in surface waters, and groundwater as well.

Ester formulations of 2,4-D have persistence in soil similar to amine salt formulations because 2,4-D esters are rapidly converted to the acid or anionic form (Grover, 1973; Wilson et al., 1997). Microbial breakdown of 2, 4-D in soil begins with the removal of the carboxyl side chain (1-C position) or the either linkage (2-C position) (Foster and McKercher, 1973; Roberts et al., 1998), forming 2, 4-dichlorophenol (2, 4-DCP) and other phenolic metabolites that are further degraded by cleavage and oxidation of the phenyl ring (Smith and Aubin, 1991; Roberts et al., 1998). Complete mineralization of herbicides is desirable from an agri-environmental standpoint because the entire herbicide molecule is reduced to carbon dioxide and other inorganic compounds.

Since the herbicide 2, 4-D is one of the most widely applied agrochemicals, much effort has been put into investigations for its degradation by advanced oxidation processes (AOPs) which are based on the oxidation of pollutants by  $\cdot\text{OH}$ -radicals. For 2, 4-D removal mainly photocatalytical and photo-Fenton treatment as well as the combination of these methods with ozone have been applied (Sun and Pignatello, 1995; Modestov and Lev, 1998; Muller et al., 1998; Piera et al., 2000). 2, 4-Dichlorophenol (2, 4-DCP) was found as an intermediate product (Herrmann et al., 1998; Sun and Pignatello, 1993b). Figure II-D-6 presents the proposed pathway for the degradation of 2, 4-D by the  $\text{Fe(II)}/\text{UV}/\text{H}_2\text{O}_2$  method (Carla et al., 2006).

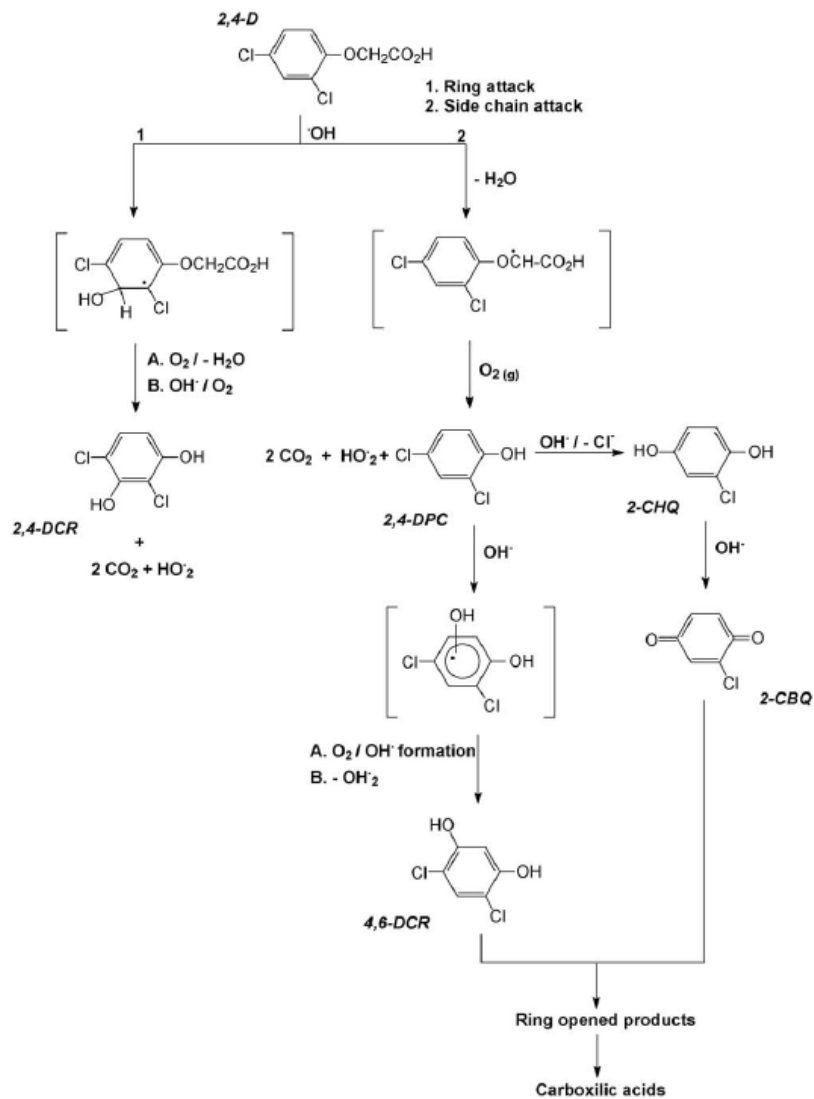


Figure II-D-6. Pathway for degradation of 2, 4-D by the Fe(II)/UV/H<sub>2</sub>O<sub>2</sub> (Carla et al., 2006)

### **III**

## **EXPERIMENTAL MATERIALS AND METHODS**



### **III-EXPERIMENTAL MATERIALS AND METHODS**

#### **A-REAGENTS**

Ferric perchlorate ( $\text{Fe}(\text{ClO}_4)_3 \cdot 9\text{H}_2\text{O}$ ), Fluka, > 97%.

S, S'-Ethylenediamine-N, N'-disuccinic acid Trisodium Salt Solution, (EDDS), 30% in water, Fluka

2, 4-dichlorophenoxyacetic acid, Sigma, > 99%.

2, 4-Dichlorophenol, Sigma, > 99%.

Pyruvic acid, Sigma, > 99%.

$\text{FeSO}_4 \cdot (\text{NH}_4)_2\text{SO}_4 \cdot 6\text{H}_2\text{O}$ , Aldrich, 99%.

3-(2-pyridyl)-5, 6-Diphenyl-1,2,4-triazin-4, 4'-disulfonate (ferrocine) Aldrich, 97%.

Ammonium acetate, Fisher Scientific, Analytical reagent grade.

8-Hydroxyquinoline-5-sulfonic acid hydrate (HQSA), Aldrich, > 98%.

Benzene, Shangai chemical reagent Co. LTD., > 99%.

Phenol, Shangai chemical reagent Co. LTD., > 99%.

Sodium hydroxide, Prolabo, > 97%.

Ammonium acetate, Aldrich, > 98%.

Potassium Ferrioxalate, synthesized in LPMM laboratory.

Sulfuric acid, Merck, made in EEC, > 95%.

Ferric chloride, Fluka, 99%.

Phosphoric acid, sigma-Aldrich, > 85%.

Acetic acid, Aldrich, > 99%.

Perchloric acid, Merck, > 97%.

1, 10-phenanthroline, Fluka, > 99%.

Potassium hydrogen phthalate, Nacalai tesque, Inc. KYOTO. Japan.

Sodium carbonate, Nacalai tesque, Inc. KYOTO, Japan.

Sodium hydrogen, Nacalai tesque, Inc. KYOTO, Japan.

Methanol, Carlo Erba Reagenti, HPLC grade.



Acetonitrile, Carlo Erba Reagenti, HPLC grade.

Ammonia (NH<sub>3</sub> aq solution 25%).

Isopropanol, Aldrich, > 99.5%

Goethite( $\alpha$ -FeOOH), synthesized in LPMM laboratory.

## **B-PREPARATION OF SOLUTIONS**

### **B-1-Preparation of stock solutions**

#### **(a) Fe(III) stock solution (2 mmol L<sup>-1</sup>)**

Great care was taken to prepare the solutions of Fe(III) in order to prevent evolution and/or precipitation of Fe(III). A certain quantity of Fe(ClO<sub>4</sub>)<sub>3</sub>·9H<sub>2</sub>O (0.2582 g) was diluted to 250 ml by adding an appropriate volume of Milli-Q water to get the desired concentration of Fe(III) and the pH value of the stock solution was adjusted to pH 2.0 by perchloric acid.

#### **(b) [S, S']-stereoisomer of ethylenediaminedisuccinic acid (EDDS) stock solution (2 mmol L<sup>-1</sup>)**

0.4776 g of EDDS was diluted to 200 ml by adding an appropriate volume of Milli-Q water to get the desired concentration of EDDS.

#### **(c) Pyruvic acid (Pyr) stock solution (2 mmol L<sup>-1</sup>)**

0.035 ml of Pyr was diluted to 250 ml by adding an appropriate volume of Milli-Q water to get the desired concentration of Pyr.

#### **(d) Ferric-EDDS complex stock solution (2 mmol L<sup>-1</sup>)**

1.194 g of EDDS and 0.5164 g of Fe(ClO<sub>4</sub>)<sub>3</sub>·9H<sub>2</sub>O were mixed and diluted to 500 ml by adding an appropriate volume of Milli-Q water to get the concentration

$$[\text{Fe(III)}]/[\text{EDDS}] = 2\text{mmol L}^{-1}/2\text{mmol L}^{-1}.$$

**(e) Fe (II) stock solution (0.45 mmol L<sup>-1</sup>)**

0.0882 g of  $\text{FeSO}_4 \cdot (\text{NH}_4)_2\text{SO}_4 \cdot 6\text{H}_2\text{O}$  was diluted to 500 ml by adding an appropriate volume of Milli-Q water to get the desired concentration of Fe (II).

**(f) 2, 4-dichlorophenoxyacetic acid (2, 4-D) stock solution (1 mmol L<sup>-1</sup>)**

0.05526 g of 2, 4-D was diluted to 250 ml by adding an appropriate volume of Milli-Q water to get the desired concentration of 2, 4-D.

**(g) Atrazine stock solution (30 mg L<sup>-1</sup>)**

0.03 g of atrazine was diluted to 1000 ml by adding an appropriate volume of Milli-Q water to get the desired concentration of atrazine.

**(h) Benzene stock solution (10 mmol L<sup>-1</sup>)**

Benzene was diluted to 1 L Milli-Q water. The solution was stirred with a magnetic bar to insure the complete dissolution of benzene.

**(i) Acetic sodium buffer**

The buffer of acetic sodium was prepared by mixing 600 mL of acetic sodium (1 N) and 360 mL of sulfuric acid (1 N) with end volume of 1 L by adding an appropriate volume of Milli-Q water.

**(j) Potassium ferrioxalate**

Potassium ferrioxalate used for actinometry was prepared from potassium oxalate and ferric chloride, according to the procedure proposed by Calvert and Pitts

(Calvert et al., 1966), and carefully stored in the dark.

**(k) 8-Hydroxyquinoline-5-sulfonic acid hydrate (HQSA) solution (0.1 mol. L<sup>-1</sup>)**

The HQSA solution was prepared by dissolution of HQSA (1.21 g) in 50 mL of NaOH (0.12 mol L<sup>-1</sup>). Great care was taken to wash the flask by HNO<sub>3</sub> to avoid that Fe adhered to the flask surface.

**(l) Hydroxylamine chlorhydrate**

Hydroxylamine chlorhydrate solution was prepared by mixing 104.25 g of Hydroxylamine chlorhydrate and 200 mL of hydrochloric acid (32%) with end volume of 500 mL by adding an appropriate volume of Milli-Q water.

**(m) Ammonium buffer**

192.7 g of ammonium acetate was diluted by adding 200ml of Milli-Q water. It was solution of ammonium acetate. Ammonium buffer was prepared by mixing ammonium acetate solution and 170mL of ammonia (25%) with the end volume of 500ml by adding an appropriate volume of Milli-Q water.

**(n) Ferrozine**

0.197 g of ferrozine was diluted to 20 ml by adding an appropriate volume of Milli-Q water. Solution was stock at 4 °C.

**B-2-Preparation of reaction solutions**

All the reaction solutions were all prepared with Milli-Q water. The pH values were adjusted with perchloric acid (1 N) and NaOH (1 N) by a JENWAY 3310 pH-meter to  $\pm 0.01$  pH unit.

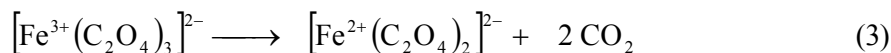
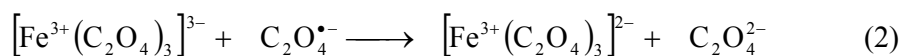
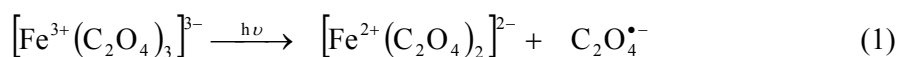
The suspension was dispersed by using an ultrasonic disperser for 20min. The particle size of the dispersed goethite was  $<2\ \mu\text{m}$ . After a shaking period, the goethite suspensions were centrifuged at 12000g for 20 min.

When necessary, reaction solutions were deaerated or oxygenated by purging with argon or oxygen before irradiation. The purging time depend on the solution volume: 20min for the big volume solutions (100 mL) and 10 min for the small volume solutions (5 mL).

## **C-IRRADIATION**

### **C-1-Ferrioxalate actinometry**

The light intensity  $I_0$  was measured by ferrioxalate potassium ( $\text{K}_3\text{Fe}(\text{C}_2\text{O}_4)_3$ ) actinometer (Calvert and Pitts, 1966). This method depend on the photochemical reactivity of  $\text{K}_3\text{Fe}(\text{C}_2\text{O}_4)_3$  in the acid solution. Under irradiation, Fe(III) was reduced to Fe(II) and oxalate ion was oxidized to  $\text{CO}_2$ . The reactions are as follows:



$\text{Fe}^{2+}$  can form stable red complex with 1, 10-phenanthroline. Fe(II) concentrations were determined by complexometry using  $\varepsilon_{510} = 1.118 \times 10^4\ \text{mol}^{-1}\ \text{L}\ \text{cm}^{-1}$  for the complex of Fe(II) with o-phenanthroline. The principle of this assay is the following: after irradiation of a volume ( $V_1$ ) of ferrioxalate potassium solution ( $0.006\ \text{mol}\ \text{L}^{-1}$ ) for a time  $t$  (expressed in seconds), we added at 2 mL ( $V_2$ ) of this irradiated solution, 1 mL of acetate buffer, and 0.5 mL of 1, 10-phenanthroline (0.1%

by mass). The solution is then filled with pure water up to 5 mL ( $V_3$ ). After agitation, the solutions were kept in the dark for 1h and then the UV-vis measurement was carried out at 510nm in a cell with an optical path equal to  $\ell$ .

The number of Fe(II) formed during the photo reaction was calculated with the following formula:

$$n_{Fe^{2+}} = \frac{6.023 \cdot 10^{20} \cdot V_1 \cdot V_3 \cdot \log(I_0 / I_T)}{V_2 \cdot l_{510} \cdot \epsilon_{510}} = \frac{6.023 \cdot 10^{20} \cdot V_1 \cdot V_3 \cdot OD_{510}}{V_2 \cdot l_{510} \cdot \epsilon_{510}}$$

With  $OD_{510} = (OD_{\text{solution}} - OD_{\text{blank}})_{510}$ , the value of the absorbance at 510 nm of the blank is obtained with the same solution of potassium ferrioxalate, but not irradiated and prepared as before.

The number of  $Fe^{2+}$  formed is proportional to the fraction of absorbed light by the solution during this time  $t$ . Then the intensity emitted by the system, in photons per second for the volume  $V_1$ , is equal to:

$$I_0 = \frac{n_{Fe^{2+}}}{\phi_{Fe^{2+}} \cdot t \cdot (1 - 10^{-OD})} \text{ photons s}^{-1}$$

$(1 - 10^{-OD})$  is the percentage of photons absorbed by the solution at the wavelength of irradiation at time  $t = 0$ .

Then:

$$I_0 = \frac{6.023 \cdot 10^{20} \cdot V_1 \cdot V_3 \cdot OD_{510}}{V_2 \cdot l_{510} \cdot \epsilon_{510} \cdot \phi_{Fe^{2+}} \cdot t \cdot (1 - 10^{-OD})} \text{ photons s}^{-1} V_1 \text{ mL}$$

These photonic flows were expressed in photons  $s^{-1} \text{ cm}^{-2}$ , because with parallel beam,  $V_1$  can be assimilated to the length of the optical path of the cell  $\ell$  irr; these flows were monitored throughout this work.

So,

$$I_0 = \frac{6.023 \cdot 10^{20} \cdot V_3 \cdot l_{irr} \cdot DO_{510}}{V_2 \cdot l_{510} \cdot \epsilon_{510} \cdot \phi_{Fe^{2+}} \cdot t \cdot (1 - 10^{-DO})} \quad \text{photons s}^{-1} \text{ cm}^{-2}$$

### **C-2-Irradiation with monochromator**

For the determination of quantum yields, solutions were irradiated in monochromatic parallel beam in 1 cm (path length) quartz cell or 2 cm (path length) cylindrical quartz cell. The light source was a high-pressure mercury lamp Osram HBO 200W equipped with a monochromator Bausch and Lomb or Jobin Yvon. Figure III-C-1 gives a picture of the monochromatic irradiation device. The monochromatic irradiations were carried out separately at wavelength 365, 334, 313 and 296 nm. The light intensity was measured by ferrioxalate actinometry (Calvert and Pitts, 1966). The photon flux of the monochromatic irradiation at different wavelength is listed in Table III-C-1. When necessary, solutions were deaerated or oxygenated by bubbling with argon or oxygen for 10 min before irradiation.

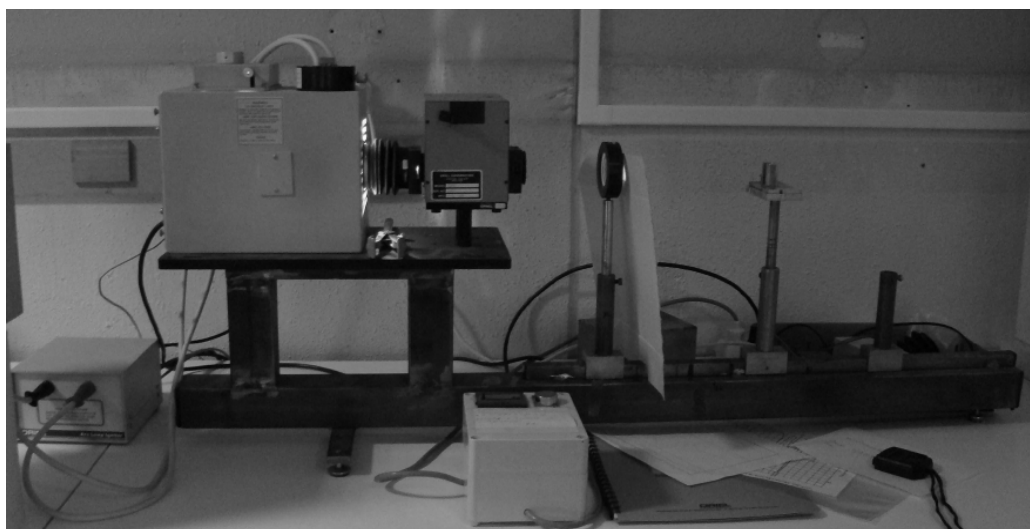


**Figure III-C-1 Monochromatic irradiation device**

**Table III-C-1. The photonic flux at 365, 334, 313 and 296 nm**

$\lambda_{irr}(nm)$	365	334	313	296
$I_0 (10^{14} \text{ photons} \cdot \text{s}^{-1} \cdot \text{cm}^{-2})$	4.47	3.15	5.41	1.42

All the quantum yield calculations depend on the following formulas (1), (2), (3) and (4):

$$\Phi = \frac{\Delta C \cdot 6.023 \cdot 10^{20} \cdot l}{I_a \cdot \Delta t} \quad (1)$$

$$\frac{I_a}{I_0} = 1 - 10^{-DO_{\lambda_{irr}}} \quad (2)$$

Where  $(1 - 10^{-DO_{\lambda_{irr}}})$  represents the percentage of the light absorption by the solution when  $t = 0$ ,  $I_0$  is the number of the photons entering the reaction cell per second determined by actinometry and  $l$  is the length of irradiation cell in cm.

So we can get formula (3).

$$\Phi = \frac{\Delta C \cdot 6.023 \cdot 10^{20} \cdot l}{I_0 \cdot \Delta t \cdot (1 - 10^{-DO_{\lambda_{irr}}})} \quad (3)$$

For the organic pollutants 2, 4-D and atrazine used in the thesis, the quantum yield can be calculated by the change of their concentrations ( $\Delta C$ ) using formula (3). For the calculation of Fe(II) generation quantum yield, we can use formula (4),  $\Delta DO_{510nm}/\varepsilon_{510nm}$  also represents the change of the Fe(II) concentration during the irradiation.

$$\Phi = \frac{\Delta OD \cdot 6.023 \cdot 10^{20} \cdot \ell}{\varepsilon \cdot L \cdot I_0 \cdot (1 - 10^{-OD_{\lambda_{irr}}}) \cdot t} \quad (4)$$

L is the length of the cell used for the measurement of the optical density (OD).

### **C-3-Irradiation at 365nm**

The irradiation experiments were performed in a home-made photoreactor placed in a cylindrical stainless steel container. The reaction device consists of four tubes (Philips TLD 15W / 05), whose emission spectrum is from 300nm to 450nm with a maximum irradiation at 365 nm (Figure III-C-2). These four tubes were separately placed in the four different axes, while the photoreactor, a water-jacketed Pyrex tube of 2.8 cm diameter, was placed in the center of the setup (Figure III-C-3). The solution (usually 100 mL) was continuously magnetically stirred with a magnetic bar during irradiation to insure its homogeneity. Control experiments showed that no degradation of 2, 4-D or atrazine occurred in Fe(III) or Fe(III)-Carboxylate complexes without irradiation in this photoreactor.

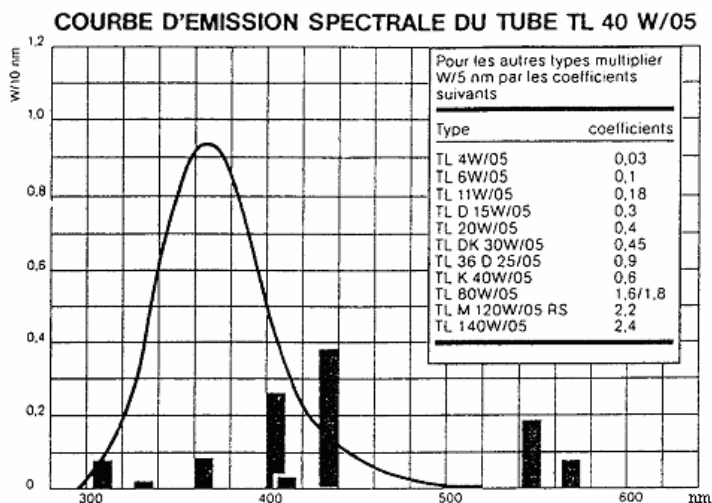


**Figure III-C-2. Emission spectra of tube Philips, TLD 15W/05.**



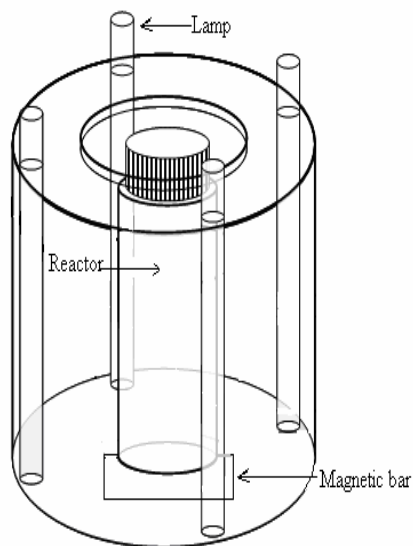


**Figure III-C-3 Home-made photoreactor with four tubes (Philips TLD 15W / 05)**

## **D-ANALYSIS METHODS**

### **D-1-Spectroscopy methods**

#### **UV-vis Spectrophotometer**

The UV–visible spectra of the solutions were recorded on a Cary 300 double beam spectrophotometer.

#### **D-2-Chromatography methods**

HPLC was used for products analysis:

A Waters chromatograph equipped with two pumps Waters 510, an auto-sampler 717 and a Waters 996 photodiode array detector.

Two HPLC columns were used in the work:

- a. Merck C-18 column (150 mm × 2.1 mm × 5 μm).

- b. An Agilent ZORBAX Eclipse XDB-C8 (reverse phase) of 4.6 mm (ID)  $\times$  150 mm (length) with a particle diameter of 5  $\mu\text{m}$ .

The mobile phases used in the research are the following:

a. To analyze 2, 4-D and its photoproducts (2,4-DCP), a mixture of Ammonium acetate (20 mmol  $\text{L}^{-1}$ ) and methanol (40/60, v/v) was used as mobile phase and the flow rate was 1.0  $\text{mL min}^{-1}$ . The detection wavelength was at 284 nm.

b. To analyze atrazine and its photoproducts, a mixture of acetonitrile/water mixture (50/50, v/v) was used as mobile phase and the flow rate was 1.0  $\text{mL min}^{-1}$ . The detection wavelength at 240 nm.

c. The formation of phenol from benzene was monitored at 270 nm and the eluent was acetonitrile/water mixture (30/70, v/v) at a flow rate of 1.0  $\text{mL min}^{-1}$ .

### **D-3-Dosage methods**

#### **Fe(II)**

Under irradiation, Fe(II) is formed in aqueous solutions in the presence of Fe(III). The concentration of Fe(II) was determined by complexometry with 1, 10-phenanthroline taking  $\epsilon_{510\text{ nm}} = 1.118 \times 10^4 \text{ L mol}^{-1} \text{ cm}^{-1}$  (Calvert and Pitts, 1966).

A certain quantity of  $\text{Fe}(\text{NH}_4)_2\text{SO}_4$  solution was used as Fe(II) sources to make a calibration curve (as shown in Figure III-D-4). The molar absorption coefficient was  $11450 \text{ L mol}^{-1} \text{ cm}^{-1}$ , which is nearly the same as the reference value  $\epsilon_{510\text{ nm}} = 11180 \text{ L mol}^{-1} \text{ cm}^{-1}$ . By means of the calibration curve, it was carefully checked that no interference in the analysis was observed when 2, 4-D or atrazine was present in the solution.

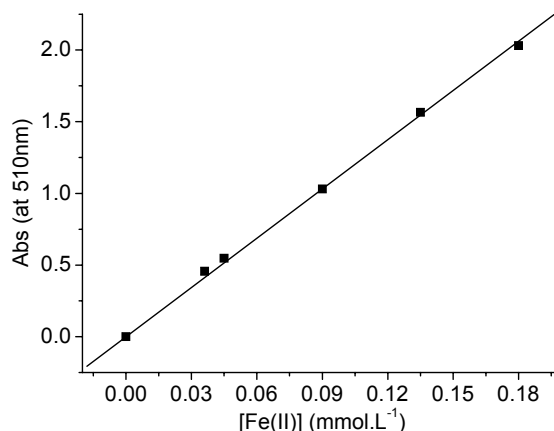


**Figure III-D-4. Calibration curve of Fe(II) concentration**

### $Fe(OH)^{2+}$

The concentration of the most photoactive species,  $[Fe(OH)^{2+}]$ , was determined by using 8-hydroxyquinoline-5-sulfonic acid (HQSA) (Faust et al., 1990). The absorbance of the tris complex  $Fe(HQSA)_3$  was measured at  $\lambda = 572$  nm ( $\epsilon = 5000$  mol<sup>-1</sup> .L .cm<sup>-1</sup>). The molar fraction of  $Fe(OH)^{2+}$  ( $x_{Fe(OH)^{2+}}$ ) was expressed as the ratio of  $[Fe(OH)^{2+}]$  to total Fe in solution.

$$\%Fe(OH)^{2+} = \frac{[Fe(OH)^{2+}]}{[Fe]_{total}}$$

### Total iron

Total iron was determined using ferrocene by the reaction of complexometry method described by Stookey (1970). Ferrocene is a disodium salt of 3-(2-pyridyl)-5, 6-diphenyl-1,2,4-triazin-4,4'-disulfonate. This compound reacts with divalent iron to form stable magenta complex species which is very soluble in water and may be used for the direct determination of iron in water. The visible absorption spectrum of the ferrous complex of ferrocene exhibits a single peak with maximum absorbance at 562 nm (figure III-D-5). Figure III-D-6 shows the Calibration curves of total iron.

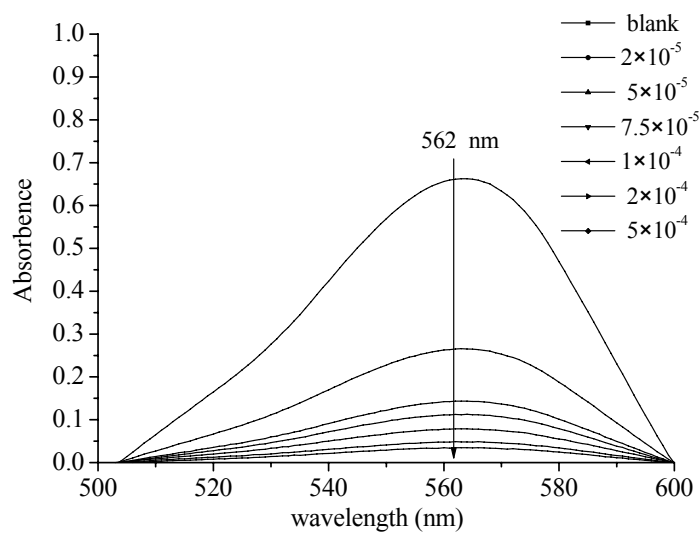


**Figure III-D-5 visible absorption spectrum of the ferrous complex of ferrozine**

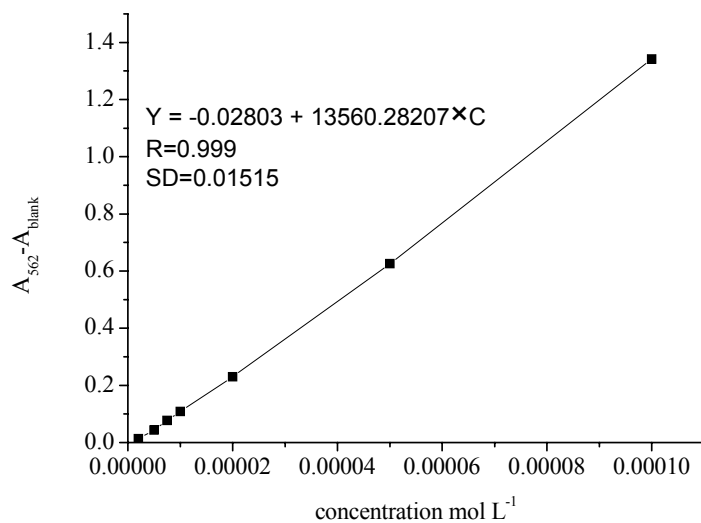
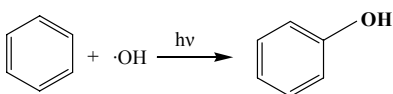


**Figure III-D-6 Calibration curves of total iron**

The molar absorption coefficient was  $13560 \text{ L mol}^{-1} \text{ cm}^{-1}$ .

### Hydroxyl radicals



Scavenging of  $\bullet\text{OH}$  by high concentrations of benzene has been used to determine the yield  $\bullet\text{OH}$  radicals formation. Aromatic hydroxylation is one of the typical reactions of  $\bullet\text{OH}$  and is used for detection of  $\bullet\text{OH}$  in the case of Fenton reaction and of the photolysis of aqueous of  $\text{HNO}_2$ ,  $\text{NO}_3^-$  and  $\text{NO}_2^-$  (Arakaki et al., 1999). Benzene is very unreactive toward  $\text{O}_2(^1\Delta_g)$  (Zepp et al., 1987). The hydroxylation of benzene by  $\bullet\text{OH}$  to produce phenol is a fairly selective process. Given the high reactivity of benzene with  $\bullet\text{OH}$  ( $k \approx 8 \times 10^9 \text{ L.mol}^{-1}.\text{s}^{-1}$ ) (Kochany and Bolton, 1992; Pan and Schuchmann, 1993) and under the conditions of these experiments, virtually all of the  $\bullet\text{OH}$  should have been scavenged by benzene. The destruction rate of phenol by direct photolysis and by peroxy radicals,  $\text{O}_2(^1\Delta_g)$  and other oxidants is expected to be slow by comparison to the rate of phenol formation from the  $\bullet\text{OH}$  through the oxidation of benzene (Liu et al., 2004).

It was thought that  $\bullet\text{OH}$ -mediated oxidation of benzene forms phenol with a nearly 100% yield (Faust and Allen, 1993; Joseph et al., 2001; Wang et al., 2006), and thus the concentrations of photochemically formed hydroxyl radicals were determined as equation (a), where,  $C_{\text{Phenol}}$  is the concentration of phenol at time t.

$$C_{\bullet\text{OH}} = C_{\text{Phenol}} \quad (\text{a})$$

#### **D-4-Molar ratio method**



M represents the metal ion; L represents the acid ions (ligand).

The method is based on the spectrophotometric measurements. We keep constant the concentration of metal ions in aqueous solution and the concentration of the relative acid is increased in the experiment. The absorbance of the aqueous solution increase with the increase of the acid concentration until it becomes stable, which

indicate that the metal ions are totally complexed by the acids.

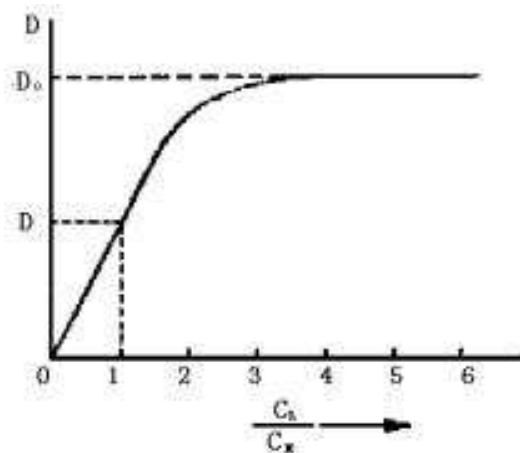


**Figure III-D-7. Measurements of the absorbance as a function of the composition of the complex  $n=C_L/C_M$**

As shown in Figure III-D-7, the absorbance of the aqueous solutions was set as  $Y$  axis, the corresponding ratio of  $C_L / C_M$  was set as  $X$  axis. Then the ratio of  $C_L / C_M$  represents the composition of the complexes. The stoichiometry of the complex corresponds to the ratio ( $C_L / C_M$ ) where the absorbance starts to be stable; no more increase is measured with the supplementary addition of acids.



## **RESULTS AND DISCUSSION**





## **IV-study on photoactivity of Fe(III)-EDDS complex**

### **IV-A-physicochemical property of Fe(III)-EDDS complex**

#### **A-1-Properties of Fe(III) solutions**

The absorption spectrum of an aqueous solution with  $0.3 \text{ mmol L}^{-1} \text{ Fe}(\text{ClO}_4)_3$  as a function of time after preparation is shown in Figure IV-A-1. Freshly prepared solutions presents a maximum absorption at about 297 nm characteristic of the monohydroxy complex  $[\text{Fe}(\text{OH})(\text{H}_2\text{O})_5]^{2+}$ . Upon standing in the dark, the absorption spectrum gradually increased in intensity and shifted to longer wavelengths; this can be rationalized by assuming a gradual and irreversible conversion of monomeric iron species to oligomeric ones (Flynn, 1984).

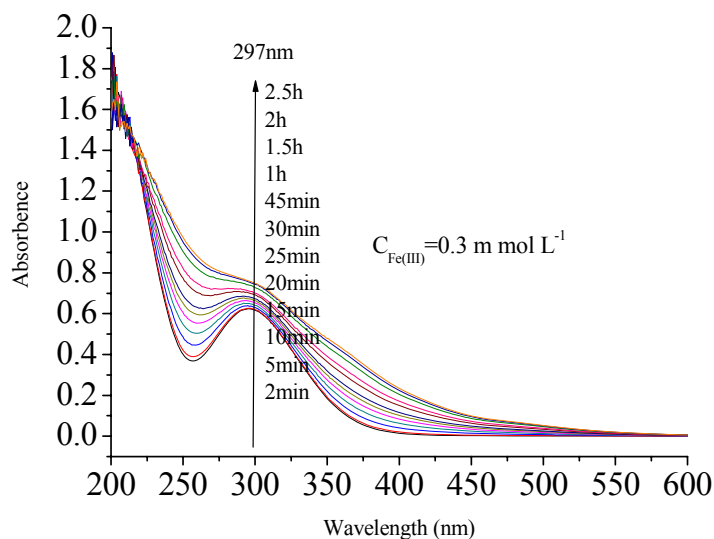


**Figure IV-A-1 UV-Visible absorption spectra of an aqueous solution with  $0.3 \text{ mmol L}^{-1}$  of  $\text{Fe(III)}$  (different time after the preparation)**

Since pH value plays an important role on the distribution of  $\text{Fe(III)}$  species in the

aqueous solutions, experiments to control this important effect were carried out in the previous works (Wang, 2008). The pH values of the aqueous solutions with 0.3 mmol L<sup>-1</sup> of Fe(ClO<sub>4</sub>)<sub>3</sub> were adjusted to 1.5, 2.5, 3.15, 4.3, 5.4, 6.8, 7.6 and 8.5. Figure IV-A-2 presents the variation of the UV-visible spectra as function of the pH value. Fe(OH)<sup>2+</sup> was the predominant species when pH value ranged from 2.5 to 4.0. While at pH below 2.0, [Fe(H<sub>2</sub>O)<sub>6</sub>]<sup>3+</sup> become the major species. From pH 5.0 to 6.0, Fe(OH)<sub>2</sub><sup>+</sup> gradually become the major species but this species rapidly disappears with time. When pH is over 7.0, Fe(OH)<sub>3</sub> is formed in the aqueous solutions and precipitate.

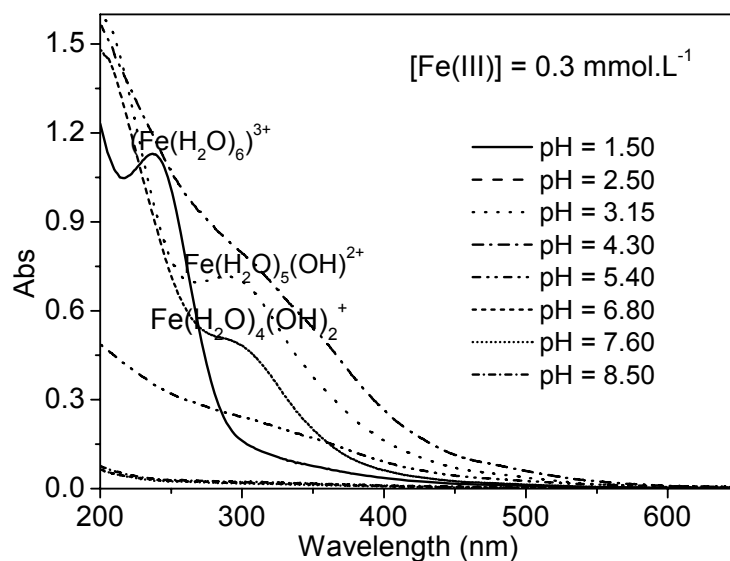
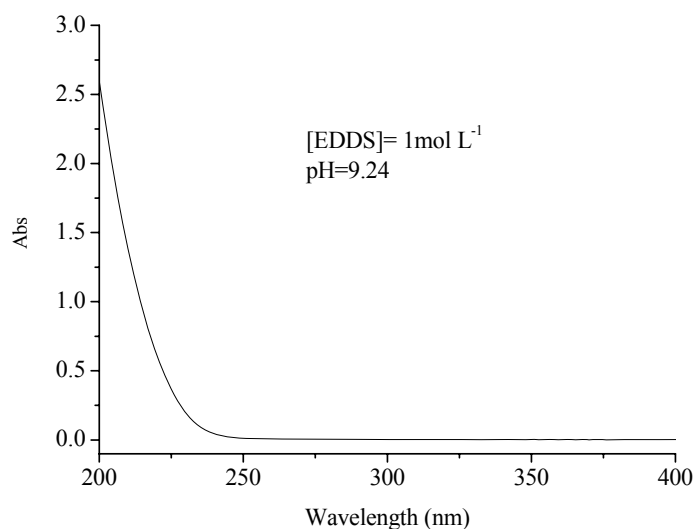


Figure IV-A-2 pH effect on the distribution of Fe(III) species in aqueous solutions(Wang, 2008).

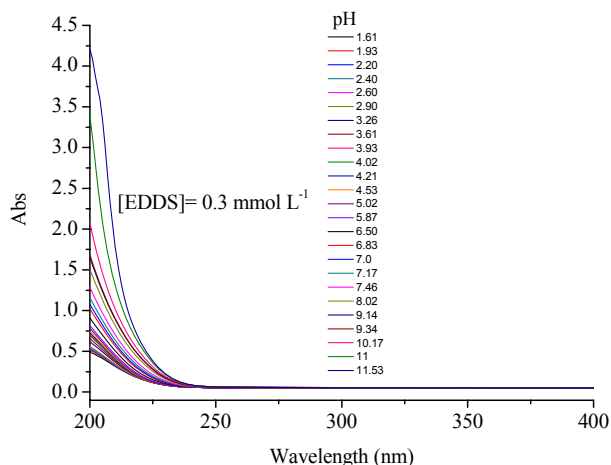
### A-2-Property of the EDDS

Carboxylic acids are important components of the Fe complexes in natural environment. Many references have reported the physical and chemical properties of Fe(III)-Carboxylate complexes, such as Fe(III)-EDTA, Fe(III)-Citrate, Fe(III)-oxalate, Fe(III)-NTA (NTA = nitrilotriacetic acid) and Fe(III)-pyruvate complexes. However,

little bibliography reports about the Fe-EDDS complex. EDDS is one kind of important carboxylic acids. EDDS can be made from ethylene diamine and maleic anhydride (Ramsey-Downey and Kerzerian, 1963). This route yields a mixture of stereoisomers consisting of 25%[S, S], 50%[R, S]/[S, R], and 25%[R, R]-form. Alternatively, single stereoisomers of EDDS can be prepared using 1, 2-dibromoethane and a selected form of aspartic acid, i.e. [S, S]-EDDS from 1-aspartic acid, [R, R]-EDDS from d-aspartic acid (Neal and Rose, 1968). S, S'-ethylenediaminedisuccinic acid (EDDS) is a biodegradable chelating agent that is a structural isomer of EDTA. Biodegradation work was done on the most degradable form, i.e. [S, S]-EDDS, in a variety of environmental compartments. Interestingly, the [S, S]-isomer of EDDS was also reported to be produced naturally by a number of microorganisms (Nishikiori et al., 1984), such as *Amycolatopsis japonicum* sp. nov. (Goodfellow et al., 1997). So, it is necessary to study the basic properties of S, S'-EDDS used in this work before studying the physical properties of carboxylate complex. Figure IV-A-3 presents the UV-visible spectra of EDDS.



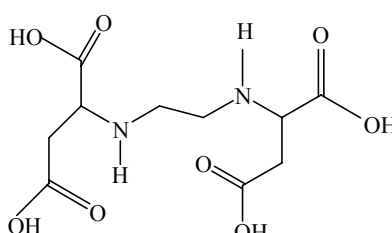
**Figure IV-A-3 the UV-visible spectra of EDDS ([EDDS]=1 mol L<sup>-1</sup>).**



**Figure IV-A-4 UV-Visible absorption spectra of EDDS as function of pH. ([EDDS] = 0.3 mmol L<sup>-1</sup>)**

Experiments were performed under different pH values. pH values of EDDS ([EDDS] = 0.3 mmol L<sup>-1</sup>) solutions ranged from 1.6 to 11.5. Figure IV-A-4 presents the UV-Visible absorption spectra of EDDS as function of pH. Results show that the absorbance increases between 200 nm and 240 nm when the pH increases. This effect was accelerated from pH higher than 7.0. Table IV-A-1 lists the EDDS base dissociation constants of EDDS in the form of pKa, which is the negative of the logarithm of the acid dissociation constant Ka (Vandevivere et al., 2001).

**Table IV-A-1. Molecular structures and acidity constants of ethylenediamine-disuccinic acid (EDDS) (25 °C, 0.1 M KNO<sub>3</sub>). (Vandevivere et al., 2001)**

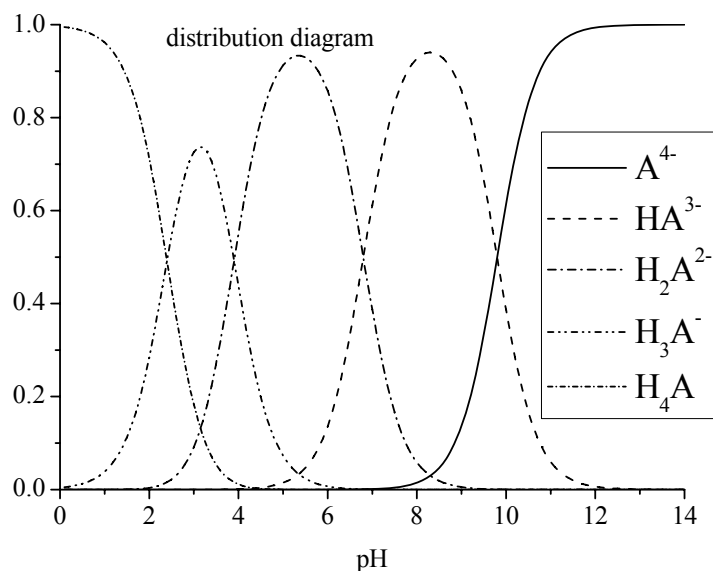
EDDS molecular formula	pKa	
	pK <sub>1</sub>	2.1
	pK <sub>2</sub>	3.0
	pK <sub>3</sub>	6.4
	pK <sub>4</sub>	10.4

Consequently, EDDS equilibrium for the solutions is described here, Eq. (1) - (4).

For simplification, EDDS molecules will not be included in the chemical formulae. EDDS molecules were substituted by  $\text{H}_4\text{A}$ .



Figure IV-A-5 was the distribution diagram of the EDDS in the aqueous solutions as a function of pH values range from 0 to 14. And the distribution diagram was calculated with equilibrium constants from (Vandevivere et al., 2001), 25 °C.  $[\text{H}_2\text{A}^{2-}]$  was the dominant species in EDDS aqueous solutions between pH 5.3 and 6.8.

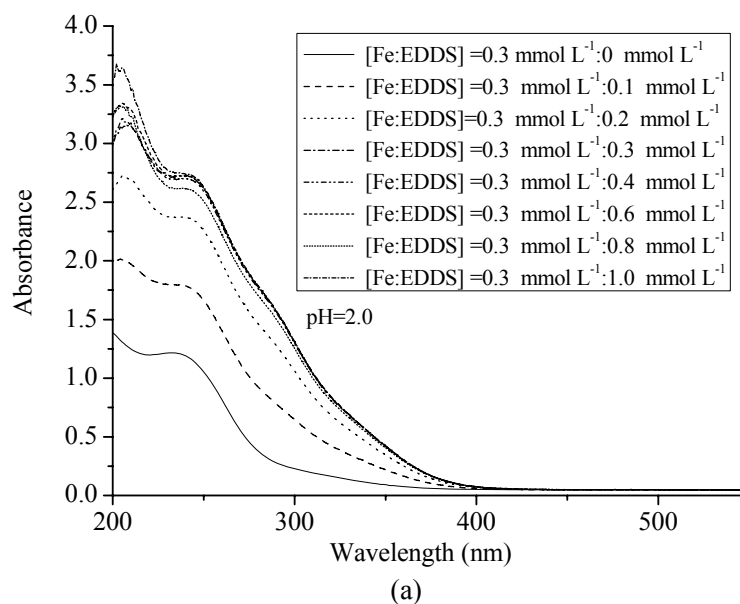


**Figures IV-A-5. the distribution diagram of EDDS aqueous solution as a function of pH values range from 0 to 14, calculated with equilibrium constants from (Vandevivere et al., 2001), 25 °C.**

### **A-3-Study of the stoichiometric composition of Fe(III) in complexes with EDDS**

Measurements of the composition of complexes formed by Fe(III) and carboxylic acids were carried out using molar ratio method mentioned in part II experimental methods.

The stoichiometric composition of Fe(III)-EDDS complex was studied by the molar ratio method. The concentration of Fe(III) was kept constant at  $0.3 \text{ mmol L}^{-1}$ . Then the concentration of EDDS was increased from 0 to  $1.0 \text{ mmol L}^{-1}$ . In order to prevent evolution and/or precipitation of Fe(III) ions, the iron aqueous solutions pH was fixed at pH 2.0. Figure IV-A-6 presents the UV-Visible absorption spectra of mixtures of EDDS and Fe(III) in aqueous solutions and the evolution of the absorbance at 340 nm as a function of the EDDS concentration.



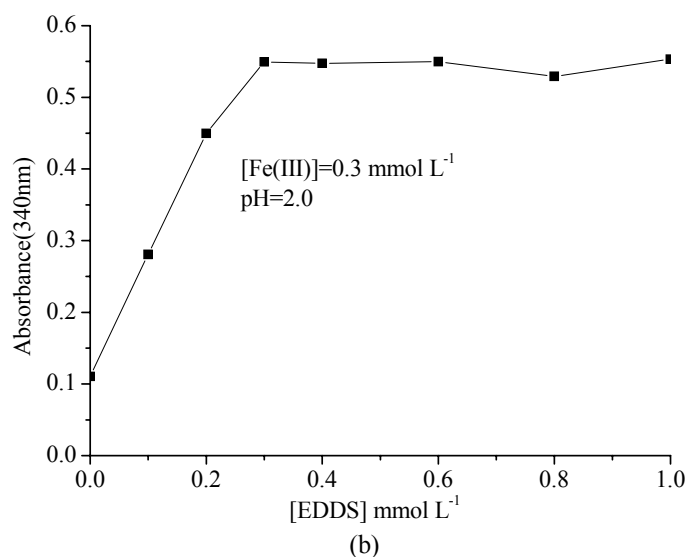


**Figure IV-A-6. (a) the UV-Visible absorption spectra of mixtures of EDDS and Fe(III) in aqueous solutions; (b) the evolution of the absorbance at 340 nm as a function of the EDDS concentration.**

340 nm was chosen as the characteristic absorbance of the Fe(III)-EDDS complex: the organic moiety no longer absorbs at that wavelength and the absorbance of Fe(III) aquacomplexes is far lower at pH = 2.0. The absorbance at 340 nm increased with the increase of the EDDS concentration. However, the absorbance became stable when the concentration of EDDS reached around 0.3 mmol L<sup>-1</sup>. This observation indicated that Fe(III) was totally complexed by EDDS. It can be concluded that the stoichiometric ratios of Fe(III)-EDDS complex is 1:1.

#### **A-4-Property of Fe(III)-EDDS complex**

Fe(III)-EDDS complexes and Fe(III)-pyruvate complexes were used in this work. So it is necessary to know the basic properties, such as their stabilities with the time at room temperature and with the variation of the pH. But the property of Fe(III)-EDDS complex was integrated studied in the previous works, experiments was carried out to study the property of Fe(III)-EDDS complex in this thesis.



#### **A-4-1 Stability of Fe(III)-EDDS complex**

In order to study the stability of the Fe-EDDS complex, the stock solutions with  $2 \text{ mmol L}^{-1}$  Fe(III) and  $2 \text{ mmol L}^{-1}$  EDDS was kept in the dark place and at room temperature at least 10 days. Equilibrium was reached within 24 hours for all solutions in which precipitation did not occur. Figure IV-A-7 presents the UV-Visible absorption spectra of the solutions. The results show that Fe-EDDS complex is stable in our conditions. The stock solutions were kept at  $4^\circ\text{C}$ . The stability of solutions used for the irradiation experiments with low concentration  $\text{Fe(III)/EDDS} = 0.3 \text{ mmol L}^{-1}/0.3 \text{ mmol L}^{-1}$  was also measured in 2 days. As shown in Figure IV-A-8, it presents the same stability as the stock solution within two days.

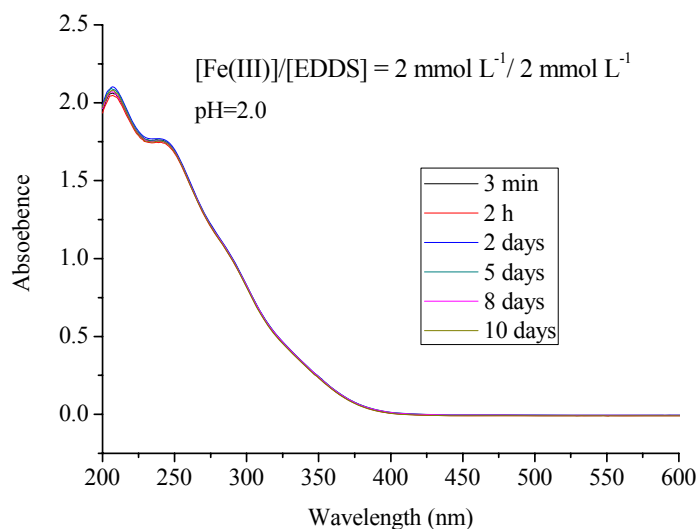


**Figure IV-A-7 Stability of the Fe(III)-EDDS complexes ( $[\text{Fe(III)}/\text{EDDS}] = 2 \text{ mmol L}^{-1}/2 \text{ mmol L}^{-1}$ ) as a function of time, in the dark and at room temperature.**

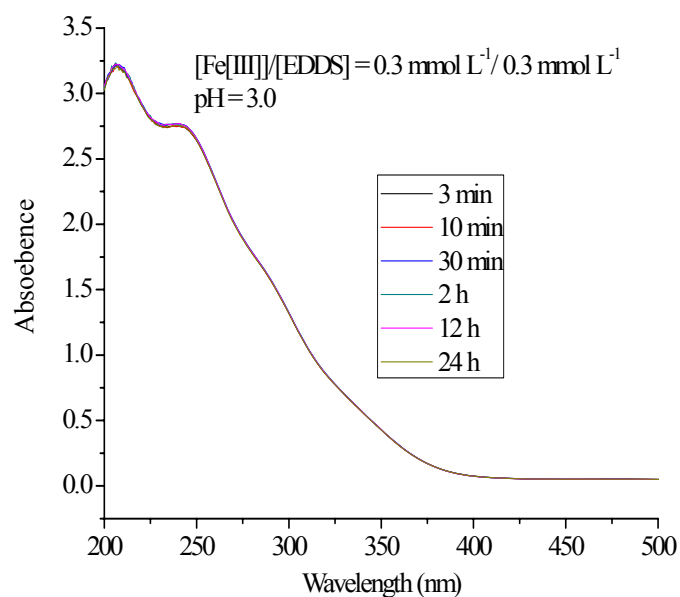


**Figure IV-A-8 Stability of the Fe(III)-EDDS complex ( $[\text{Fe(III)}]/[\text{EDDS}] = 0.3 \text{ m mol L}^{-1}/0.3 \text{ m mol L}^{-1}$ ) as a function of time, in the dark and at room temperature**

#### **A-4-2 pH effect**

Since Fe(III) and EDDS can form stable complex with a 1:1 molar ratio, experiment was performed with the stock solution of the complex. Experiments were performed to study the pH effect on the stability of Fe(III)-EDDS complex. As shown in Figure IV-A-9, the UV-Visible absorption spectra of aqueous solutions with  $0.3 \text{ mmol L}^{-1}$  Fe(III) and  $0.3 \text{ mmol L}^{-1}$  EDDS change according to the modification of the pH value between 1.52 and 11.0. Figure IV-A-9 (b) shows the variation of the absorbance at 340 nm. Figure IV-A-9 (b) also indicated an inflexion point near pH 4.3, 7.08 and 10.

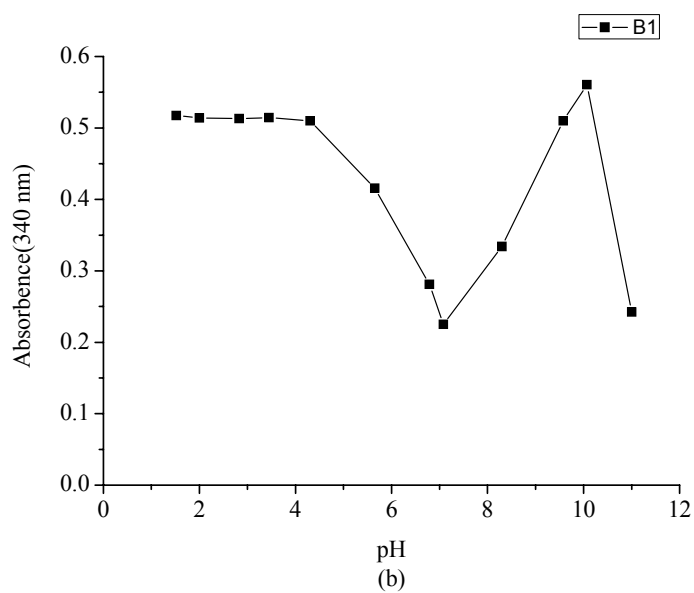
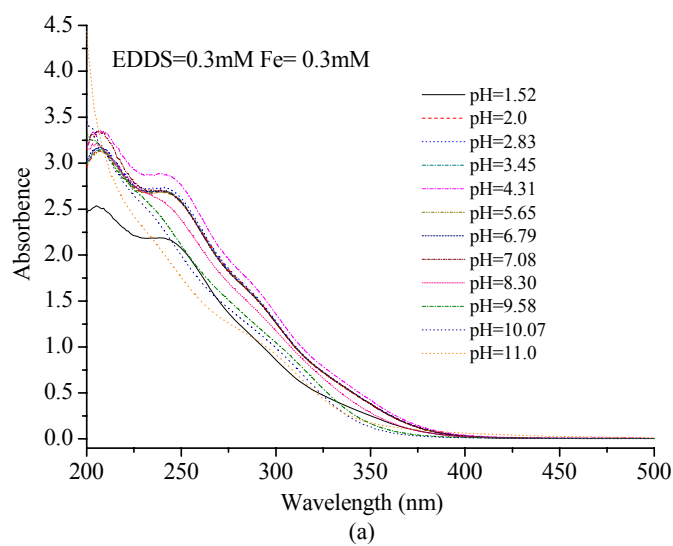


**Figure IV-A-9 UV-Visible absorption spectra of Fe-EDDS complex solution as function of pH.**

$$[\text{Fe(III)}]/[\text{EDDS}] = 0.3 \text{ mmol L}^{-1}/0.3 \text{ mmol L}^{-1}$$

**(a) UV-Visible spectra of Fe(III)-EDDS complex; (b) Absorbance at 340 nm**

### **A-4-3 Irradiation effect**

Photolysis of Fe (III)-EDDS complex ( $[\text{Fe(III)}]/[\text{EDDS}] = 0.1 \text{ mmol L}^{-1}/0.1 \text{ mmol L}^{-1}$ )

$L^{-1}$ ) was studied in the aqueous solution under irradiation. Results were shown in Figure IV-A-10. In 30 min of irradiation, the UV-Visible absorbance of the solution strongly decreased. These results indicated that under 365 nm, these complexes were easily photolyzed and it provided the possibility for the formation of excited state complexes and further generated many kinds of radicals. Further experiments have been carried out and this conclusion has been confirmed in the later part of the thesis.

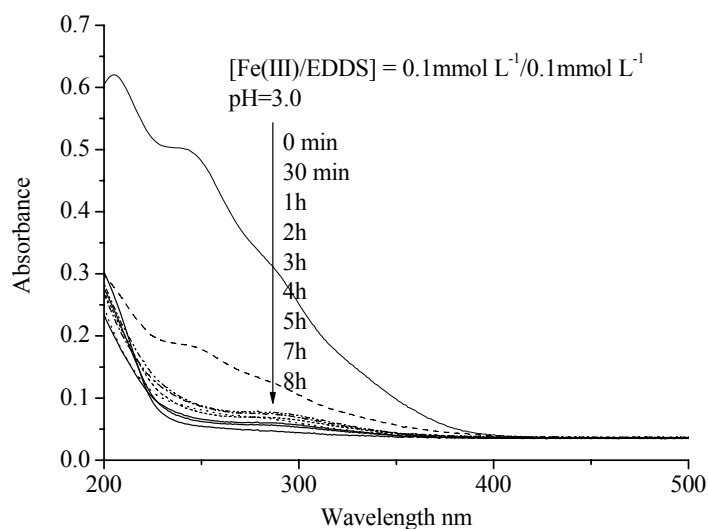


**Figure IV-A-10. Variation of UV-visible spectra of Fe(III)-EDDS complex ( $[Fe(III)/EDDS] = 0.1 \text{ mmol L}^{-1} / 0.1 \text{ mmol L}^{-1}$ ) under irradiation (365 nm)**

## **Conclusions**

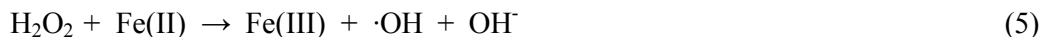
In our experimental conditions, we demonstrated that Fe(III) was complexed by EDDS with a ratio 1:1. We also checked the stability of Fe-EDDS complex in the dark and at room temperature. Fe(III)-EDDS is stable in the aqueous solutions in our experimental conditions ( $\text{pH} = 2.0$  and  $\text{pH} = 3.0$ ). Our results show that the pH is an important parameter for the stability of the complex and its speciation. At lower pH ( $< 2.0$ ) a phenomenon of decomplexation can be observed.

#### **IV-B-Determination of hydroxyl radicals from photolysis of Fe(III)-EDDS complex in aqueous solutions**

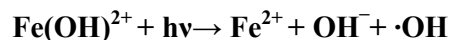
The presence of carboxylic acids, such as oxalate acid, citrate acid, pyruvic acid, and so on, has a significant effect on the speciation and the photoactivity of Fe(III) ions in acidic conditions. They can form stable complexes with Fe(III) ions. Free Fe(III) ions absorb weakly in the solar UV region (290 nm~400 nm), but the absorption spectra of hydrated or otherwise complex iron species (iron pairs) are shifted toward the visible, which might make their use in sunlight possible (Lente and Fábíán, 2001). In natural waters, photochemically induce electron transfer from the complexing organic ligand to Fe(III) in the excited of Fe(III)-org complexes can take place, and subsequently, the electron deficient Fe(III)-org complexes further reduce  $O_2$  to  $O_2^{\bullet-}$ .  $O_2^{\bullet-}$  rapidly reacts to yield the hydroxyl radicals (Zuo and Hoigné, 1992; Joseph et al., 2001; Zepp et al., 1987). In the previous works, photogeneration of hydroxyl radicals were in the aqueous solutions of Fe(III)-citrate, Fe(III)-pyruvate and so on. In this work, we studied the photogeneration of hydroxyl radicals in the aqueous solutions in the presence of Fe(III)-EDDS complex.

Photogeneration of  $\bullet OH$  by the photolysis of Fe(III)-EDDS complexes in aqueous solution has been determined using benzene ( $7 \text{ mmol L}^{-1}$ ) as a scavenger and the selected typical reaction was the formation of phenol from benzene. Due to the big difference of concentration between benzene and phenol formed, we can consider that  $\bullet OH$  radicals react mainly with the benzene. Through detecting the phenol formed in the reaction solution, we can quantify  $\bullet OH$  generated in the reaction. The mechanism of photoproduction of  $\bullet OH$  in the aqueous solutions containing Fe(III)-EDDS complexes can presumably be interpreted as the following reactions scheme: eq. (1)-eq. (5):





### **B-1-Generation of hydroxyl radicals in the irradiated aqueous solution containing Fe(III)-EDDS complex**



The concentration of the  $\cdot\text{OH}$  radicals production by the photolysis of the Fe(III)-EDDS complex was determined. As shown in Figure IV-B-1, under the condition of 8h irradiation and at pH 3.0, the concentration of  $\cdot\text{OH}$  generated in the system containing the Fe(III)-EDDS complex was  $42 \mu\text{mol L}^{-1}$ . The possible production of the hydroxyl radical in the thermal reaction was experimentally checked and no hydroxyl radicals were generated. The presence of oxygen in the aqueous solution was found to be an important factor for the  $\cdot\text{OH}$  production, because in anaerobic conditions, the experiments showed that no  $\cdot\text{OH}$  was generated (Figure IV-B-1).

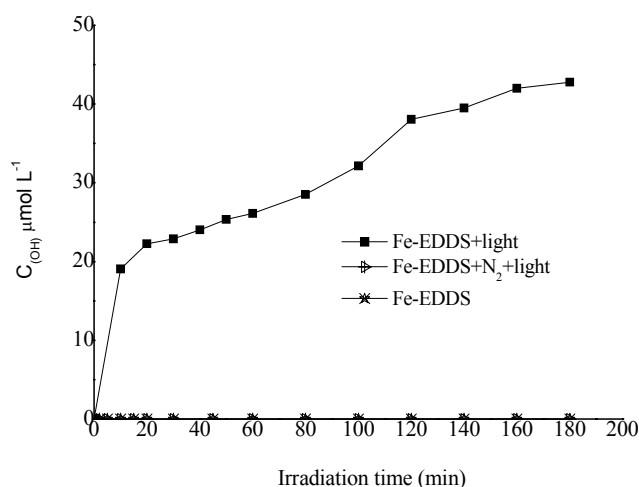


**Figure IV-B-1. Comparison of  $\cdot\text{OH}$  formation under different conditions for an aqueous**

solution with  $C_{\text{Fe(III)}} = 300 \mu\text{mol L}^{-1}$ ,  $C_{\text{EDDS}} = 300 \mu\text{mol L}^{-1}$ . Initial pH of the aqueous solution was 3.0.

### **B-2-Effect of pH on the generation of hydroxyl radicals in the irradiated aqueous solution containing Fe(III)-EDDS complex**

The experiments were performed in the homogeneous aqueous solutions at pH value of 3.0, 4.0, 5.0 and 6.0, which were provided by an addition of hydrochloric acid. An effect of pH on the  $\cdot\text{OH}$  yield was observed (Figure IV-B-2). The  $\cdot\text{OH}$  concentration at pH = 6.0 appeared to be higher than that at all other pH values in the range studied after 3h of irradiation. This is very interesting, because in the previous works with aquacomplexes of Fe(III), the  $\cdot\text{OH}$  concentration at pH = 3.0 appeared to be much higher than at pH 6.0. The same effect of pH on the production of  $\text{H}_2\text{O}_2$  upon the photolysis of different Fe(III)-carboxylate complexes was reported previously (Deng et al., 1998; Gao and Zepp, 1998; Wu et al., 2004).

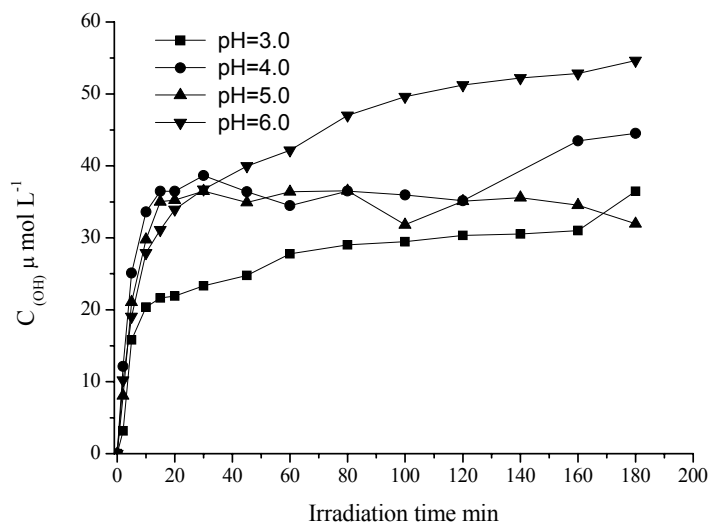


**Figure IV-B-2. Effect of the initial pH value on the total  $\cdot\text{OH}$  concentration for an aqueous solution with  $C_{\text{Fe(III)}} = 300 \mu\text{mol L}^{-1}$ ,  $C_{\text{EDDS}} = 300 \mu\text{mol L}^{-1}$ .**

We believe that the influence of pH on the photolysis of the Fe(III)-EDDS complex could be explained by two reasons. First, as we know, pH can influence Fenton reaction and the equilibrium between  $\text{HO}_2^\bullet/\text{O}_2^{\bullet-}$  and as a consequence the rate of  $^\bullet\text{OH}$  radical formation. Second, pH can also affect the distribution of different species (Fe(III) complexes) present in the solution. These species [(Fe(III)-EDDS,  $\text{Fe}(\text{OH})^{2+}$ ,  $\text{Fe}(\text{OH})_2^+$ ,  $\text{Fe}^{3+}_{\text{aq}}$ , EDDS] have different photochemical reactivity, and it would affect the  $^\bullet\text{OH}$  formation yield. This second reason is has probably a key role for the results of the  $^\bullet\text{OH}$  concentration at pH = 6.0 where the formation is higher. The species of the complex Fe(III)-EDDS present at pH 6.0 must be more reactive to photogenerated hydroxyl radicals.

### **B-3-Effect of Fe(III) and EDDS concentrations on the photogeneration of hydroxyl radicals in aqueous solution**

The concentration ratio Fe(III)/EDDS is another important factor. To evaluate this factor, experiments in solutions at pH = 3.0 were performed. Results are shown in Figure IV-B-3 and IV-B-4. It can be concluded that both the Fe(III) and EDDS concentrations affect the  $^\bullet\text{OH}$  formation yield. The  $^\bullet\text{OH}$  concentration increased with an increase of the EDDS concentration in the range from 100 to 300  $\mu\text{mol L}^{-1}$ . With an increase in the Fe(III) concentration in the range from 100 to 300  $\mu\text{mol L}^{-1}$ , the  $^\bullet\text{OH}$  concentration increased slowly and almost the same concentration of  $^\bullet\text{OH}$  photoproducted after 3h of irradiation is observed whatever the iron concentration (Figure IV-B-4). At a given pH value, a change in the Fe(III) / EDDS ratio can lead to a change in the relative content of different Fe(III)-EDDS complexes in the solution. When the EDDS concentration was much higher than that of Fe(III), the formation of  $^\bullet\text{OH}$  radical is higher. This phenomenon can be explain by the fact that EDDS is a complexing agent of Fe(III) and can strongly enhance the oxidation of Fe(II) into Fe(III) via the formation of Fe(III)-EDDS complex, which is a photoactive species for the generation of  $^\bullet\text{OH}$  radicals..



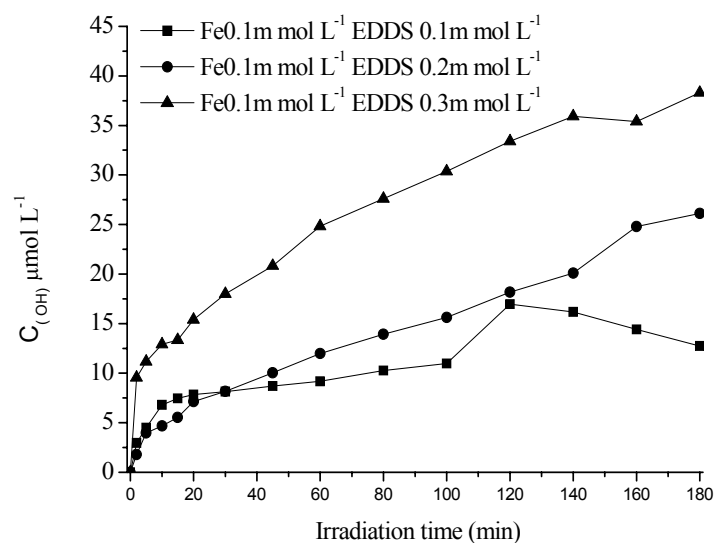


**Figure IV-B-3. Effect of the EDDS concentration on the  $\cdot\text{OH}$  formation under irradiation with  $C_{\text{Fe(III)}} = 100 \mu\text{mol L}^{-1}$  (Initial pH of the aqueous solution was 3.0).**

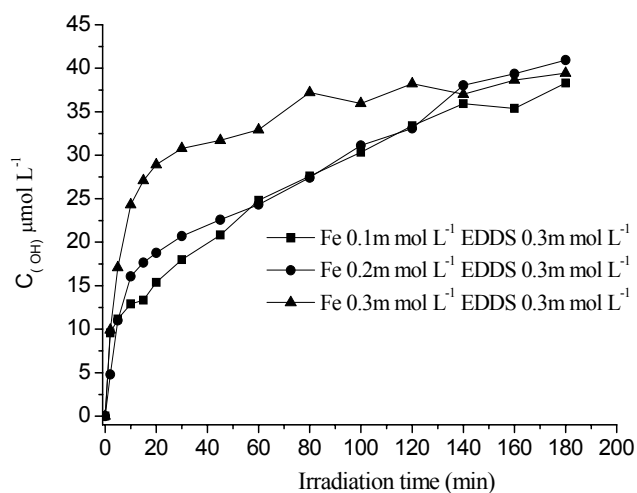


**Figure IV-B-4. Effect of the Fe(III) concentration on the  $\cdot\text{OH}$  formation under irradiation with  $C_{\text{EDDS}} = 300 \mu\text{mol L}^{-1}$ . (Initial pH of the aqueous solution was 3.0).**

## Conclusions

In the present study, formation of phenol from benzene was used to determine the concentration of  $\cdot\text{OH}$  radicals by the photolysis of Fe(III)-EDDS complex. Parameters, such as pH, concentration of Fe(III) or EDDS, oxygen were all considered in the study. Results show that the pH value has great effect on the photolysis of Fe(III)-EDDS complex in producing  $\cdot\text{OH}$ . Interestingly, the maximum concentration of  $\cdot\text{OH}$  radicals were observed at pH 6.0 (pH ranged from 3.0 to 6.0).

The  $\cdot\text{OH}$  concentration generated in the system increased also with the increase of Fe(III) or acid concentrations. The presence of high concentration of acid strongly favored the reoxidation of Fe(II) after the first photoredox process in the complex. This step (reoxidation of Fe(II)) is a limiting step in the photocatalytic process based on the couple Fe(III)/Fe(II) (Poulain et al., 2003).

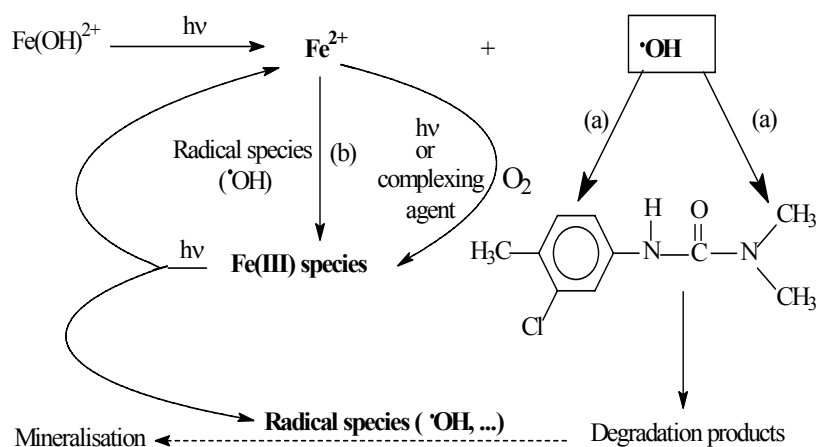


**Figure IV-B-5 Photochemical cycle Fe(III)/Fe(II) in the presence of organic pollutant (Poulain et al, 2003).**

But for the Fe(III)-EDDS complex, the speciation of the complex, depending on the pH, leads to different forms of the complex which possess different photochemical reactivity, and it would affect the  $\cdot\text{OH}$  formation yield. Oxygen is a crucial factor for

the formation of active radicals in aqueous solutions. Without oxygen no formation of  $\bullet\text{OH}$  radical is observed from the Fe-EDDS complex even under irradiation.

Results show that the concentration of  $\bullet\text{OH}$  in the solution containing Fe(III)-EDDS complex is higher than that of the system only containing Fe(III) ( $[\text{Fe(III)}] = 300 \mu\text{mol L}^{-1}$ ). It was confirmed that EDDS has positive effects on the photogeneration of  $\bullet\text{OH}$  in the aqueous solution. So, the Fe(III)-EDDS complex has the potential of utilizing sunlight as an irradiation source. Interestingly, the [S, S']-isomer of EDDS was reported to be produced naturally by a number of microorganisms, such as *Amycolatopsis japonicum* sp. nov. So in the natural surface waters, such as lakes, which contain Fe(III)/Fe(II) and [S, S']-EDDS, photochemical reactions can be induced by sunlight, and it will play an important role in the oxidation of organic/inorganic pollutants in natural waters. Further experimental and theoretical work is needed to fully understand the system and its application in natural aquatic or atmospheric environments.

## **V-Photodegradation of 2, 4-D photoinduced by the Fe(III)-EDDS complex and goethite-EDDS complex**

### **A-Photodegradation of 2, 4-D induced by the Fe(III)-EDDS complex**

2, 4-D was used as model compound in this work to study the photochemical properties of Fe(III)-EDDS complex. Experiments were carried out under monochromatic and polychromatic irradiation. Irradiation experiments were carried out separately under monochromatic irradiation for short times and under irradiation in the photoreactor (emission between 300 and 500 nm) for long times. Parameters such as wavelength of irradiation, complex concentration, pH, oxygen were all studied in the work.

#### **A-1-Properties of 2, 4-D in aqueous solution**

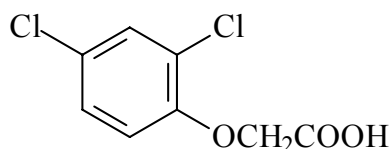


**Figure V-A-1 2 4-Dichlorophenoxyacetic acid (2, 4-D)**

Figure V-A-1 was the molecular formula of 2, 4-Dichlorophenoxyacetic acid (2, 4-D). The UV-visible spectrum of the solutions with different concentrations of 2, 4-D is presented in Figure V-A-2. It has two bands with maximum absorption at 230 nm and 284 nm. In this work, molar absorption at 284nm was only concerned. And the molar absorption coefficients is  $1870 \text{ L mol}^{-1} \text{ cm}^{-1}$  at 284 nm (Figure V-A-3).

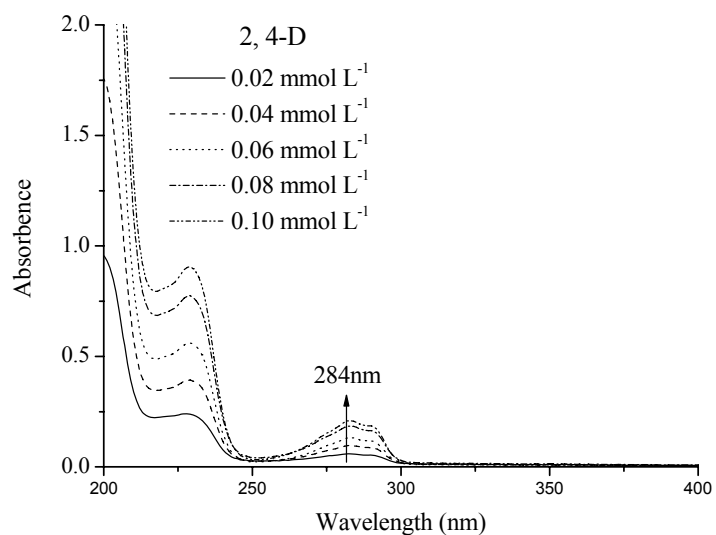


**Figure V-A-2 UV-visible spectra of 2, 4-D at different concentrations.**

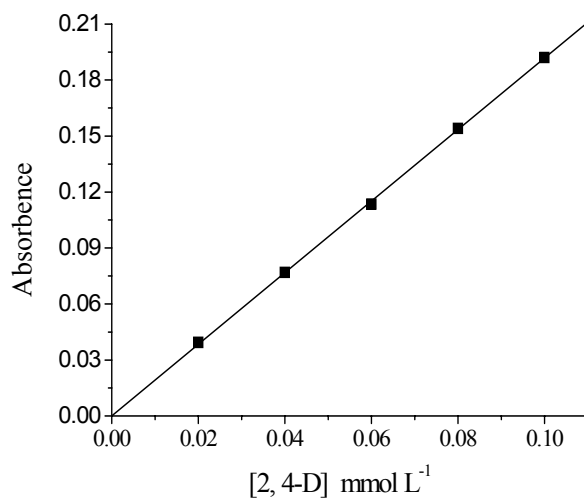


**Figure V-A-3 Molar absorption coefficients at 284 nm.**

It was reported that 2, 4-D is an organic acid with pKa of 2.6 and high water solubility (Tatiane et al., 2007). Experiment was carried out to confirm the pKa value of the 2, 4-D used in this work. Figure V-A-4 presents the UV-visible spectra of 2, 4-D as the function of pH ranged from 1.5 to 5.0 ( $[2, 4-D] = 3.6 \times 10^{-5} \text{ mol L}^{-1}$ ). Figure V-A-5 shows the variation of the absorbance at 235 nm of 2, 4-D. It indicate

that the pKa value of 2, 4-D used in this work is 2.9.

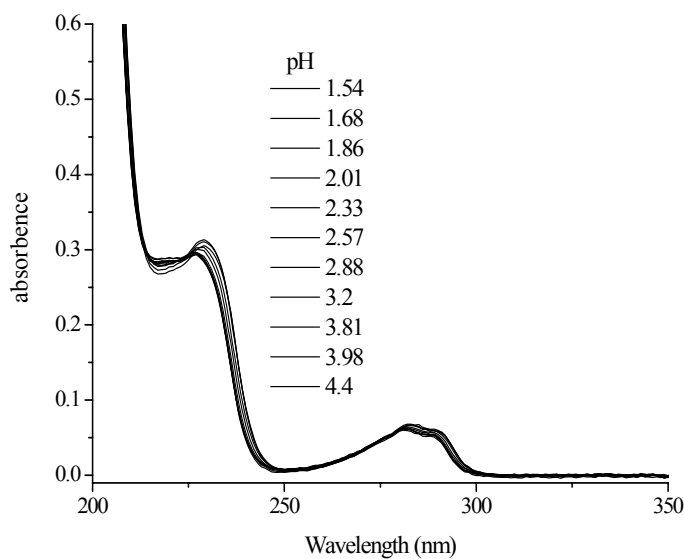


**Figure V-A-4 UV-visible spectra of 2, 4-D as the function of pH ranged from 1.5 to 5.0**

**([2, 4-D] =  $3.6 \times 10^{-5} \text{ mol L}^{-1}$ )**

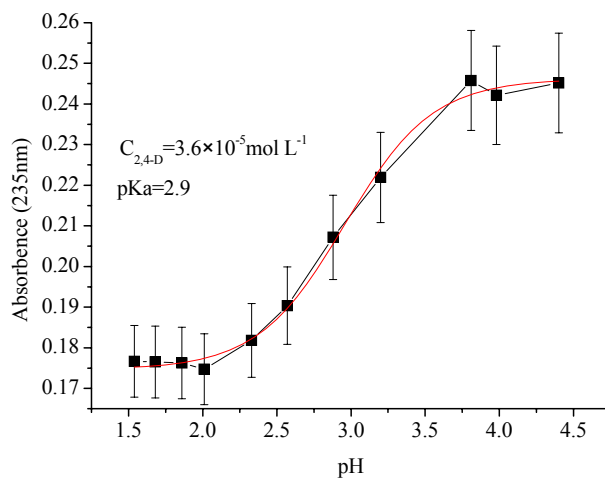


**Figure V-A-5 pKa of 2, 4-D ([2, 4-D] =  $3.6 \times 10^{-5} \text{ mol L}^{-1}$ )**

Experiments were performed to study UV-visible spectra of different aqueous solutions: (a)  $0.3 \text{ mmol L}^{-1}$  of Fe(III); (b)  $0.1 \text{ mmol L}^{-1}$  of 2, 4-D; (c) mixture of 0.3

mmol L<sup>-1</sup> Fe(III) and 0.1 mmol L<sup>-1</sup> 2, 4-D; (d) sum of Fe(III) and 2, 4-D spectra. Figure V-A-5 shows the UV-Visible absorption spectra of the solutions 3 min after the preparation. The spectrum of the mixture (Fe(III) + 2, 4-D) correspond to the sum of the spectra of the both components. This result shows that there is no interaction (complexation) between 2, 4-D and Fe(III) in the aqueous solution and in the dark.

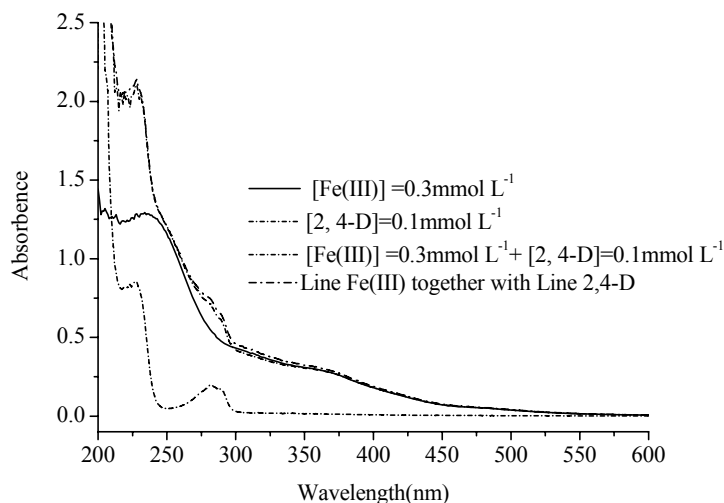


**Figure V-A-6 UV-Visible absorption spectra of aqueous solution 3 min after the preparation with 0.3 mmol L<sup>-1</sup> of Fe(III) and 0.1 mmol L<sup>-1</sup> of 2, 4-D**

### **A-2-Quantum yields of 2, 4-D degradation and Fe(II) formation**

The monochromatic irradiation was carried out separately at 296, 313, 334 and 365 nm. 2, 4-D does not absorb at such wavelengths: no degradation was observed when 2, 4-D was irradiated alone at these four wavelengths. The reaction times was well controlled to make sure that all the degradation of 2, 4-D and the generation of products not exceed 10%. This condition permits to determine the initial quantum yields. Therefore, the quantum yields of 2, 4-D degradation ( $\Phi_{2, 4-D}$ ) and Fe(II) generation ( $\Phi_{Fe(II)}$ ) were calculated with an error of less than 5%. Parameters such as pH, oxygen and concentrations of Fe-EDDS complex that may influence the reaction were all studied.

**A-2-1-Influence of the irradiation wavelength on the quantum yields of Fe(II) and 2,4-D in Fe(III) -EDDS complex aqueous solution**

The quantum yields of Fe(II) formation and 2, 4-D disappearance has been evaluated at different wavelength (296, 313, 334 and 365 nm) in the aqueous solutions:

- (1) with 0.3 mmol L<sup>-1</sup> of Fe(III) and 0.1 mmol L<sup>-1</sup> of 2, 4-D,
- (2) with 0.3 mmol L<sup>-1</sup> of Fe(III)-EDDS complex ,
- (3) with 0.3 mmol L<sup>-1</sup> of Fe(III)-EDDS complex and 0.1 mmol L<sup>-1</sup> of 2, 4-D.

All of the experiments were carried out at pH 3.0. Table V-A-1 shows the results.

**Table V-A-1 Quantum yields of disappearance of 2, 4-D and generation of Fe(II) as a function of the irradiation wavelength (at pH 3.0).**

	$\lambda$ (nm)	$I_0, (\times 10^{14})$ Photons s <sup>-1</sup> cm <sup>-2</sup>	$\Phi_{\text{Fe(II)}} (\Delta t=40 \text{ s})$		$\Phi_{2, 4\text{-D}}$ ( $\Delta t=30 \text{ min}$ )
			Without 2, 4-D	With 2, 4-D	
[Fe(III)] 0.3 mmol L <sup>-1</sup>	296	1.42		0.065	0.028
	313	5.41		0.031	0.019
	334	3.15		0.025	0.15
	365	4.47		0.026	0.011
[Fe(III)-EDDS] 0.3 mmol L <sup>-1</sup>	296	1.42	0.26	0.33	0.016
	313	5.41	0.25	0.28	0.015
	334	3.15	0.19	0.22	0.011
	365	4.47	0.16	0.17	0.008

As the results showed, we confirm that wavelength has obvious effect on the quantum yields of both Fe(III) solutions and Fe(III)-EDDS solutions. Both  $\Phi_{\text{Fe(II)}}$  and  $\Phi_{2, 4\text{-D}}$  increased with the decrease of the wavelength. Quantum yields of Fe(II) formation and 2, 4-D disappearance almost have an opposite tendency. The photoreduction of Fe(III) is enhanced in the presence of ligands. So the  $\Phi_{\text{Fe(II)}}$  is higher in the presence of acid carboxylic than in the presence of water or hydroxide group as ligands ( $\text{Fe}(\text{OH})^{2+}$ ). This difference can be also attributed to the fact that in the case of organic ligands Fe(II) formed is less reoxidized, and radical species



formed under irradiation attack pollutants as well. However, for Fe(III)-EDDS complex, the  $\Phi_{2,4-D}$  is lower than in the presence of  $\text{Fe}(\text{OH})^{2+}$ . This result may be due to the competition between organic substrates (EDDS and oxidized EDDS) and less radicals are available for the 2, 4-D degradation at the beginning of the irradiation.

**A-2-2-influence of oxygen on the quantum yields of Fe(II) and 2, 4-D with Fe(III)-EDDS complex ( $\lambda_{\text{irr}}=365\text{nm}$ )**

As we know, Oxygen plays a very important role in the photochemical process. Effects on the quantum yield of Fe(II) formation and on the quantum yield of 2, 4-D degradation were studied. Different gas medium of reaction solutions were obtained by bubbling oxygen or argon 15 min into the solutions before irradiation. The experiment was carried out in the presence of Fe(III)-EDS complex at pH = 3.0 with monochromatic irradiation at 365 nm. Table V-A-2 presents the results in detail. In deaerated solution, the quantum yield of 2, 4-D is negligible ( $\Phi_{2,4-D}=0.003$ ). The quantum yield of Fe(II) formation in oxygenated solution is almost five times higher than those obtained in aerated solution.

**Table V-A-2 Effect of oxygen on the quantum yields of 2, 4-D disappearance and of Fe(II) generation. pH = 3.0. ( $\lambda_{\text{irr}}=365\text{nm}$ )**

[Fe(III)/EDDS]= 0.3 mmol L <sup>-1</sup> :0.3 mmol L <sup>-1</sup>			
	Deaerated solution	Aerated solution	Oxygen saturated solution
$\Phi_{\text{Fe(II)}}$	0.02	0.16	0.48
$\Phi_{2,4-D}$	0.003	0.012	0.047

It can be concluded that oxygen has a strong effect on the reaction. Oxygen enhance the photoredox process involving Fe(III)-EDDS complex, thus, more Fe(II) and reactive species (such as  $\cdot\text{OH}$  radicals, organic radicals) are generated in aqueous

solution during the reaction process. Moreover, in the absence of oxygen, necessary to form the reactive species, 2, 4-D degradation is strongly inhibited.

### **A-2-3-Influence of pH on the quantum yields of Fe(II) and 2, 4-D in Fe(III)-EDDS complex ( $\lambda_{irr}=365\text{ nm}$ )**

As we know, the pH of solution is very important parameter in the photochemical reaction with Fe(III)-complexes. Experiments were carried out under monochromatic irradiation at 365 nm with different concentration of Fe(III)-EDDS complex. The concentration of Fe(III)-EDDS was 0.1, 0.2, 0.3 and 0.6 mmol L<sup>-1</sup>. Concentration of 2, 4-D was 0.1 mmol L<sup>-1</sup>. The pH values of the solutions were controlled from 2.0 to 6.0. Results about the quantum yields of Fe(II) are presented in Table V-A-3.

**Table V-A-3 Quantum yields of generation of Fe(II) as a function of pH at 365nm**

[Fe(III)-EDDS]	$I_0 \quad (\times 10^{14})$ photons·s <sup>-1</sup> ·cm <sup>-2</sup>	pH	$\Phi_{\text{Fe(II)}} \quad (\Delta t=40\text{s})$
0.3 mmol L <sup>-1</sup>	4.47	2.0	0.17
		3.0	0.18
		4.0	0.14
		5.0	0.04
		6.0	0.008

The quantum yield of Fe(II) formation decreases when the pH increases. This result is mainly due to the fact that at higher pH, Fe(II) is easily oxidized by dissolved oxygen present in water.

**Table V-A-4 Quantum yields of disappearance of 2, 4-D as a function of pH**

[Fe(III)-EDDS] (mmol L <sup>-1</sup> )	$\Phi_{2,4\text{-D}} \quad (\Delta t=30\text{min})$				
	pH=2.0	pH=3.0	pH=4.0	pH=5.0	pH=6.0
0.3	0.009	0.008	0.02	0.021	0.028

The pH effect on the quantum yields of 2, 4-D disappearance was also studied. Results are shown in Table IV-D-4. According to the values, the quantum yields of 2,

4-D disappearance were increased with the increase of the pH value. It can be concluded that higher pH value condition is more favourable for the degradation of 2, 4-D in the presence of Fe(III)-EDDS complex. The quantum yields of 2, 4-D disappearance were optimal at pH 6.0 in the presence of Fe(III)-EDDS complex.

### **A-3- Degradation of 2, 4-D photoinduced by Fe(III)-EDDS complex at 365 nm under polychromatic irradiation**

The photodegradation of 2, 4-D was studied in the presence of Fe(III)-EDDS complexes. Irradiation was with polychromatic tubes emitting between 300 and 500 nm. Concentration of complex, and oxygen, pH, and effect of isopropanol were all studied in this work.

#### **A-3-1-Effect of Fe(III)-EDDS concentration**

Fe(III)-EDDS concentration effect on the photodegradation of 2, 4-D ( $0.1 \text{ mmol L}^{-1}$ ) was studied in aqueous solution at pH 3.0. The initial concentration of Fe(III)-EDDS complex used in the work were 0.05, 0.1, 0.3 and  $0.6 \text{ mmol L}^{-1}$ . Figure V-A-6 presents the kinetics of 2, 4-D photodegradation. The disappearance of 2, 4-D increases with the increase of Fe-EDDS complex concentration. After 3 hours of irradiation, 45% of the 2, 4-D was degraded in solution with  $0.6 \text{ mmol L}^{-1}$  of Fe(III)-EDDS complex, nearly 20% of 2, 4-D with  $0.3 \text{ mmol L}^{-1}$  and  $0.05 \text{ mmol L}^{-1}$ , and only 15% with  $0.1 \text{ mmol L}^{-1}$  of Fe(III)-EDDS complex. After 8 hours of irradiation, the photodegradation efficiency of 2, 4-D have reached 55%, 48%, 25% and 20% in the solutions with 0.6, 0.3, 0.1 and  $0.05 \text{ mmol.L}^{-1}$  of Fe(III)-EDDS complexes respectively. It is obviously that the photodegradation efficiency of 2, 4-D was increased with increasing concentration of Fe-EDDS complex in aqueous solutions at pH 3.

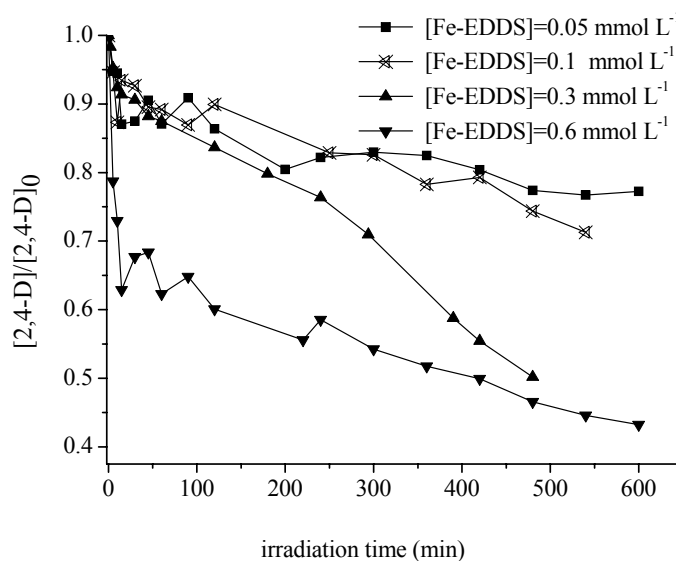


**Figure V-A-7 Kinetics of 2, 4-D photodegradation as a function of Fe-EDDS concentration**  
(Initial pH = 3.0; [2, 4-D]<sub>0</sub> = 0.1 mmol L<sup>-1</sup>)

Figure V-A-8 presents the HPLC spectrum of reaction solutions with 0.3 mmol L<sup>-1</sup> Fe(III) and 0.1 mmol L<sup>-1</sup> 2, 4-D at initial pH 3.0. As we see from Figure V-A-7, the 2, 4-DCP is the main photoproduct of photodegradation of 2, 4-D in aqueous solutions. It is obviously that the retention time of 2, 4-D is 2.3 min and the retention time of 2, 4-DCP is 7.3 min.

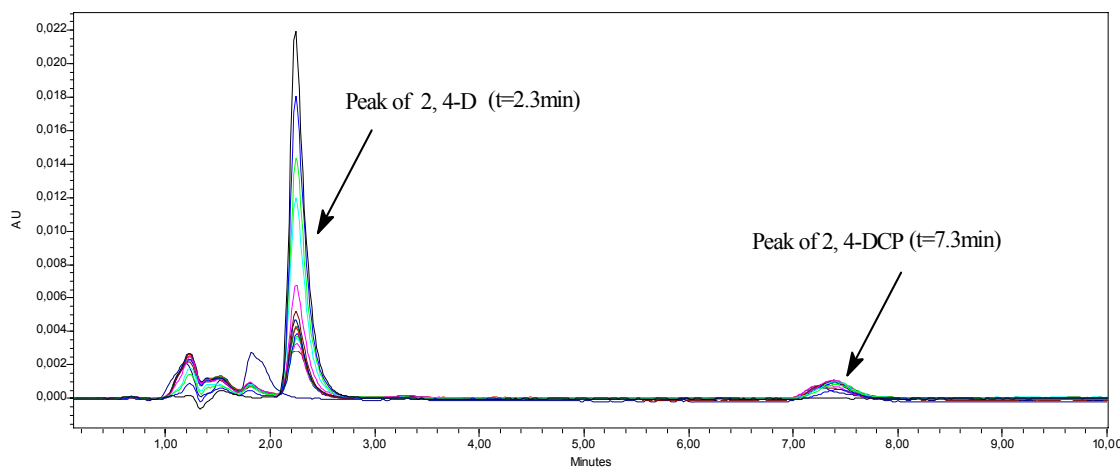


**Figure V-A-8 Evolution of HPLC spectrum of reaction solution with 0.3 mmol L<sup>-1</sup> Fe(III)**  
**and 0.1 mmol L<sup>-1</sup> 2, 4-D at pH = 3.0**

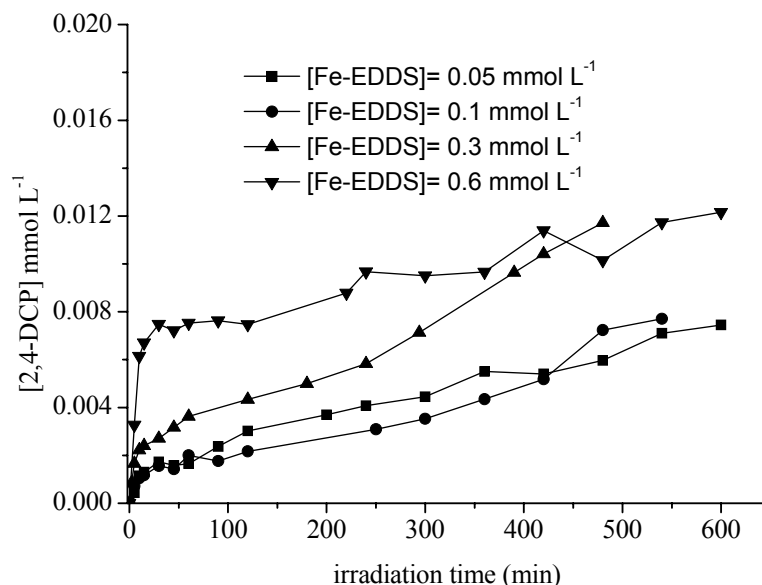


**Figure V-A-9 Photoproduction concentration of 2, 4-DCP in solutions with different concentration of Fe-EDDS under irradiation (Initial pH = 3.0; [2, 4-D]<sub>0</sub> = 0.1 mmol L<sup>-1</sup>)**

During the reaction process, 2, 4-DCP was generated from the photodegradation of 2, 4-D. Figure V-A-9 presents the results of photoproduction of 2, 4-DCP in solutions with different concentration of Fe(III)-EDDS complex. The concentration of 2, 4-DCP in the solutions containing 0.6 mmol L<sup>-1</sup> Fe(III)-EDDS complex is higher than in the other three solutions. 2, 4-DCP was generated faster at the beginning of the reaction process. After 8 hours irradiation, 2, 4-DCP concentration was almost the same ( $\approx 5 \mu\text{mol L}^{-1}$ ) in the solutions with 0.05 and 0.1 mmol L<sup>-1</sup> of Fe(III)-EDDS but lower than 2, 4-DCP concentration formed with 0.3 and 0.6 mmol L<sup>-1</sup> of Fe(III)-EDDS. In this latter case the concentration of 2, 4-DCP is around two times higher ( $\approx 10 \mu\text{mol L}^{-1}$ ).

In the photochemical process, Fe(III) was reduced to Fe(II) species. The concentration of Fe(II) was also detected in this work. Figure V-A-10 presents the results, which indicate that the Fe(III) was reduced during irradiation period. The formation of Fe(II) is very fast at the beginning of irradiation but, contrary to Fe(III)

aquacomplexes where around 100% of Fe(III) is reduced, no more than 50% of Fe(III) has been reduced to Fe(II) after 60 min of irradiation. After that the photochemical process continues with a stable concentration of Fe(II) species. There is no significant variation of the concentration of Fe(II) from 1 h to 8 h of irradiation in all the conditions. The concentration of Fe(II) represents between 30% and 45% of the total iron concentration after 8 h of irradiation.

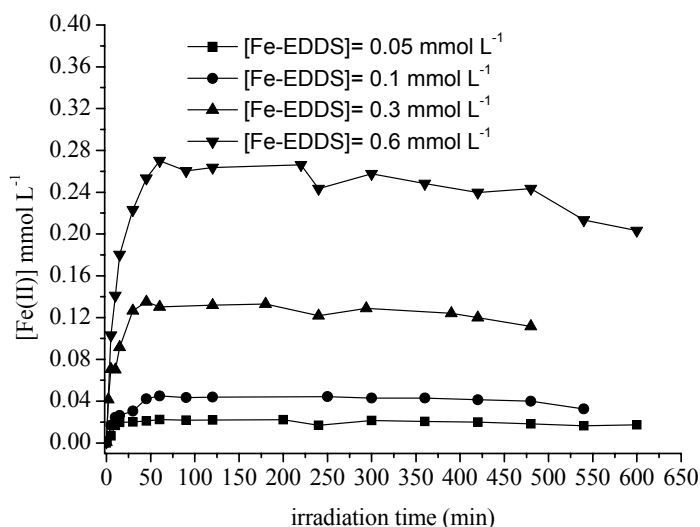


**Figure V-A-10 Photogeneration of Fe(II) as a function of Fe(III)-EDDS concentration in solutions ( Initial pH = 3.0; [2,4-D]<sub>0</sub> = 0.1 mmol L<sup>-1</sup>).**

### **A-3-2 Effect of oxygen on the 2, 4-D photodegradation**

As we know, oxygen is a very important parameter in the photoreaction process. A lot of experiments have proved its effects on the photodegradation of pollutants in the previous study. Experiments were performed in the solutions with 0.3 mmol L<sup>-1</sup> of Fe(III)-EDDS complex and 0.1 mmol L<sup>-1</sup> of 2,4-D. The initial pH of solution was fixed at 3.0. Different reaction medium was obtained by bubbling oxygen or argon into the solutions before irradiation. The time of bubbling O<sub>2</sub> or Ar was both 15min. Results are presented in Figure V-A-10. It is obvious that oxygen has a very strong

effect on the photodegradation of 2, 4-D. In the oxygen saturated condition, the photodegradation efficiency of 2, 4-D, nearly 85%, is higher than in the air saturated and deaerated conditions after a long time of irradiation. At the beginning of the reaction, the degradation rate is faster in the oxygen saturated condition than in the other conditions. The photodegradation efficiency of 2, 4-D after 8 hours of irradiation is 82% in the oxygen saturated solution, 50% in the air saturated solution and 18% in the deaerated solution.

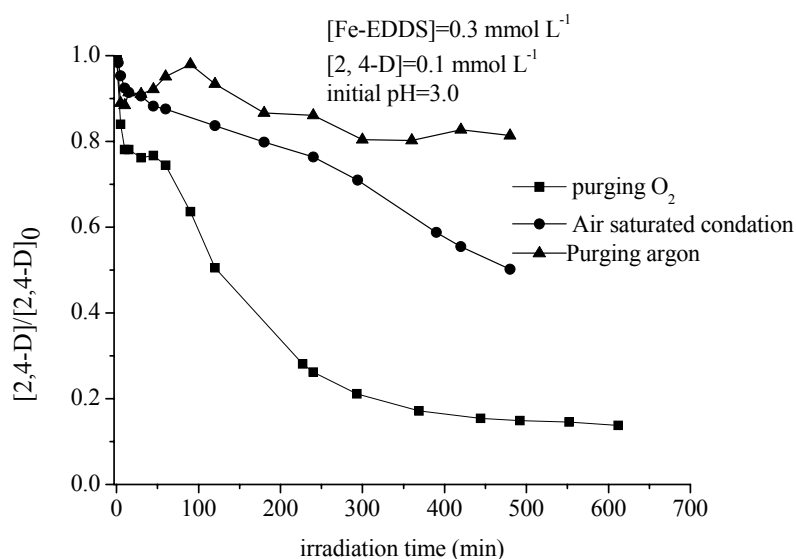


**Figure V-A-11 Impact of oxygen on 2, 4-D photodegradation in the presence of Fe(III)-EDDS.**

2, 4-DCP was also detected in the same time. Figure V-A-12 presents the results of photoproduct concentration of 2, 4-DCP in aqueous solution. 2, 4-DCP was not photogenerated in the solution purged with argon. And both in solutions of air saturated condition and oxygen saturated condition, 2, 4-DCP was detected. From the results, in the O<sub>2</sub> saturated condition, 2, 4-DCP in solutions can be also clearly photodegraded. In this condition (O<sub>2</sub> saturated) the progress of the photochemical reaction is higher. That is why the concentration of 2, 4-DCP in air saturated condition was higher than oxygen saturated condition after 6 hours of irradiation.

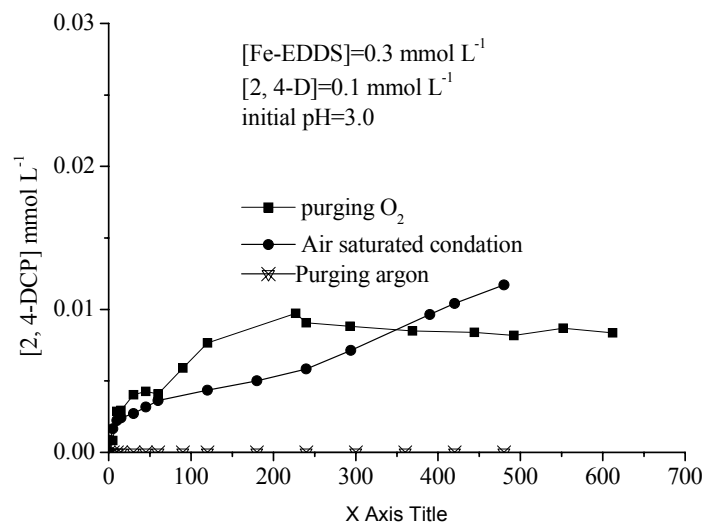


**Figure V-A-12 Impact of oxygen on 2, 4-DCP formation**

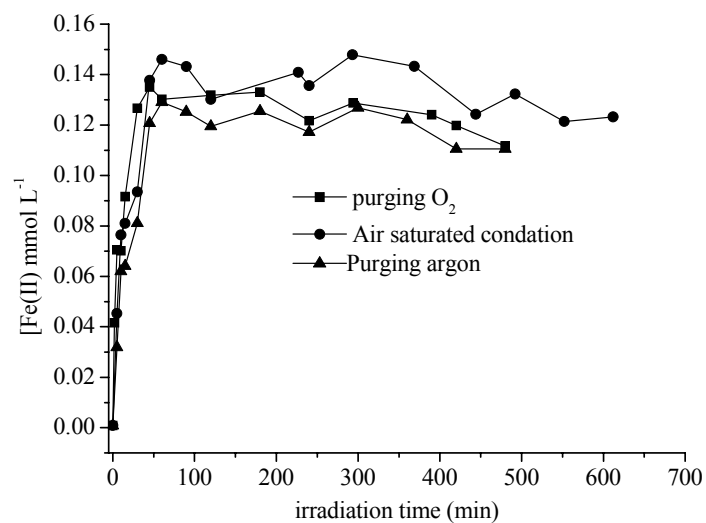


**Figure V-A-13 Photogeneration of Fe(II) as function of oxygen in solutions with an initial pH = 3.0.  $[\text{Fe(III)-EDDS}]_0 = 0.3 \text{ mmol L}^{-1}$ ,  $[\text{2,4-D}]_0 = 0.1 \text{ mmol L}^{-1}$ .**

Oxygen effects on the formation of Fe(II) was performed under irradiation. Figure V-A-13 presents the results. In all the conditions, the formation of Fe(II) was



fast at the beginning of the reaction. Oxygen presents a slight negative effect on the formation of Fe(II) before 60 min of irradiation. However we can conclude that it does not appear any significant effect of oxygen on Fe(II) formation.

### **A-3-3-Effect of pH on photodegradation of 2, 4-D**

Experiments were carried out with  $0.1 \text{ mmol L}^{-1}$  of Fe(III)-EDDS complex and  $0.1 \text{ mmol L}^{-1}$  of 2, 4-D. With the increase of pH, the photodegradation efficiency of 2, 4-D increased before 6 hours of irradiation. The optimal photodegradation process of 2, 4-D was obtained at pH 6.0. As shown in Figure V-A-14, the photodegradation rate is faster before 30 min of irradiation at pH 6.0 and then the degradation continues with a slower rate. At pH 3.0, further degradation of 2, 4-D occurred and 55% of 2, 4-D was degraded after 8 h of irradiation. The photodegradation efficiency is about 55% at pH 3.0 and 25% at pH 6.0 after 8 h of irradiation.

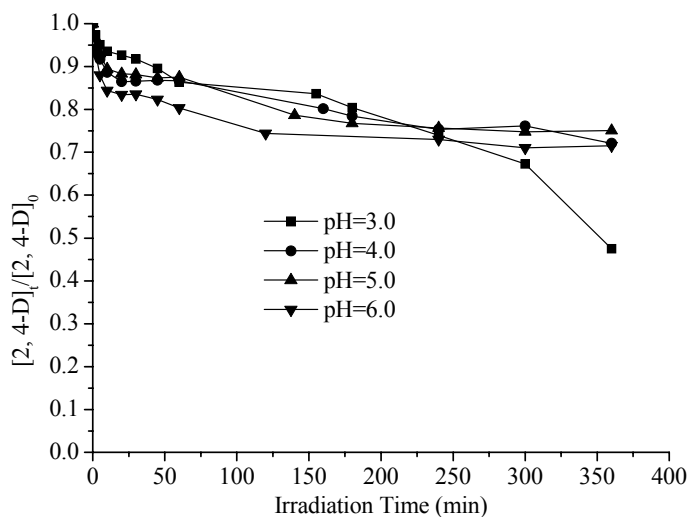


**Figure V-A-14 Influence of pH on the photodegradation of 2, 4-D in the presence of Fe(III)-EDDS complex.  $[\text{Fe(III)-EDDS}]_0 = 0.1 \text{ mmol L}^{-1}$ ,  $[\text{2,4-D}]_0 = 0.1 \text{ mmol L}^{-1}$ .**

Fe(II) formation was strongly affected by the pH (FigureV-A-15). Especially at relative higher pH 6.0, the formation of Fe(II) was obviously lower, the maximum

concentration of Fe(II) corresponded to only 30% of total Fe in the aqueous solution after 4 hours of irradiation. This value decreased to 20% after 6 hours of irradiation at pH 6.0.

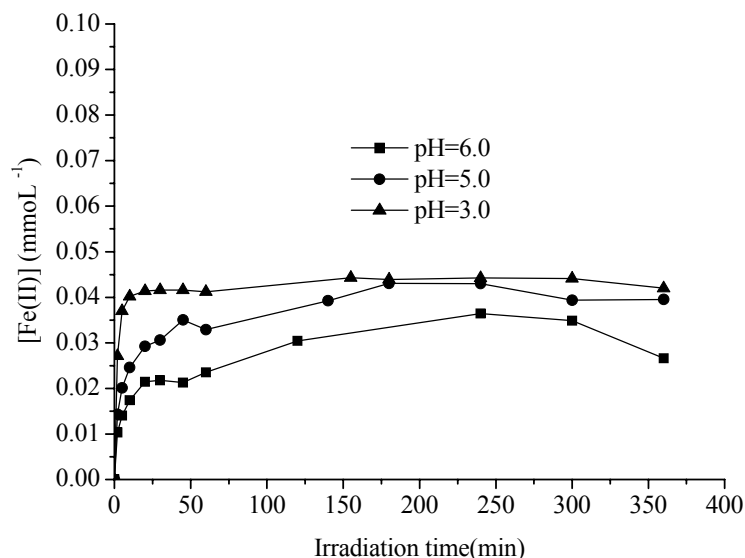


**Figure V-A-15 Influence of pH on the photogeneration of Fe(II) in the presence of Fe-EDDS complex.  $[\text{Fe(III)-EDDS}]_0 = 0.1 \text{ mmol L}^{-1}$ ,  $[\text{2,4-D}]_0 = 0.1 \text{ mmol L}^{-1}$ .**

#### **A-3-4-study on the effect of isopropanol on photodegradation of 2, 4-D**

Experiments were carried out in the solution with  $0.3 \text{ mmol L}^{-1}$  of Fe(III)-EDDS complex,  $0.1 \text{ mmol L}^{-1}$  of 2, 4-D and 0.5% isopropanol at pH 3.0. It is obvious from Figure V-A-16 that 2, 4-D photodegradation efficiency was 50% in solution without isopropanol after 8 h of irradiation. On the contrary no photodegradation was observed in the solution with isopropanol even after more than 8 h of irradiation. Figure V-A-17 presents that 2, 4-DCP was not detected in the solution with isopropanol even after 8 h of irradiation. Without isopropanol, more than  $0.01 \text{ mmol L}^{-1}$  of 2, 4-DCP was detected in solution.

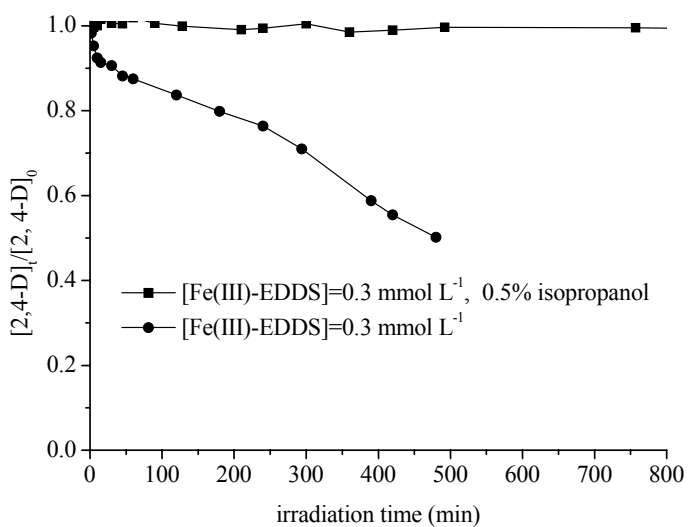


**Figure V-A-16 Influence of isopropanol on the photodegradation of 2, 4-D in presence of Fe-EDDS complex at pH 3.0.  $[2, 4-D]_0 = 0.1 \text{ mmol L}^{-1}$ .**

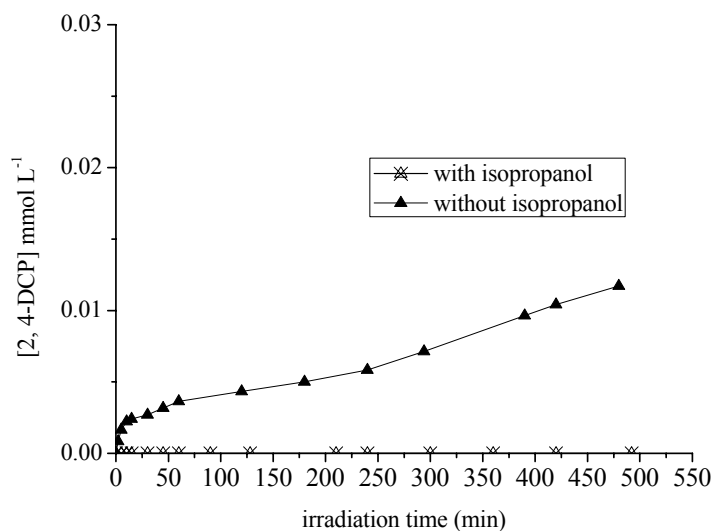


**Figure V-A-17 Influence of isopropanol on the photogeneration of 2, 4-DCP in presence of Fe-EDDS complex at pH 3.0.  $[Fe(III)-EDDS] = 0.3 \text{ mmol L}^{-1}$ ,  $[2,4-D]_0 = 0.1 \text{ mmol L}^{-1}$ .**

The spectra of the solutions as a function of the irradiation times are presented in the Figure V-A-18. The solution is a mixture of  $0.1 \text{ mmol L}^{-1}$  2, 4-D and  $0.3 \text{ mmol L}^{-1}$  of Fe(III)-EDDS at pH = 3.0. There is a sharp decrease after 15 min of irradiation.

This observation is due to the efficient photoredox process taking place in the Fe(III)–EDDS under irradiation. The absorbance of complex from 300 to 400 nm decreased. It is in agreement with the fact that the Fe(II) formation, resulting from the photoredox process, is very fast at the beginning of the irradiation and that in this condition 2, 4-D is efficiently degraded.

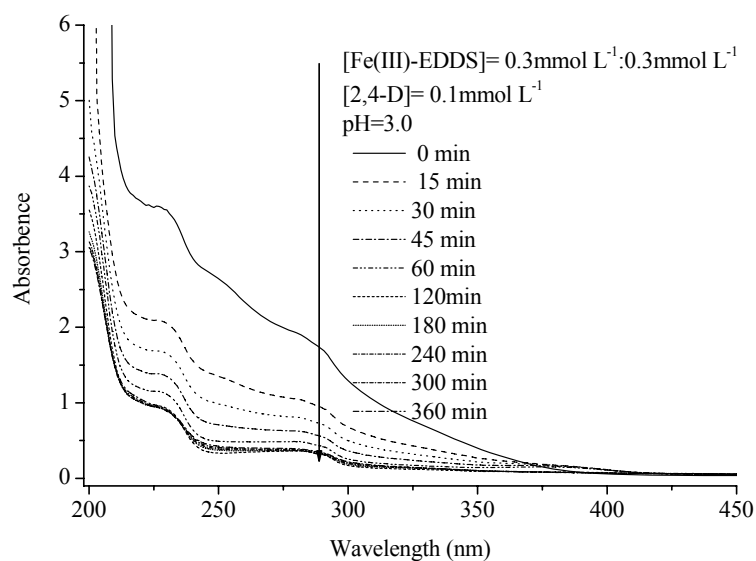


**Figure V-A-18 UV-visible spectrum of the Fe(III)-EDDS and 2, 4-D solutions as a function of irradiation time.**

## **Conclusions**

Photodegradation of 2, 4-D photoinduced by Fe(III)-EDDS complex was investigated in this study. Results indicate that irradiation wavelength, pH, oxygen, ratio and concentration of Fe(III)-EDDS complex and isopropanol, all have effect on the quantum yields of Fe(II) formation and 2, 4-D degradation. Irradiation wavelength has a great effect on the quantum yields, both  $\Phi_{\text{Fe(II)}}$  and  $\Phi_{2, 4\text{-D}}$  increase with the decrease of wavelength of irradiation.

The pH 6.0 and high concentration of oxygen are all favorable for the photodegradation of 2, 4-D. In the presence of high concentration in oxygen and at pH

6.0 the total degradation of 2, 4-D and photogeneration of 2, 4-DCP are observed after 8 h of irradiation. Oxygen is necessary for an efficient degradation of 2, 4-D and the experiment with isopropanol show that  $\cdot\text{OH}$  radicals are responsible for the degradation of 2, 4-D.

## **B-Photodegradation of 2, 4-D induced by the Goethite in the presence of EDDS**

Iron oxides, hydroxides, and oxy-hydroxides are efficient sorbents for inorganic and organic species and have a great potential in industrial applications. They are also of substantial interest in environmental sciences since some of them are frequently occurring in soil minerals (e.g., goethite and ferrihydrite) having significant impact on the behavior of pollutants in soils. The mineral solid-water interface plays a central role in regulating the concentrations of a large number of reactive elements in natural aqueous systems by influencing their biogeochemical cycles, and also in water treatment technologies. Goethite is the most abundant iron oxide in nature, whose surface reactivity has been extensively studied. In this work, experiments were carried out to study the influence of 2, 4-D degradation in the suspension of goethite with or without EDDS. The goethite that was used in this study was synthesized from LPMM of Blaise Pascal University.

A goethite suspension was dialyzed in deionized ultra pure aerated water until its conductivity equaled that of fresh deionized ultra pure aerated water. Then, the suspension was dispersed by using an ultrasonic bath for 20 min. The particle size of the dispersed goethite was  $< 2 \mu\text{m}$ . For the analysis of the solution, the goethite suspensions were centrifuged at 12000 rpm for 20 min.

### **B-1-Adsorption of 2, 4-D on goethite**

The concentration of goethite in the suspension is an important factor for the adsorption of 2, 4-D. To evaluate this factor, the experiments in suspension at pH = 4.0 were performed. Concentrations of goethite were changed from 0.05 g L<sup>-1</sup> to 1.0 g L<sup>-1</sup>. The initial concentration of 2, 4-D was 0.1 mmol L<sup>-1</sup>. The results are shown in table V-B-1 and Figure V-B-1. The concentration of 2, 4-D was almost the same even after 39 h shaking period in the aqueous solutions with presence of goethite. It means that there was no obvious adsorption of 2, 4-D in suspension with the presence of goethite at pH 4.0.

**Table V-B-1 Adsorption data of 2, 4-D on goethite with different time in suspension at pH 4.0**

[Goethite]	[2, 4-D] mmol L <sup>-1</sup>					
	t=0 h	t=0.5 h	t=1 h	t=14 h	t=25 h	t=39 h
0.05 g L <sup>-1</sup>	0.10	0.09845	0.09977	0.10	0.09752	0.10
0.1 g L <sup>-1</sup>	0.10	0.10	0.10	0.09577	0.10	0.10
0.2 g L <sup>-1</sup>	0.09999	0.10	0.09989	0.09865	0.10	0.10
0.5 g L <sup>-1</sup>	0.10	0.10	0.0998	0.10	0.09983	0.10
1.0 g L <sup>-1</sup>	0.09999	0.09812	0.09897	0.10	0.10	0.10

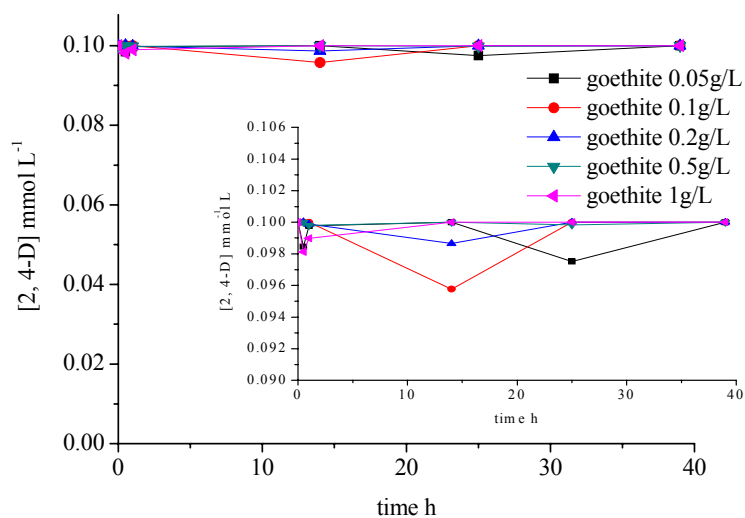


**Figure V-B-1 Adsorption of 2, 4-D on goethite with different time in suspension at pH 4.0**

Since effect of the concentration of goethite is negligible at pH 4.0, adsorption of 2, 4-D on goethite ( $0.2 \text{ g L}^{-1}$ ) at different pH value in suspension was studied with the different time. The initial concentration of 2, 4-D was  $0.1 \text{ mmol L}^{-1}$ . The pH value of aqueous solution changed from 3.0 to 6.0. The results are shown in table V-B-2. With the increase of time, in evidence, nearly 9% of 2, 4-D was adsorbed on the goethite at pH 3.0, and the concentration of 2, 4-D was decreased from  $0.1 \text{ mmol L}^{-1}$  to  $0.09147 \text{ mmol L}^{-1}$  at pH 3.0 after 37 h shaking period. For the suspension at pH 4.0, 5.0 and 6.0, the adsorption of 2, 4-D on goethite was not observed. So it indicated that the pH value of solution is a more important factor for the adsorption of 2, 4-D than the concentration of goethite in suspension. 2, 4-D adsorption primarily occurs under acidic conditions, as shown in Figure V-B-2. But even at pH 3.0, no more than 4% of 2, 4-D were adsorbed on the goethite in suspension after 8h shaking period.

**Table V-B-2 Adsorption data of 2, 4-D on goethite at different pH in suspension**

pH	[2, 4-D] $\text{mmol L}^{-1}$					
	t=0 h	t=0.5 h	t=1 h	t=12.5h	t=28h	t=37h
3.0	0.10	0.10	0.09842	0.09433	0.09261	0.09147
4.0	0.10	0.10	0.10	0.0999	0.10	0.10
5.0	0.10	0.10	0.10	0.10	0.10	0.10
6.0	0.10	0.09994	0.10	0.10	0.10	0.10

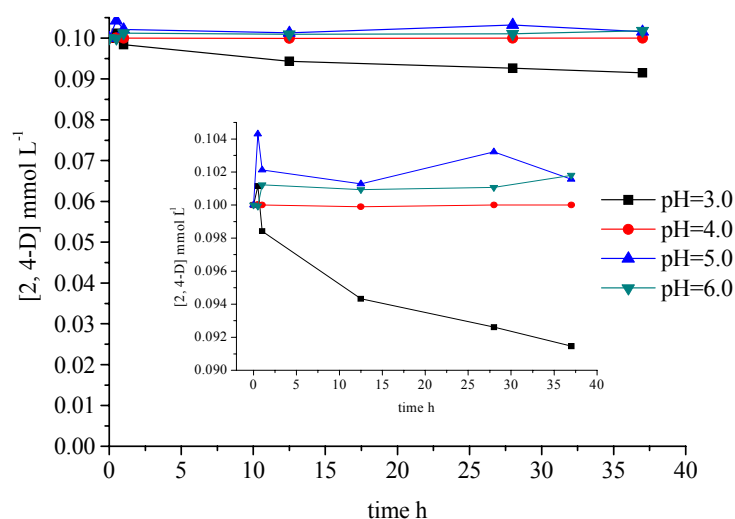


**Figure V-B-2 Adsorption of 2, 4-D on goethite at different pH in suspensions**

### **B-2-Photodegradation of 2, 4-D at 365 nm in suspension of the goethite**

Since goethite is the most abundant iron oxide in nature, the mineral solid-water interface plays a central role on degradation of organic pollutant (organic pesticide) in natural environment. Experiments were carried out to study the photodegradation of 2, 4-D at 365 nm in suspension of the goethite. Irradiation was with polychromatic tubes emitting between 300 and 500 nm. Concentration of goethite in suspension and pH were all studied in this work.

#### **B-2-1-Effect of goethite concentration in suspension**

Goethite concentration effect on the photodegradation of 2, 4-D was studied in suspension with 0.1 mmol L<sup>-1</sup> of 2, 4-D at pH 4.0. The concentration of goethite used in the work was 0.05, 0.1, 0.2 and 0.5 g L<sup>-1</sup>. Figure V-B-3 presents the photodegradation efficiency of 2, 4-D in suspension. The disappearance of 2, 4-D was decrease when the concentration of goethite is 0.5 g L<sup>-1</sup> compared to 0.2 g L<sup>-1</sup>. The photodegradation efficiency of 2, 4-D in suspension of 0.1 g L<sup>-1</sup> goethite is higher



than in suspension of  $0.05 \text{ g L}^{-1}$  goethite. After 8 h of irradiation, the photodegradation efficiency of 2, 4-D have reached 11%, 20%, 20% and 10% in the suspension with 0.05, 0.1, 0.2 and  $0.5 \text{ g L}^{-1}$  of goethite respectively.

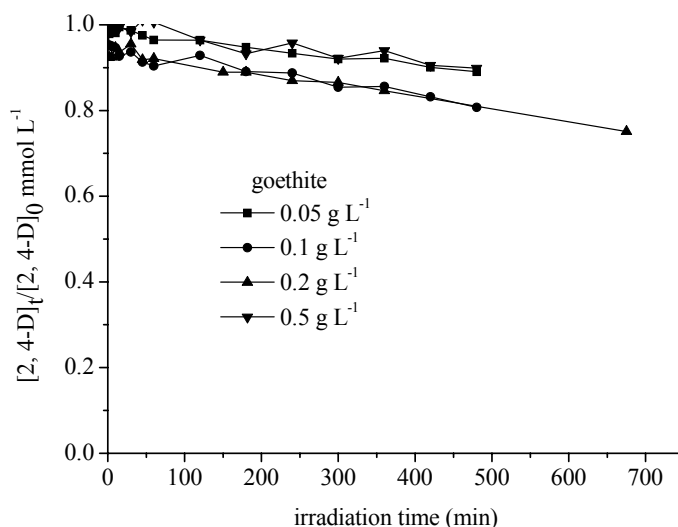


**Figure V-B-3 Photodegradation efficiency of 2, 4-D in suspension at pH 4.0 under irradiation**

As we know the 2, 4-DCP was the main photoproduct of 2, 4-D degradation. In this work we also detected the photoproduct of 2, 4-DCP in suspension. Figure V-B-4 presents the results of 2, 4-DCP photoproduction in suspension. After 8h irradiation,  $0.01 \text{ mmol L}^{-1}$  of 2, 4-DCP was observed in the suspension of goethite with the concentration of  $0.2 \text{ g L}^{-1}$ . There is no significant variation of the concentration of 2, 4-DCP photoproduction in the period of 8h irradiation at 365nm between the suspensions of different goethite concentration used in this work. It indicated that in our experimental conditions the effect of goethite concentration in suspension is negligible for the photodegradation of 2, 4-D.

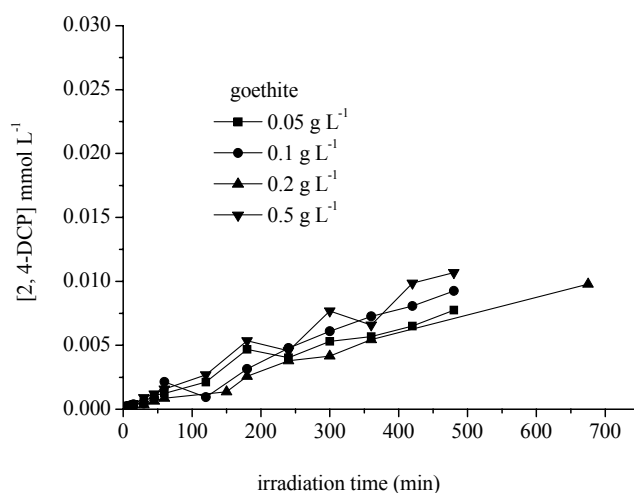


**Figure V-B-4 Results of 2, 4-DCP photoduction in suspension at pH 4.0 under irradiation**

### **B-2-2- initial pH effect of suspension on photodegradation of 2, 4-D**

Experiments were carried in the solution with 0.2 g L<sup>-1</sup> of goethite and 0.1 mmol L<sup>-1</sup> of 2, 4-D. With the increase of pH, the photodegradation efficiency of 2, 4-D decreased. The optimal photodegradation process of 2, 4-D was obtained at pH 3.0 and 4.0. As shown in Figure V-B-5, the photodegradation rate is faster at pH 3.0 and at pH 4.0. At pH 5.85, no degradation of 2, 4-D occurred after 8 h of irradiation. After 8 hours of irradiation around 20% of 2, 4-D is degraded in both pH's.

The influence of pH on photoproduction of 2, 4-DCP concentration was observed in Figure V-B-6. 2, 4-DCP photoproduction was strongly affected by the pH. Especially at relative higher pH 5.85, no 2, 4-DCP was observed. The maximum concentration of 2 4-DCP was 0.015 mmol L<sup>-1</sup> after 8h irradiation in suspension at pH 3.0. The concentration of 2 ,4-DCP is two times higher at pH 3.0 than at pH 4.0 (0.0075 mmol L<sup>-1</sup>). This observation can be due to the faster degradation of 2, 4-DCP at pH 4.0 than at pH 3.0.

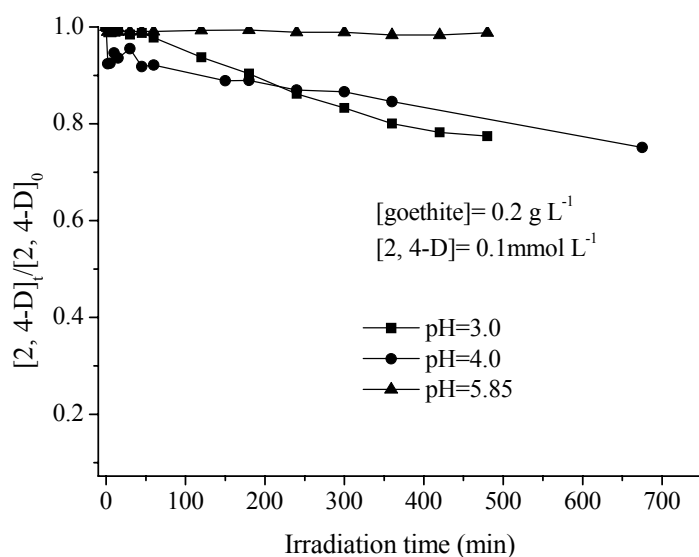


**Figure V-B-5 Influence of pH on the photodegradation of 2, 4-D in the presence of goethite**

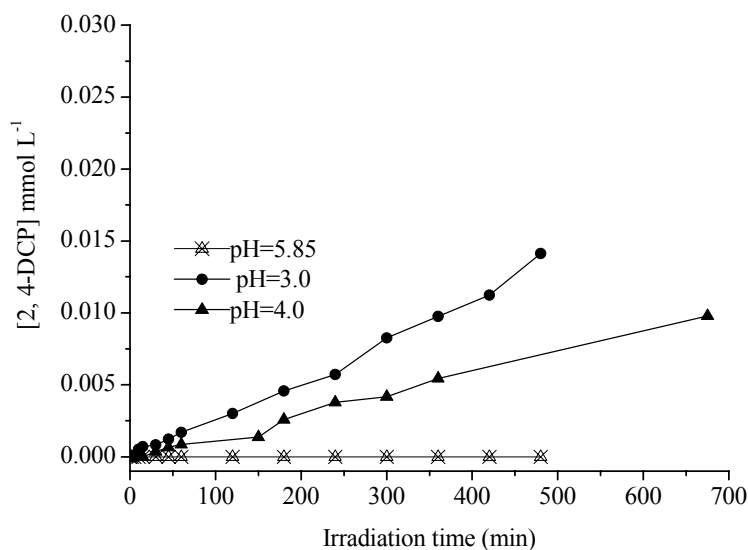


**Figure V-B-6 Influence of pH on the photoproduction of 2, 4-DCP in suspension of goethite**  
 ([Goethite]= 0.2 g L<sup>-1</sup>, [2, 4-D]= 0.1 mmol L<sup>-1</sup>)

### **B-2-3- Effect of isopropanol on photodegradation of 2, 4-D**

Experiments were performed to study influence of isopropanol on the photodegradation of 2, 4-D in the suspension of goethite at pH 4.0. Results were

shown in Figure V-B-7. The photodegradation efficiency of 2, 4-D without isopropanol in suspension is higher than that with isopropanol. No more than 10% of 2, 4-D was degraded in suspension with isopropanol after 8 h of irradiation. Around 20% of 2, 4-D was degraded in suspension without isopropanol after 8 h of irradiation. 2, 4-DCP, as main photoproducts, were detected in this period. And after 8 h of irradiation,  $0.0075 \text{ mmol L}^{-1}$  was observed in suspension with or without isopropanol (Figure V-B-8).

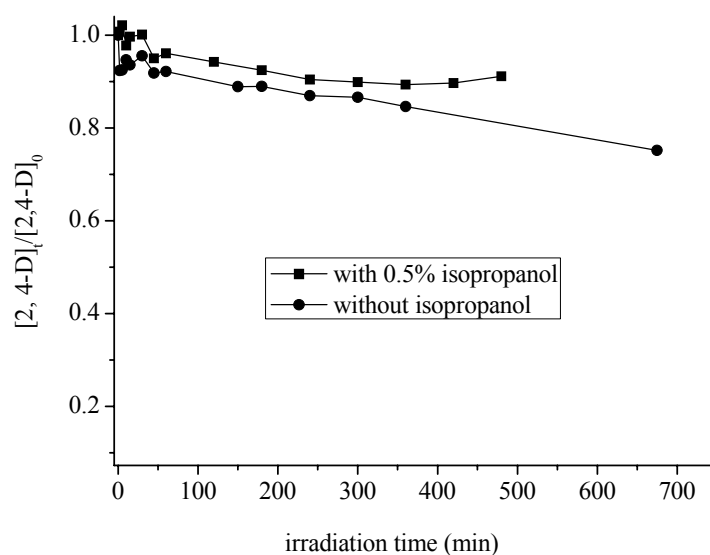


**Figure V-B-7 Influence of isopropanol on the photodegradation of 2, 4-D in suspension of goethite at pH 4.0 ([goethite]=  $0.2 \text{ g L}^{-1}$ , [2, 4-D]<sub>0</sub>=  $0.1 \text{ mmol L}^{-1}$ )**

However, the degradation of 2, 4-D in the presence of isopropanol shows that the mechanism of degradation is not only due to  $\cdot\text{OH}$  radicals photogenerated in aqueous solution. A reaction at the surface of the goethite particles can take place in such systems.

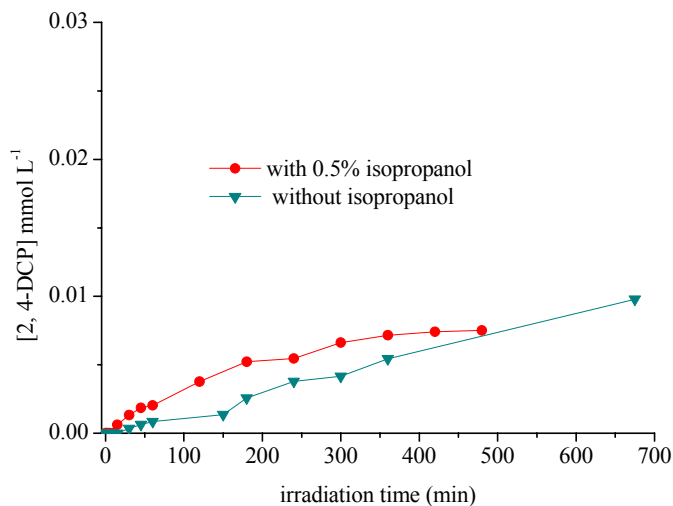


**Figure V-B-8 Influence of isopropanol on the photoproduction of 2, 4-DCP in suspension of goethite at pH 4.0([goethite]= 0.2 g L<sup>-1</sup>, [2, 4-D]<sub>0</sub>= 0.1 mmol L<sup>-1</sup>)**

The formation of 2, 4-DCP is not strongly affected by the presence of isopropanol and on the contrary of the degradation of 2, 4-D, the formation of 2, 4-DCP is higher at the beginning of the irradiation with isopropanol.

#### **B-2-4-comparison of 2, 4-D and 2, 4-DCP on photodegradation**

Since the main photoproduct of 2, 4-D degradation was 2, 4-DCP a comparison of the photodegradation of both organics were carried out. There is probably a competition of 2, 4-D and 2, 4-DCP on photodegradation in suspension. Experiments were carried out with 0.1 mmol L<sup>-1</sup> of 2, 4-D and 0.1 mmol L<sup>-1</sup> of 2, 4-DCP in the same condition in suspension (initial pH 4.0; [goethite] = 0.2 g L<sup>-1</sup>). The result was compared in figure V-B-9. After 8 h of irradiation, 0.008mmol L<sup>-1</sup> of 2, 4-DCP was degraded, and nearly 0.02 mmol L<sup>-1</sup> of 2, 4-D. It is observed that the degradation rate of 2, 4-D was faster (more than two times) than that of 2, 4-DCP at pH 4.0 in suspension of goethite.

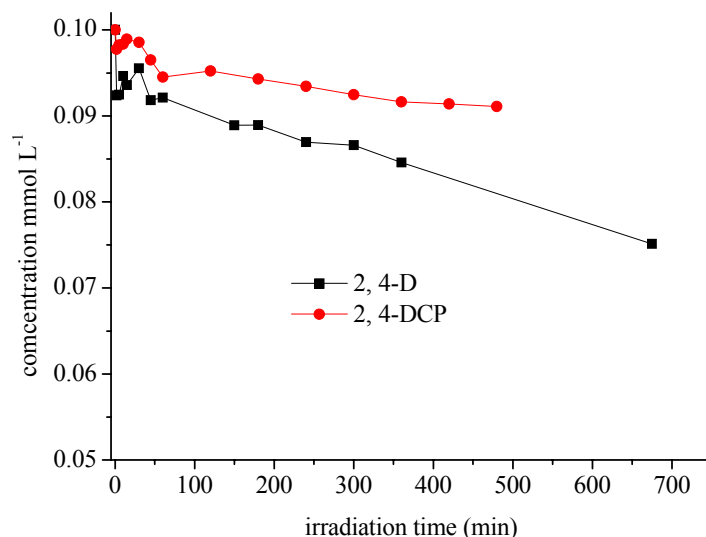


**Figure V-B-9 Comparison of 2, 4-D and 2, 4-DCP on photodegradation ( initial concentration: [2, 4-D] = 0.1 mmol L<sup>-1</sup>, [2, 4-DCP] = 0.1 mmol L<sup>-1</sup>, [goethite] = 0.2 g L<sup>-1</sup>)**

### **B-3- Photodegradation of 2, 4-D at 365 nm in suspension of goethite with EDDS**

Experiments were carried out to study the photodegradation of 2, 4-D at 365 nm in the suspension with EDDS and goethite. Concentration of EDDS and goethite, initial pH of suspension, influence of O<sub>2</sub> were all studied. Photodegradation of 2, 4-D, photoproduction of 2, 4-DCP and total iron concentrations were all detected in this work.

#### **B-3-1- influence of [EDDS] on 2, 4-D photodegradation in the suspension of goethite**

The concentration of EDDS in suspension of goethite was an important factor on photodegradation of 2, 4-D. Experiments were carried out at pH 6.0. The initial concentration of goethite used in this work was 0.2 g L<sup>-1</sup>. The concentration of EDDS are 0.1, 0.5 1.0, 2.0 and 4.0 mmol L<sup>-1</sup>. The suspension contains 0.1 mmol L<sup>-1</sup> of 2, 4-D with an initial pH value equal to 6.0. Results are shown in Figure V-B-10 and Figure

V-B-11. The photodegradation efficiency of 2, 4-D was higher with  $[\text{EDDS}] = 0.5 \text{ mmol L}^{-1}$  than that with other concentration of EDDS after 8 h of irradiation 33% of 2, 4-D was degraded in this condition. The concentrations of 0.1 and 4  $\text{mmol L}^{-1}$  of EDDS in suspension of goethite led to the same concentration of 2, 4-D degraded after 8 h of irradiation corresponding at 23% approximately. In this part, the photodegradation efficiency was not increased with the increase of EDDS concentration in suspension. Actually, if the EDDS concentration is too high, competition reactions will strongly exist between the organic substances in aqueous solutions. As a consequence, less active species are available for the degradation of 2, 4-D. For this reason, the photodegradation efficiency of 2, 4-D is almost the same in the presence of 4.0 and 0.1  $\text{mmol L}^{-1}$  of EDDS in the goethite suspension. Another reason could be also due to lower penetration of the light in the solution when the concentration of goethite is too high. Anyway, the important result is that in the presence of EDDS the degradation of 2, 4-D is effective and important at pH 6.0. No degradation of 2, 4-D is observed at this pH without EDDS.

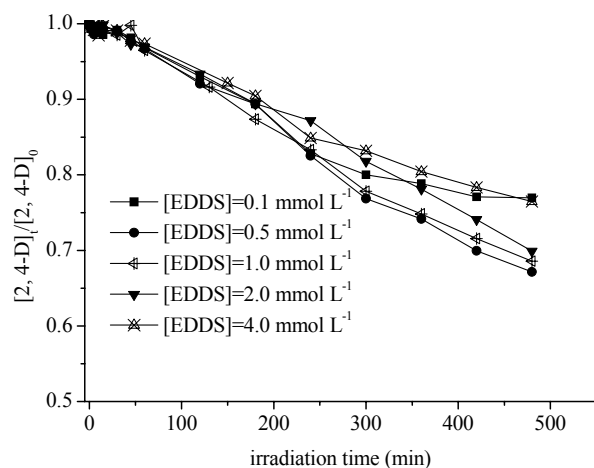


**Figure V-B-10 Influence of  $[\text{EDDS}]$  on 2, 4-D photodegradation in the suspension of goethite.**

**( $[\text{goethite}] = 0.2 \text{ g L}^{-1}$ ,  $[\text{2,4-D}]_0 = 0.1 \text{ mmol L}^{-1}$ , initial pH=6.0)**

For photoproduction of 2, 4-DCP in suspension, the concentration was also

higher in suspension with 0.5 mmol L<sup>-1</sup> of EDDS than in suspension with 0.1, 1.0, 2.0 and 4.0 mmol L<sup>-1</sup> of EDDS. These results are in good agreement with those of 2, 4-D degradation.

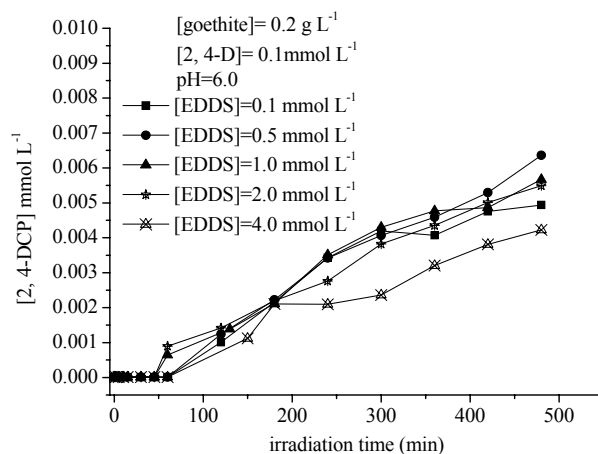


**Figure V-B-11 influence of [EDDS] on photoproduction of 2, 4-DCP in the suspension of goethite. ([goethite]=0.2 g L<sup>-1</sup>, [2,4-D]<sub>0</sub>=0.1 mmol L<sup>-1</sup>, initial pH=6.0)**

### **B-3-2- influence of goethite concentration on 2, 4-D photodegradation**

The concentration of goethite was also an important factor on the photodegradation of 2, 4-D in this work. Experiments were carried out at pH 6.0. The initial concentration of EDDS used in this work is 0.5 mmol L<sup>-1</sup>. The concentration of goethite is 0.05, 0.1, 0.2 and 0.4 g L<sup>-1</sup>. The initial concentration was 0.01 mmol L<sup>-1</sup>. Results are shown in Figure V-B-12 and Figure V-B-13. The photodegradation efficiency of 2, 4-D was highest with [goethite] = 0.05 g L<sup>-1</sup> than that with other concentration of goethite after 8 h of irradiation, 37% of 2, 4-D was degraded. The same effect was observed without EDDS; higher efficiency at 0.05 g L<sup>-1</sup> of goethite but no strong difference between all the concentrations of goethite was noticed.



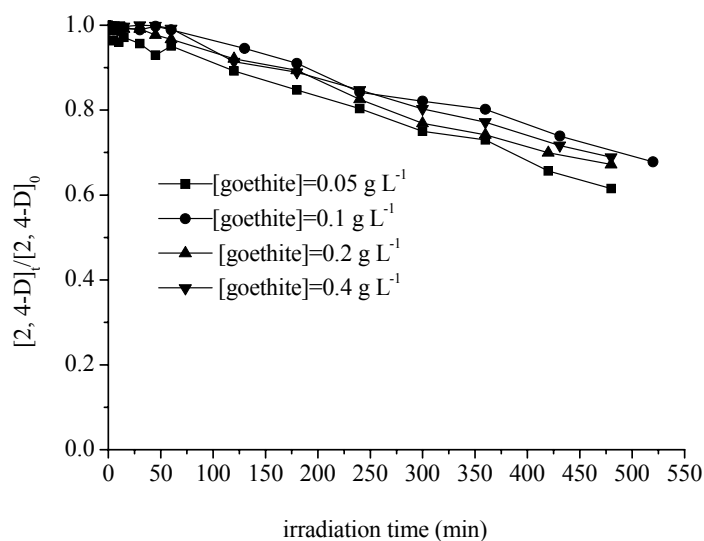


**Figure V-B-12 influence of goethite concentration on 2, 4-D photodegradation. ([EDDS]=0.5 mmol L<sup>-1</sup>, [2,4-D]<sub>0</sub>=0.1 mmol L<sup>-1</sup>, initial pH=6.0)**

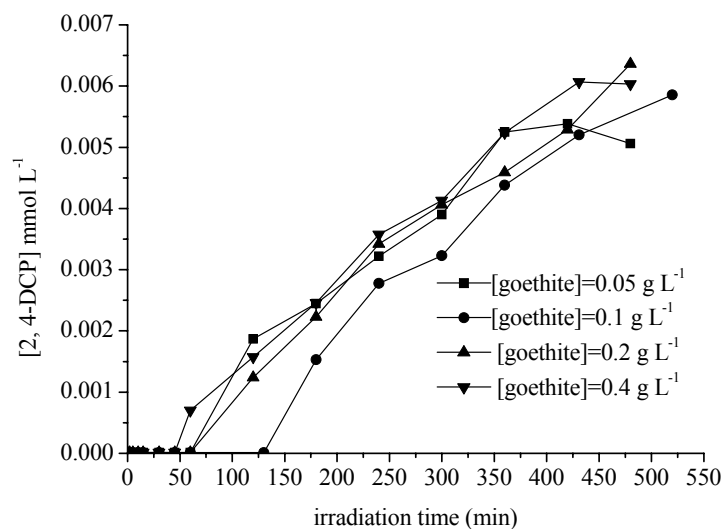


**Figure V-B-13 influence of goethite concentration on photoproduction of 2, 4-DCP in the suspension. ([EDDS]=0.5 mmol L<sup>-1</sup>, [2,4-D]<sub>0</sub>=0.1 mmol L<sup>-1</sup>, initial pH=6.0)**

The formation of 2, 4-DCP was similar whatever the goethite concentration.

### **B-3-3- influence of initial pH on 2, 4-D photodegradation in goethite suspension**

The pH is a very important parameter in many kinds of reactions. Experiments were carried out to study the pH effect on the photodegradation of 2, 4-D in suspension with  $0.2 \text{ g L}^{-1}$  of goethite,  $1.0 \text{ mmol L}^{-1}$  of EDDS and  $0.1 \text{ mmol L}^{-1}$  of 2, 4-D under irradiation at 365 nm. pH was adjusted to the desired value with NaOH or  $\text{HClO}_4$ . From the results presented in Figure V-B-14, it appears that the pH has a strong effect on the photodegradation reaction. The optimal photodegradation efficiency of 2, 4-D was observed at pH = 6.0. For example, after 8 h of irradiation, approximately 30% of 2, 4-D was degraded at pH = 6.0, but no degradation of 2, 4-D was observed at pH = 8.5, and only 18% at pH = 3.0.

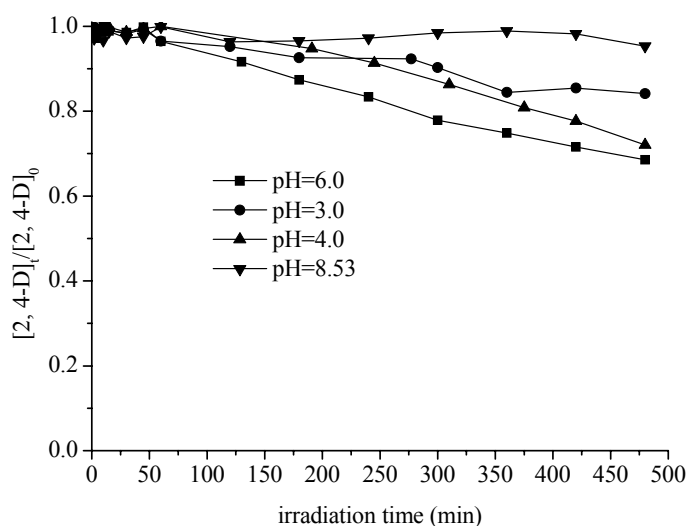


**Figure V-B-14 Influence of initial pH on photodegradation of 2, 4-D in the suspension of goethite. ([goethite] =  $0.2 \text{ g L}^{-1}$ , [EDDS] =  $1.0 \text{ mmol L}^{-1}$ ,  $[2, 4-D]_0 = 0.1 \text{ mmol L}^{-1}$ )**

2, 4-DCP concentrations were also determined at the same time. Results are presented in Figure V-B-15. The pH had also a strong effect on the photoproduction of 2, 4-DCP. At pH = 6.0 and 4.0, the maximum concentration of 2, 4-DCP was more than  $0.006 \text{ mmol L}^{-1}$ , it was  $0.004 \text{ mmol L}^{-1}$  at pH 3.0 and no 2, 4-DCP is detected at pH 8.5.

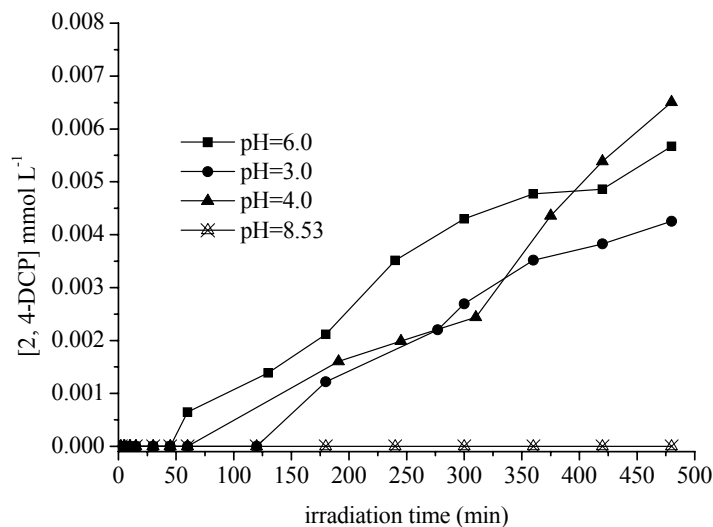


**Figure V-B-15 Influence of initial pH on photoproduction of 2, 4-DCP in the suspension of goethite. ( $[\text{goethite}] = 0.2 \text{ g L}^{-1}$ ,  $[\text{EDDS}] = 1.0 \text{ mmol L}^{-1}$ ,  $[\text{2,4-D}]_0 = 0.1 \text{ mmol L}^{-1}$ )**

## Conclusions

The concentration of 2, 4-D was almost the same even after 39 h of shaking period in the aqueous solutions in the presence of goethite. It means that there was no obvious adsorption of 2, 4-D on the surface of goethite particles at pH 4.0. With the increasing of time, in evidence, nearly 9% of 2, 4-D was adsorbed on the goethite at pH 3.0. But even at pH 3.0, no more than 4% of 2, 4-D were adsorbed on the goethite in suspension after 8 h of shaking period.

2, 4-D degradation photoinduced by goethite and goethite with or without EDDS were investigated in this study. Results indicate that pH, concentrations of goethite and EDDS and presence of isopropanol all have effect on the 2,4-D degradation.

The pH 6.0 is favorable for the photodegradation of 2, 4-D in suspension of goethite with EDDS. On the contrary without EDDS, pH 3.0 is favorable for the photodegradation of 2, 4-D and no degradation was observed at pH 6.0. The presence of isopropanol decreased the photodegradation efficiency of 2, 4-D by a factor of two

in the suspension of goethite. This is in agreement with the reaction of  $\bullet\text{OH}$  radical with isopropanol. This result shows that  $\bullet\text{OH}$  radicals are formed in this system but it is not the only reactive species or process capable to degrade 2, 4-D. Same results were observed with the photoproduction of 2, 4-DCP.

The fact that 2, 4-D is degraded by the goethite in the presence of EDDS at pH 6.0 is a very important result for the fate of organic pollutants in aquatic surface. Indeed, such process can be present in real environment and can play an important role for the transformation of organic matter.



## **VI-Photodegradation of atrazine photoinduced by the Fe(III)-EDDS complex and Fe(III)-pyruvate complex**

Atrazine (2-chloro-4-ethylamino-6-isopropylamino-1, 3, 5-triazine) was used as a model compound. Figure VI-A-1 was the chemical formula of atrazine

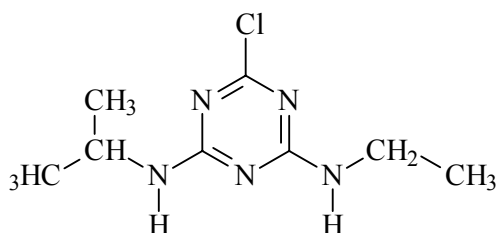


**Figure VI-A-1 Chemical formula of atrazine**

It was a selective inside-absorbing herbicide which can be used in the fields of corn, sorghum, orchard and forest, controlling broad-leaf and grassy weeds. It was not readily biodegradable and presented a relatively high persistence in soils and even reaches the groundwater. Its solubility in water was low ( $1.61 \times 10^{-4}$  mol L<sup>-1</sup>) and did not depend on pH. Atrazine, like other herbicides of the *S*-triazine group, was barely oxidized by ozone. Many methods have been developed to remove atrazine, including adsorption on activated carbon and advanced oxidation processes.

The aims of this study were as follows:

(1) studying the photochemical degradation of atrazine induced by the Fe(III)-EDDS system and examining several factors that controlled the kinetics of atrazine degradation.

(2) studying the photochemical degradation of atrazine induced by the Fe(III)-Pyr system and examining several factors that controlled the kinetics of atrazine degradation.

Experiments were carried out to study the photodegradation of atrazine induced by the Fe(III)-Carboxylate complexes, such as Fe(III)-EDDS and Fe(III)-pyruvate.

Parameters such as wavelength irradiation, complex and oxygen concentration and pH, were all studied in this work.

### **A-1-atrazine in aqueous solution**

The UV-visible spectrum of solutions with different concentrations of atrazine is presented in Figure VI-A-2. Atrazine has two bands with maximum absorption at 220 and 260 nm.

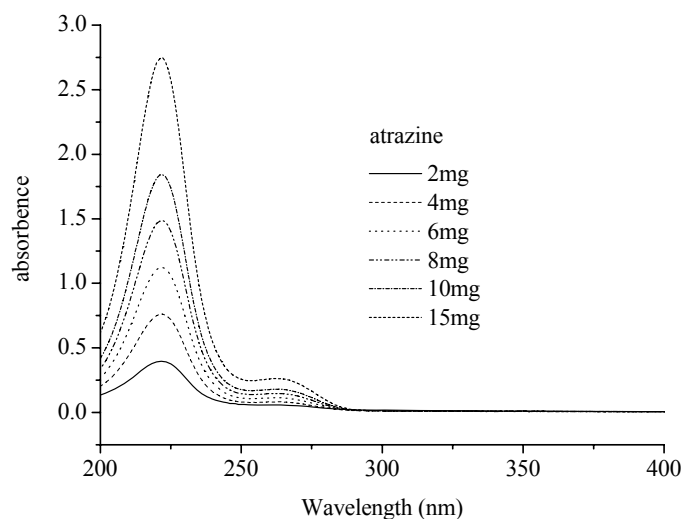


**Figure VI-A-2-UV-visible spectra of atrazine at different concentrations.**

Experiments were performed to study UV-visible spectra of different aqueous solutions: (a)  $0.3 \text{ mmol L}^{-1} \text{ Fe(III)}$ ; (b)  $10 \text{ mg L}^{-1} \text{ atrazine}$ ; (c) mixture of  $0.3 \text{ mmol.L}^{-1} \text{ Fe(III)}$  and  $10 \text{ mg L}^{-1} \text{ atrazine}$ ; (d) sum of (a) and (b) spectra. Figure VI-A-3 shows the spectra of the solutions 3 min after the preparation. The spectrum of the mixture (Fe(III) + atrazine) correspond to the sum of the spectra of the both components. This result shows that there is no interaction (complexation) between atrazine and Fe(III) in the aqueous solution and in the fundamental state.

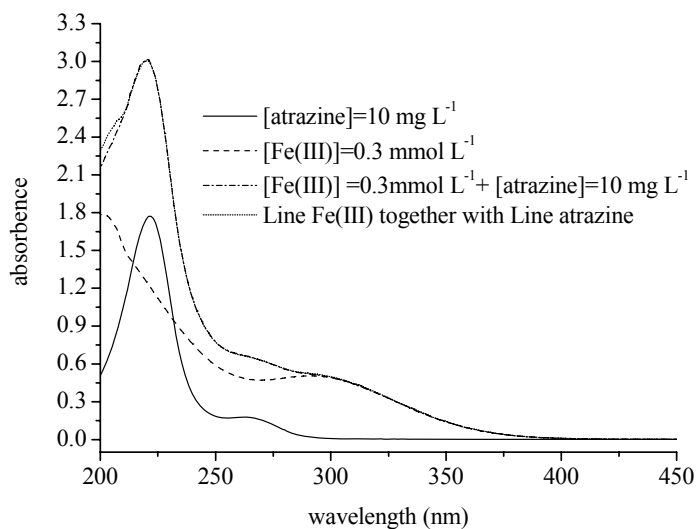


**Figure VI-A-3 UV-Visible absorption spectra of aqueous solution 3 min after the preparation with  $0.3 \text{ mmol L}^{-1}$  of Fe(III) and  $10 \text{ mg L}^{-1}$  of atrazine**

## **A-2-Degradation of atrazine photoinduced by Fe(III)-EDDS complex at 365 nm**

The photodegradation of atrazine was studied in the presence of Fe(III)-EDDS complexes. Irradiation was with polychromatic tubes emitting between 300 and 500 nm. Concentration of complex and oxygen, pH and effect of isopropanol were all studied in this work.

### **A-2-1- Effect of initial Fe(III), EDDS concentrations on the degradation of atrazine**



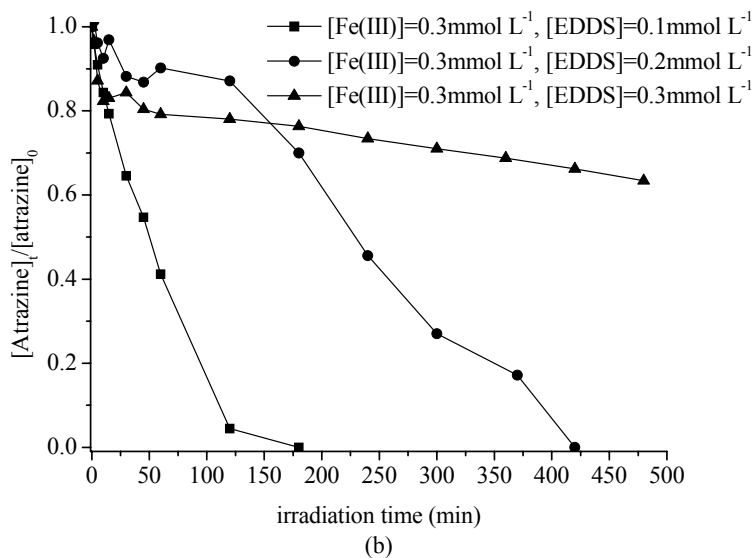
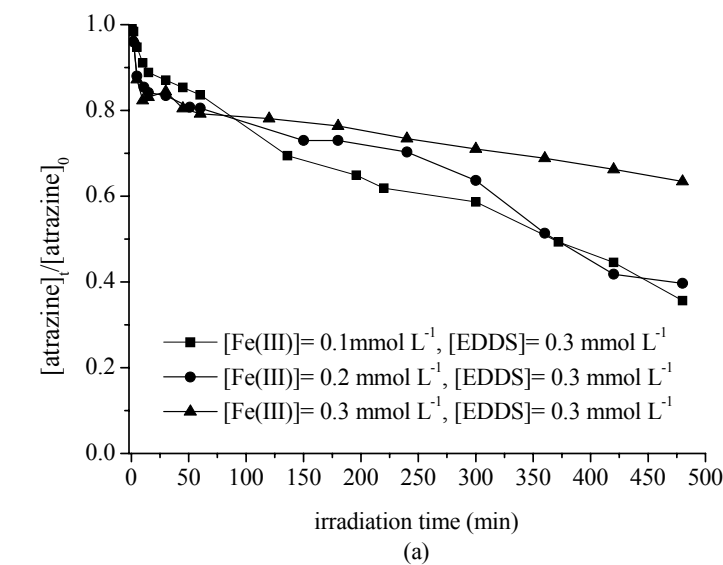
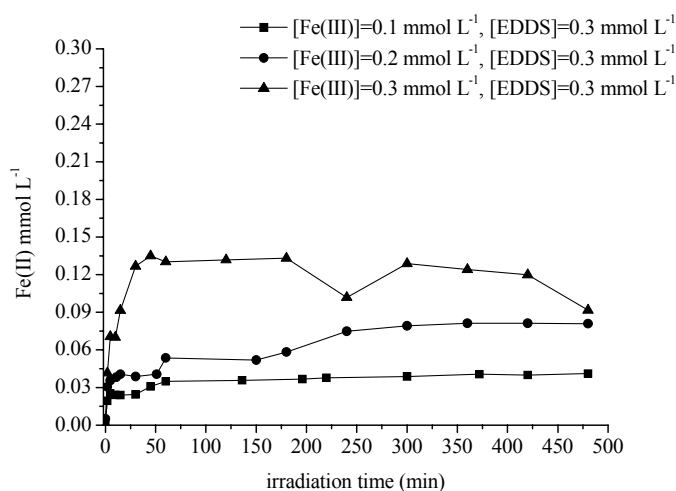


**Figure VI-A-4 Photodegradation of atrazine in the Fe(III)-EDDS systems, (a) with different Fe(III) concentrations and (b) with different EDDS concentrations. pH = 3.0.**

In this work, both Fe(III) and EDDS were the essential elements for the degradation of atrazine. It was necessary to study their effect on the reaction. Experiments were carried out to study the effect of different ratio of Fe(III)/EDDS on

the photodegradation of atrazine. Figure VI-A-4 presented results in the water with the following as the initial concentrations: 10.0 mg L<sup>-1</sup> of atrazine, 0.3 mmol L<sup>-1</sup> of EDDS and different Fe(III) concentrations under irradiation at pH 3.0. With an increase of the initial concentration of Fe(III) from 0.1 to 0.3 mmol L<sup>-1</sup>, after 8 hours of irradiation, the photodegradation efficiency of atrazine have reached 60%, 55% and 25% in the solutions. The photodegradation efficiency of atrazine was also decreased from 100% to 25% with the increase of EDDS concentration from 0.1 mmol L<sup>-1</sup> to 0.3 mmol L<sup>-1</sup> after 3 hours of irradiation.

In these experimental conditions (pH = 3.0), Fe(III) species seems to be more photoreactive than Fe(III)-EDDS complex for the degradation of atrazine. When the concentration of EDDS decreases from 0.3 to 0.1 mmol L<sup>-1</sup>, the complexation of iron is not complete and the degradation of atrazine strongly increases. This result can be also explained by the competition of •OH radicals reaction on atrazine or on EDDS and its oxidized degradation products. Moreover, when the concentration of Fe(III) decreases from 0.3 to 0.1 mmol L<sup>-1</sup> the degradation efficiency of atrazine is divided by a factor of two. In this case the lower degradation of atrazine is mainly due to the lower concentration of iron.



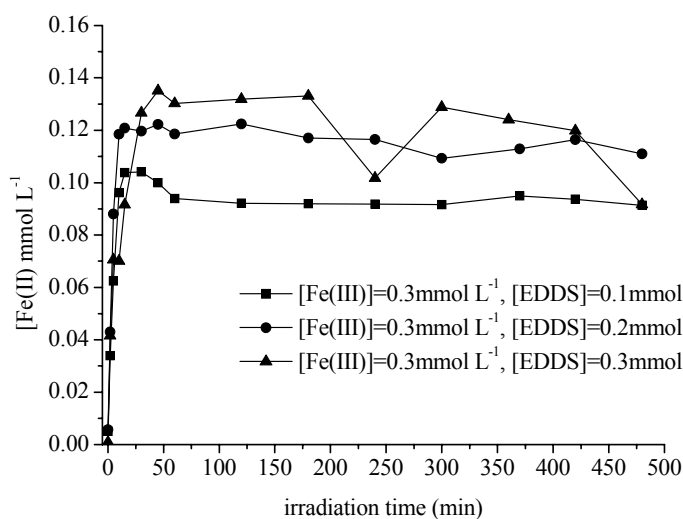


**Figure VI-A-5 Influence of ratio of Fe(III)/EDDS on the photogeneration of Fe(II) in aqueous solution.**

The formation of Fe(II) was very fast at the beginning of the irradiation and in 10 to 15 minutes reached a constant value (Figure VI-A-5). This constant value was higher when the concentration of Fe(III) was higher and also when the concentration of EDDS was higher. In the case of 0.3 mmol L<sup>-1</sup> of each component, the complexation of iron was complete and the formation of Fe(II) was higher. This result indicated that, contrary to the disappearance of atrazine, the photoredox process from the complex Fe(III)-EDDS was more efficient for the formation of Fe(II) than with Fe(III) aquacomplexes. This is in agreement with the quantum yield calculation for the formation of Fe(II).

#### **A-2-2- Effect of initial pH on the degradation of atrazine**

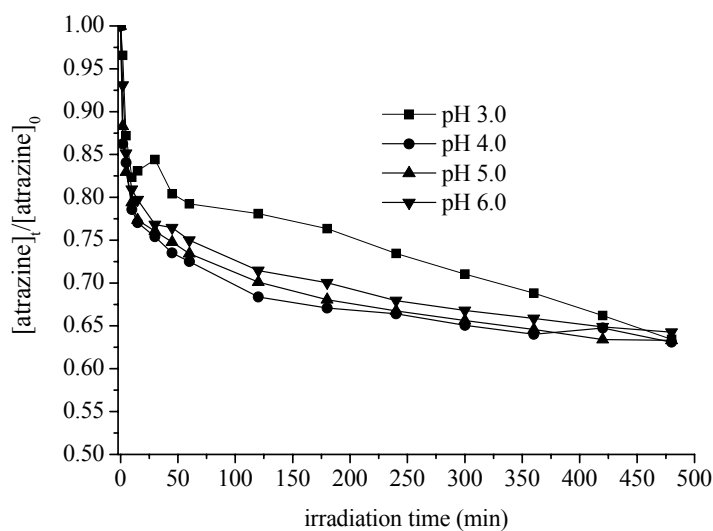


**Figure VI-A-6 Influence of initial pH on photodegradation of atrazine in the Fe(III)-EDDS systems.  $[\text{Fe(III)-EDDS}] = 0.3 \text{ mmol L}^{-1}$ ;  $[\text{atrazine}] = 10 \text{ mg L}^{-1}$ .**

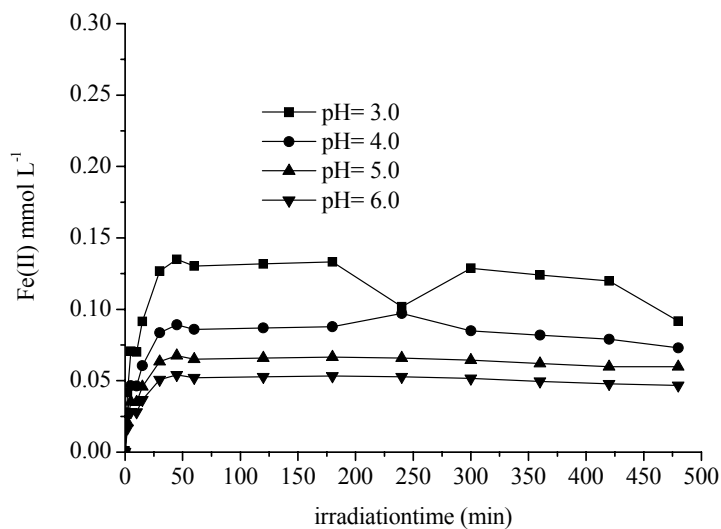


**Figure VI-A-7 Influence of initial pH on photoproduction of Fe(II) in the Fe(III)-EDDS systems.  $[\text{Fe(III)-EDDS}] = 0.3 \text{ mmol L}^{-1}$ ;  $[\text{atrazine}] = 10 \text{ mg L}^{-1}$ .**

The pH as an important parameter was studied in the solution with  $[\text{Fe(III)-EDDS}] = 0.3 \text{ mmol L}^{-1}$  and  $[\text{atrazine}] = 10.0 \text{ mg L}^{-1}$  under irradiation. Figure VI-A-6 and Figure VI-A-7 illustrates the experiment results. More than 30% of the atrazine was

degraded at pH 6.0 after 180 min of irradiation. The photodegradation efficiency of atrazine was lower at pH =3.0; only 22% of atrazine was degraded after 180 min of irradiation. It appeared that the pH can be an important parameter in the photodegradation of atrazine induced by Fe(III)-EDDS complex, but after 8 h of irradiation the percentage of atrazine degraded was the same whatever the starting pH (35%). Interestingly, acidic condition was favorable for the photocycling of Fe(III)/Fe(II) and the formation of active oxygen species, which was the main reason for the degradation of atrazine. For Fe(III)-EDDS complex, pH 6.0 is better for the photodegradation efficiency of atrazine than pH 3.0. But for longer irradiation times the degradation continue only at pH = 3.0 where the Fe(III)/Fe(II) cycle was still efficient for the photogeneration of oxidative species.

#### **A-2-3- Effect of initial atrazine concentration on the degradation of atrazine**

Experiments were carried out under different atrazine initial concentrations in the Fe(III)-EDDS ( $0.3 \text{ mmol L}^{-1}$ ) system at pH 3.0. Results are shown in Figure VI-A-8 and Figure VI-A-9. The number of atrazine molecules degraded increased when the atrazine concentration increased. When the concentration of atrazine was higher, the radical species photogenerated from Fe(III)-EDDS complex reacted preferentially on atrazine than in other organic compounds. This result shows that there is a real competition for  $\bullet\text{OH}$  radical attack between atrazine ( $k = 1.2 \text{ to } 3.0 \times 10^9 \text{ mol}^{-1} \text{ L s}^{-1}$ ) and EDDS or oxidized EDDS compounds.

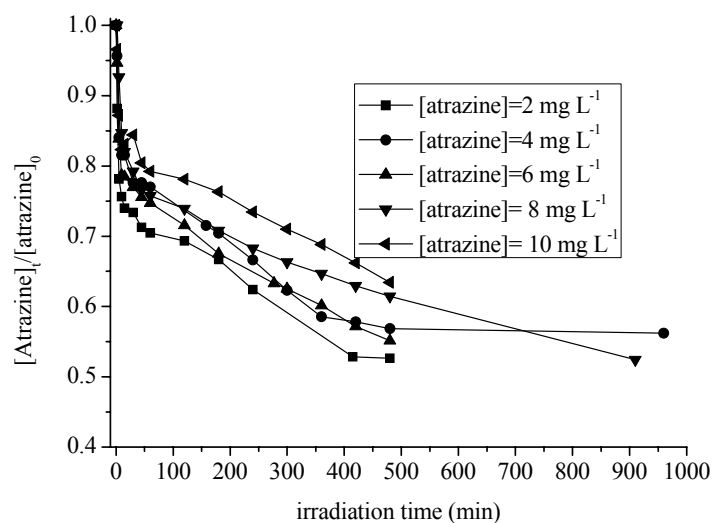


**Figure VI-A-8 Influence of initial concentration of atrazine on photodegradation efficiency.  $[\text{Fe(III)}\text{-EDDS}] = 0.3 \text{ mmol L}^{-1}$**

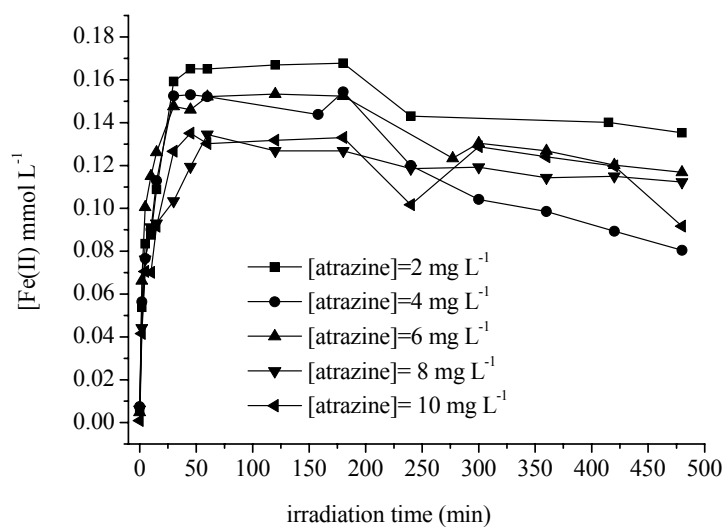


**Figure VI-A-9 Influence of initial concentration of atrazine on photoproduction of Fe(II) in the Fe(III)-EDDS system.  $[\text{Fe(III)}\text{-EDDS}] = 0.3 \text{ mmol L}^{-1}$**

Photogenerated concentration of Fe(II) was slightly smaller with the increase of atrazine initial concentration.

## **B-Photodegradation of atrazine in the aqueous solutions containing Fe(III)-Pyr complex**

The composition and photochemical properties of the Fe(III)-Pyruvate (Fe(III)-Pyr) complexes in the aqueous solution was studied in previous work (Wang, 2008). Fe(III) was complexed by Pyr in the ratio of 1:3. Photodegradation of atrazine induced by the photolysis of Fe(III)-Pyr was studied. Parameters such as pH, the initial concentrations of Fe(III), Pyruvate (Pyr) and atrazine were all investigated. Photoproducts were detected by the LC-MS and the photodegradation scheme was proposed.  $\bullet\text{OH}$  radical was the main reactive species involving for the atrazine degradation.

### **B-1-control experiment on photodegradation of atrazine**

The control experiments were carried out in the systems with  $20\ \mu\text{mol L}^{-1}$  Fe(III) or  $20\ \mu\text{mol L}^{-1}$  Pyr or  $20.0\ \mu\text{mol L}^{-1}/60\ \mu\text{mol L}^{-1}$  Fe(III)-Pyr complex. The initial concentration of atrazine was  $10\ \text{mg L}^{-1}$ . The dark reaction was carried out to keep the mixture of atrazine, Fe(III) and pyruvate in the dark. From the results in Figure VI-B-1, no degradation of atrazine was observed after 150 min in the dark. The presence of light was an essential parameter for the degradation of atrazine. Direct irradiation of  $10\ \text{mg L}^{-1}$  of atrazine showed no degradation of atrazine. The photolysis of atrazine was not present between 300 and 500 nm. The photodegradation efficiency of atrazine was much higher in the aqueous solution with Fe(III)-Pyr complex than in the one with the only presence of Pyr or Fe(III). Although  $\bullet\text{OH}$  radicals could be produced by the direct photolysis of Fe(III) and Pyr, the amount of the radicals produced was less important than in the Fe(III)-Pyr system. In this case, Fe(III)-Pyr complex overlapped with the entire spectrum of the tubes (300 to 500 nm), allowing

the effective use of irradiation. After 150 min of irradiation, nearly 85% atrazine was degraded in the Fe(III)-Pyr system and only 35 and 26% with Fe(III) and pyruvate respectively.

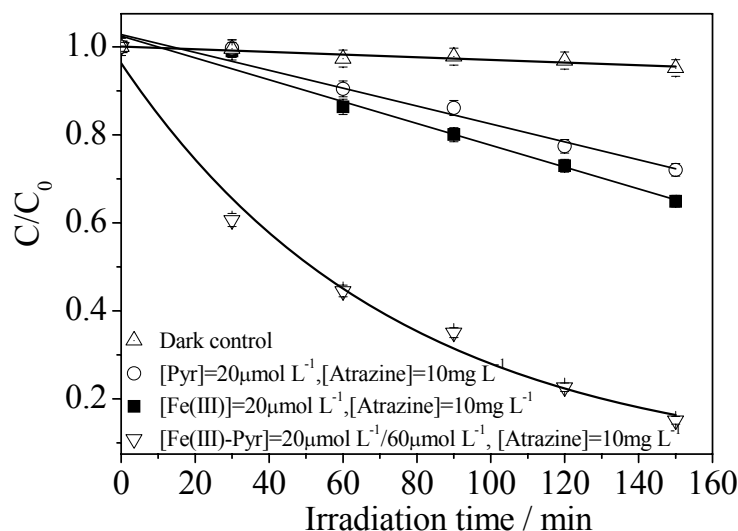


Figure VI-B-1 Photodegradation of atrazine under different conditions at pH 3.0

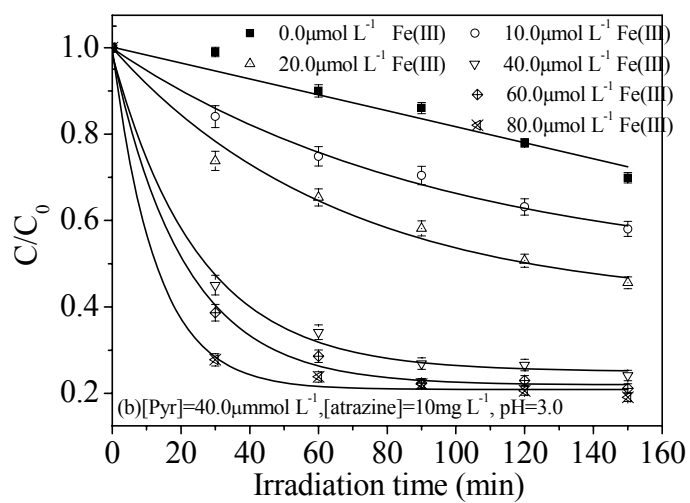
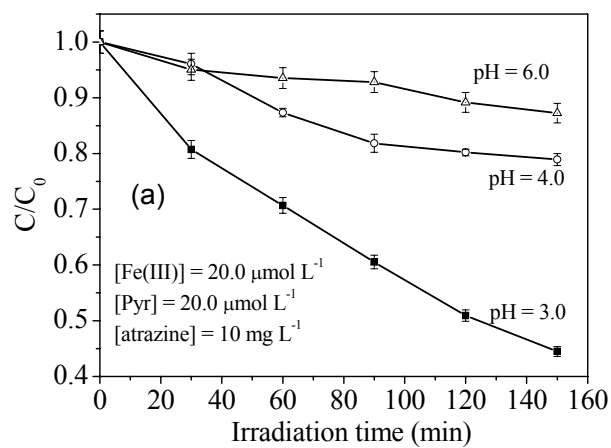
### **B-2-Effect of pH, initial Fe(III), Pyr and atrazine concentrations on the degradation of atrazine**

The pH as an important parameter was studied in the solution with 20 μmol L<sup>-1</sup> Fe(III) and 20.0 μmol L<sup>-1</sup> Pyr and 10.0 mg L<sup>-1</sup> atrazine under irradiation. Figure VI-B-2 (a) illustrates the experiment results. More than 55% of the atrazine was degraded at pH 3.0 after 150 min of irradiation. The photodegradation efficiency was lower at high pH. Only 20% of atrazine was degraded at pH 4.0 and 13% at pH 6.0 after 150 min of irradiation. It appeared that the pH played an important role in the photodegradation of atrazine. Acidic condition was favorable for the photocycling of Fe(III)/ Fe(II) and the formation of active oxygen species, which was the main reason



for the degradation of atrazine.

In this work, both Fe(III) and Pyr were the essential elements for the degradation of atrazine. It was necessary to study their effect on the reaction. Experiments were carried out to study the effect of different ratio of Fe(III)/Pyr on the photodegradation of atrazine. Figure VI-B-2 (b) presents the results in the water with the following as the initial concentrations: 10.0 mg L<sup>-1</sup> of atrazine, 40.0 μmol L<sup>-1</sup> of Pyr and different Fe(III) concentrations under irradiation at pH 3.0. With an increase of the initial concentration of Fe(III) from 0 to 80 μmol L<sup>-1</sup>, the photodegradation efficiency increased from 30% to 80% after 150min irradiation. As presented in Figure VI-B-2 (c), the photodegradation efficiency of atrazine was also increased from 35% to 84% with the increase of Pyr concentration from 0 to 80 μmol L<sup>-1</sup>. The enhancement of atrazine degradation efficiency was attributed to the high concentration of Fe(III)-Pyr complex, producing more active oxygen radicals in the system. For high activity of •OH radicals, it was found that they were the most efficient radicals for the pollutant degradation. From the photolysis processes of Fe(III)-Pyr, both reagents were found to be essential to promote organic compounds degradation under this type of irradiation. Experiments were carried out under different atrazine initial concentrations in the Fe(III)-Pyr system at pH 3.0. Results are shown in Figure VI-B-4 (d). From the table VI-B-1 it was evidence that the initial rate of atrazine degradation increased with the concentration of atrazine. At higher concentration •OH radicals reacted preferentially with atrazine.



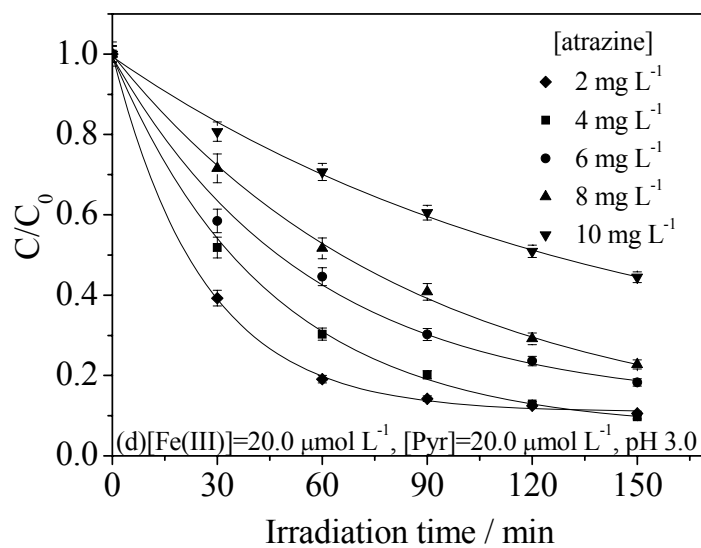
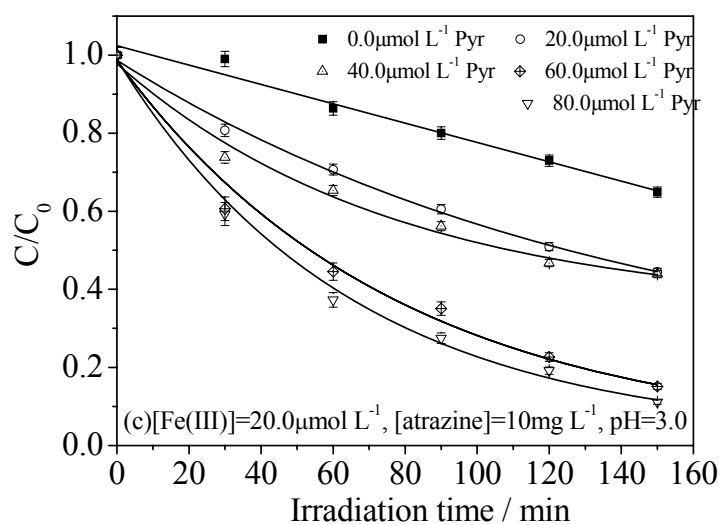


**Figure VI-B-2. Photodegradation of atrazine in the Fe(III)-Pyr systems, (a) at different pH values; (b) with different Fe(III) concentrations; (c) with different Pyr concentrations; (d) with different atrazine concentrations.**

Table VI-B-1 Kinetics analysis of the photodegradation of atrazine

System	R	Initial Rate (mg L <sup>-1</sup> min <sup>-1</sup> )
Pyr (μM)	[Fe(III)]= 20.0μ mol L <sup>-1</sup> , [atrazine]=10mg L <sup>-1</sup> , pH=3.0	
10	0.9761	0.025
20	0.9965	0.061
40	0.9887	0.088
60	0.9971	0.141
80	0.9906	0.168
Fe(III) (μM)	[Pyr]= 40.0μM, [atrazine]=10mg L <sup>-1</sup> , pH=3.0	
10	0.9704	0.021
20	0.9870	0.091
40	0.9972	0.314
60	0.9981	0.388
80	0.9881	0.637
pH	[Fe(III)-Pyr]= 20.0μM/20.0μM, [atrazine]=10mg L <sup>-1</sup>	
3.0	0.9966	0.061
4.0	0.9695	0.029
6.0	0.9574	0.011
Atrazine (mg L <sup>-1</sup> )	[Fe(III)-Pyr]= 20.0μM/20.0μM, pH=3.0	
2.0	0.9997	0.069
4.0	0.9993	0.087
6.0	0.9942	0.097
8.0	0.9989	0.088

According to the time evolution of atrazine under different conditions, we analyzed the reaction kinetics. The photodegradation of atrazine fitted well with the first order reaction kinetics. Results were presented in Table VI-B-1. Through comparing the formation of Fe(II) and degradation of atrazine under the same reaction conditions, it was concluded that the initial rate  $k_{\text{Fe(II)}}$  was higher than the  $k_{\text{atrazine}}$  as shown in Figure VI-B-3. This result is not surprising because the formation of Fe(II) is obtained from the first primary photochemical reaction. As a contrary the degradation of atrazine is due active species photogenerated after a chain of reaction.

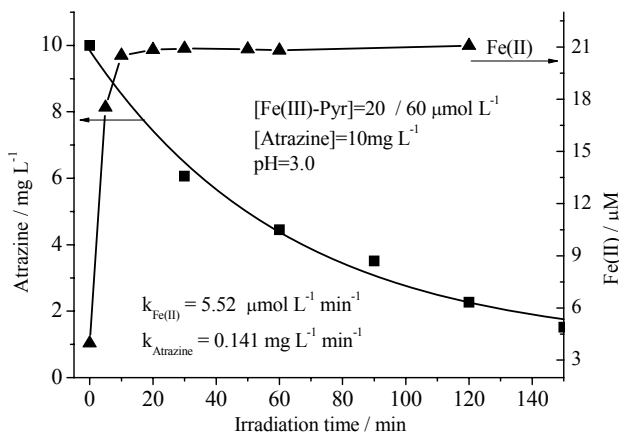
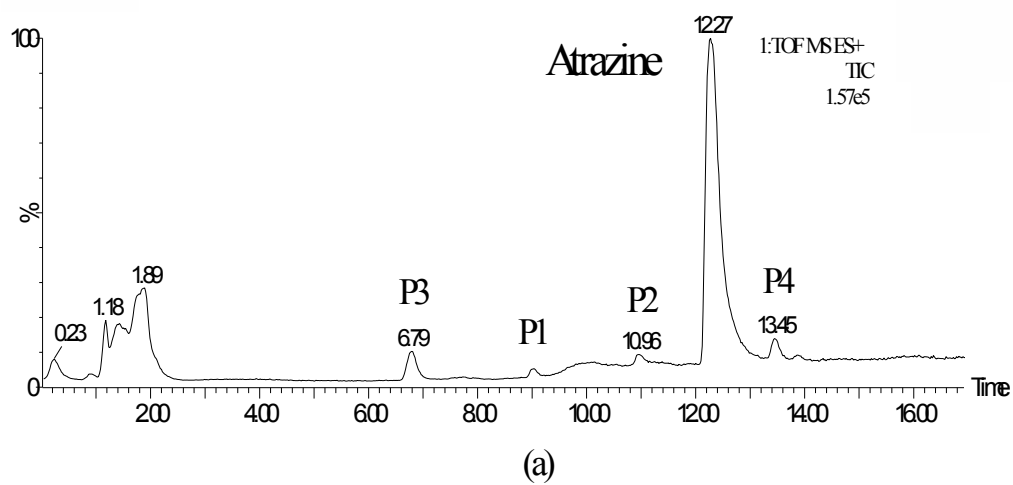


Figure VI-B-3 Kinetics analysis of atrazine degradation and Fe(II) formation

### B-3- Degradation products of atrazine

In the Fe(III)-Pyr system and under irradiation, atrazine was attacked by the active radicals, especially  $\bullet\text{OH}$  radicals. LC-MS was used to identify the intermediate photoproducts. The mass spectra were presented in Figure VI-B-4. As expected the most intense peak was observed at  $m/z$  216 corresponding to atrazine compound  $[\text{M}+\text{H}]^+$ . The four main fragments-ions  $m/z$  174, 188, 197 and 146 clearly demonstrated the formation of the degradation products 2-Chloro-4-ethylamino-6-amino-1,3,5-triazine (P1), 2-Chloro-4-isopropylamino-6-amino-1, 3, 5-triazine (P2), 2-Hydroxy-4-ethylamino-6-isopropylamino-1, 3, 5-triazine (P3) and 2-Chloro-4,6-diamino-1, 3, 5-triazine (P4).

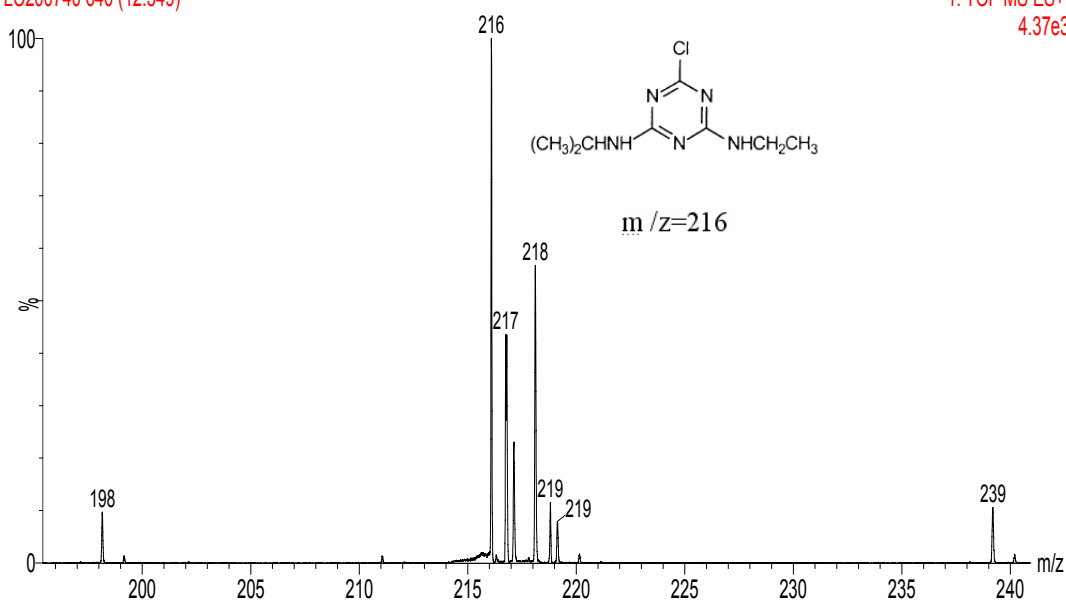


(a) total ions chromatogram from LC-MS

# **ATRAZINE T4H**

LC200740 640 (12.349)

1: TOF MS ES+  
4.37e3

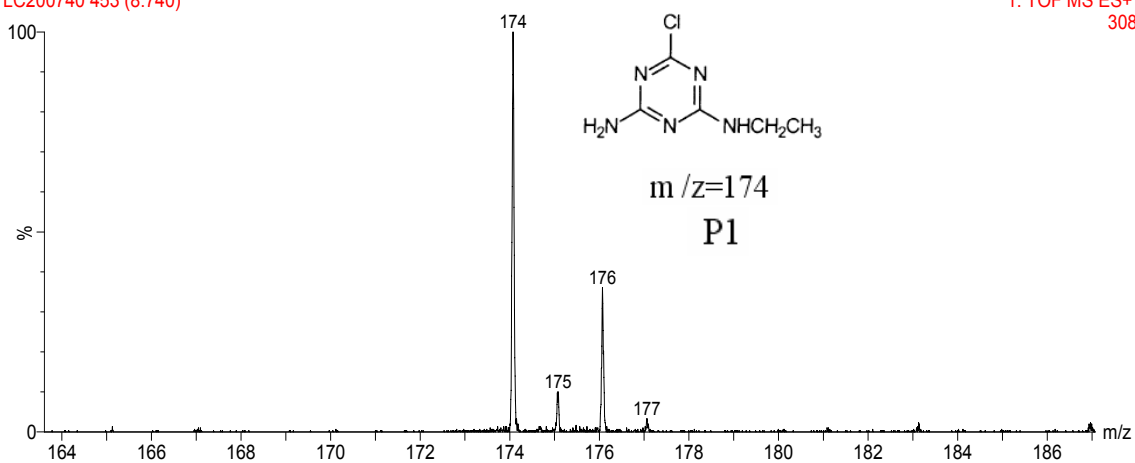


(b) LC-MS spectra of Atrazine

**ATRAZINE T4H**

LC200740 453 (8.740)

1: TOF MS ES+  
308

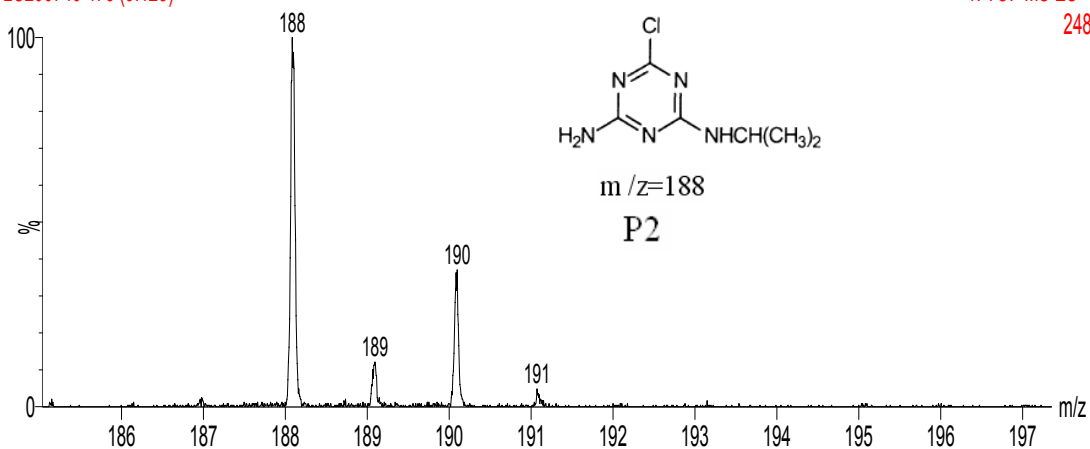


(c) LC-MS spectra of CEAT

**ATRAZINE T4H**

LC200740 473 (9.125)

1: TOF MS ES+  
248

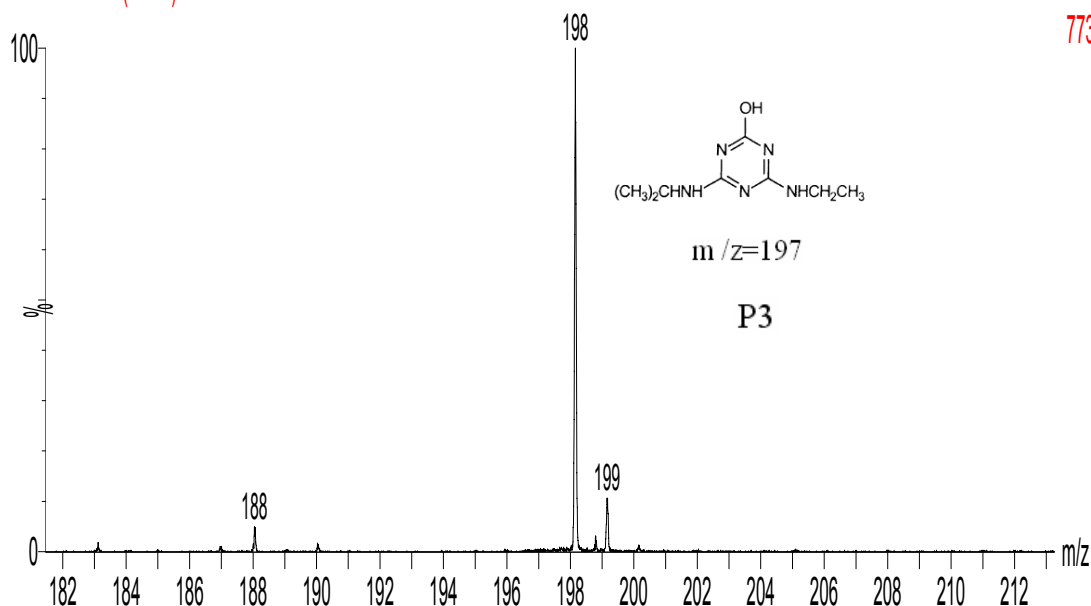


(d) LC-MS spectra of CIAT

# ATRAZINE T4H

LC200740 360 (6.946)

1: TOF MS ES+  
773

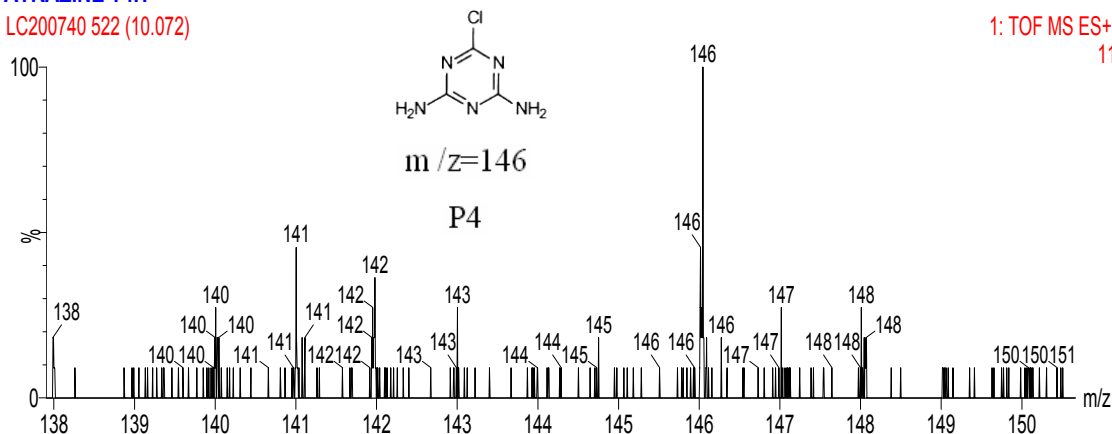


(e) LC-MS spectra of HEIT

# ATRAZINE T4H

LC200740 522 (10.072)

1: TOF MS ES+  
11



(f) LC-MS spectra of CAAT

Figure VI-B-4 LC-MS spectra of the atrazine degradation in Fe(III)-Pyr systems after 4 h of irradiation: [Atrazine] = 10 mg mL<sup>-1</sup>, [Fe(III)/Pyr] = 10 μM/30 μM, pH = 3.0.

In the Fe(III)-Pyr system and under irradiation, atrazine was attacked by the active radicals, especially the •OH radicals,. The main intermediate photoproducts



were identified by LC-MS. The four main fragments-ions  $m/z$   $[M-H^+]$  197, 188, 174 and 146 clearly demonstrated the formation of the P1, P2, P3 and P4. Figure 8 presented the scheme of the atrazine photodegradation in the Fe(III)-Pyr system.

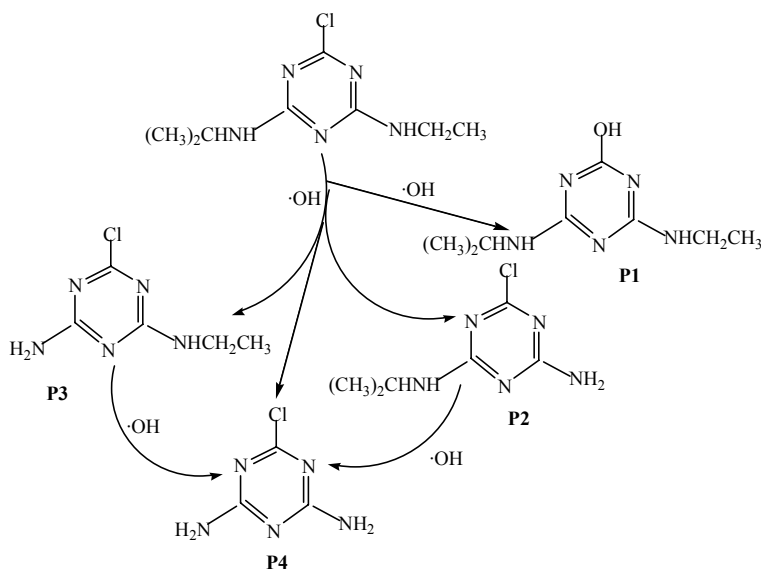


Figure VI-B-5 Proposed photodegradation mechanism

The main attack of  $\cdot\text{OH}$  radicals are i) the attack on the aromatic ring and the substitution of Cl atom by OH ii) the abstraction of H atom of the isopropyl group and iii) the H abstraction from the ethyl group.

## Conclusions

This kind of complex was stable in the aqueous solution. Under irradiation, the photolysis of Fe(III)-Pyr complexes could represent the source of active oxygen radicals, such as  $\cdot\text{OH}$ ,  $\text{CO}_3^{\cdot-}$ ,  $\text{CO}_2^{\cdot-}$ ,  $\text{H}^{\cdot}$  and  $\text{RCO}_2^{\cdot}$ . However it is well known that free Fe(III) species could generate  $\cdot\text{OH}$  radicals through the reaction  $\text{Fe(III)} + \text{H}_2\text{O} + h\nu \rightarrow \text{Fe(II)} + \cdot\text{OH} + \text{H}^+$ .  $\cdot\text{OH}$  radicals could also be generated by direct photolysis of pyruvic acid with a relative quantum yield of  $5 \pm 3\%$  (Pozdnyakov, I. P. et al., 2000). Oxygen was always involved in the formation of active oxygen species. Acidic

condition was favorable for these two photochemical reactions.

Under irradiation Fe(III)-Pyr complex could enhance the photodegradation of atrazine in the aqueous solution. High degradation efficiency was obtained at high concentrations of Fe(III)/Pyr and at lower pH (3.0). Four kinds of primary photoproducts were identified in this system. This type of complexes could be formed in the natural aquatic environment due to the presence of carboxylic acids and iron. Thus, such complexes could influence the fate of inorganic and organic pollutants existing in the natural environment. This work could help us to fully understand the photoreaction processes under solar irradiation concerning Fe(III)/Pyr complex and its potential for the degradation of pollutants in the natural surface and atmospheric water.



## **VII**

# **GENERAL CONCLUSIONS**



## **VII-General conclusions**

In our experimental conditions, we demonstrated that Fe(III) was complexed by EDDS with a ratio 1:1. We also checked the stability of Fe-EDDS complex in the dark and at room temperature. Fe(III)-EDDS is stable in the aqueous solutions in our experimental conditions (pH = 3.0 to pH = 6.0). Our results show that the pH is an important parameter for the stability of the complex and its speciation. At lower pH (< 2.0) a phenomenon of decomplexation can be proposed.

In the present study, formation of phenol from benzene was used to determine the concentration of  $\cdot\text{OH}$  radicals by the photolysis of Fe(III)-EDDS complex. Parameters, such as pH, the concentration of Fe(III) or EDDS, oxygen were all considered in the study. Results shows that the pH value has great effect on the photolysis of Fe(III)-EDDS complex in producing  $\cdot\text{OH}$ . Interestingly, the maximum concentration of  $\cdot\text{OH}$  radicals were observed at pH 6.0 (pH ranged from 3.0 to 6.0). This particular point is fully in agreement with the disappearance of 2, 4-D which is higher at pH 6.0 than 3.0 in the presence of Fe(III)-EDDS complexes. The  $\cdot\text{OH}$  concentration generated in the system increased also with the increase of Fe(III) or acid concentrations. The presence of high concentration of acid strongly favored the reoxidation of Fe(II) after the first photoredox process in the complex and as a consequence increased the efficiency of  $\cdot\text{OH}$  radicals photoproduction.. Oxygen is a crucial factor for the formation of active radicals in the aqueous solutions. Without oxygen no formation of  $\cdot\text{OH}$  radical is observed in the containing Fe-EDDS complex even under irradiation.

EDDS has positive effects on the photogeneration of  $\cdot\text{OH}$  in the aqueous solution. So, the Fe(III)-EDDS complex has the potential of utilizing sunlight as an irradiation source. Interestingly, the [S, S']-isomer of EDDS was reported to be produced naturally by a number of microorganisms, such as *Amycolatopsisjaponicum sp. nov.* So in the natural surface waters, such as lakes, which contain Fe(III)/Fe(II) and [S, S']-EDDS, photochemical reactions can be induced by sunlight, and it will play an

important role in the oxidation of organic/inorganic pollutants in natural waters. Further experimental and theoretical work is needed to fully understand the system and its application in natural aquatic or atmospheric environments.

Photodegradation of 2, 4-D and atrazine photoinduced by Fe(III)-EDDS complex was investigated in this study. Results indicate that irradiation wavelength, pH, oxygen, ratio and concentration of Fe(III)-EDDS complex and isopropanol, all have effect on the quantum yields of Fe(II) formation and 2,4-D degradation. Irradiation wavelength has a great effect on the quantum yields, both  $\Phi_{\text{Fe(II)}}$  and  $\Phi_{2,4\text{-D}}$  increase with the decrease of wavelength of irradiation. The pH 6.0 and high concentration of oxygen are all favorable for the photodegradation of 2, 4-D. In the presence of high concentration in oxygen and at pH 6.0 the total degradation of 2, 4-D and photogeneration of 2, 4-DCP are observed after 8 h of irradiation. Oxygen is necessary for an efficient degradation of 2, 4-D.

In the presence of goethite particles, the concentration of 2, 4-D was almost the same even after 39 h shaking period in the aqueous solutions. It means that there was no obvious adsorption of 2, 4-D in suspension with the presence of goethite at pH 4.0. With the increasing of time, in evidence, nearly 9% of 2, 4-D was adsorbed on the goethite at pH 3.0, But even at pH 3.0, no more than 4% of 2, 4- D were adsorbed on the goethite in suspension after 8 h shaking period.

Degradation of 2, 4-D photoinduced by goethite with or without EDDS complex were investigated in this study. Results indicate that pH, concentrations of goethite and EDDS in suspension, isopropanol all have effect on the 2,4-D degradation. The pH 6.0 is favorable for the photodegradation of 2, 4-D in suspension with goethite and EDDS. This is fully in agreement with the results obtained in the presence of the complex Fe(III)-EDDS and prove that the degradation is effective through the formation of this complex in the system goethite, EDDS and light. As a contrary, in the presence of goethite without EDDS, pH 3.0 is favorable for the photodegradation of 2, 4-D. Isopropanol depress the photodegradation efficiency of 2, 4-D in all the cases. This is in agreement with the formation of  $\bullet\text{OH}$  radical which react with isopropanol. The same results were observed with the photoproduction of 2, 4-DCP.

Under irradiation, the photolysis of Fe(III)-Pyr complexes could represent the source of active oxygen radicals, such as  $\cdot\text{OH}$ ,  $\text{CO}_3\cdot^-$ ,  $\text{CO}_2\cdot^-$ ,  $\text{H}\cdot$  and  $\text{RCO}_2\cdot$ . In the Fe(III)-Pyr system, free Fe(III) species could generate  $\cdot\text{OH}$  radicals through the reaction  $\text{Fe(III)} + \text{H}_2\text{O} + h\nu \rightarrow \text{Fe(II)} + \cdot\text{OH} + \text{H}^+$ .  $\cdot\text{OH}$  radicals could also be generated by direct photolysis of pyruvic acid with a relative quantum yield of  $5 \pm 3 \%$ . Oxygen was always involved in the formation of active oxygen species. Acidic condition was favorable for this photochemical reaction.

Fe(III)-Pyr complex could enhance the photodegradation of atrazine in the aqueous solution and under irradiation. High degradation efficiency was obtained at high concentrations of Fe(III)/Pyr and at low pH, as a contrary of the complex Fe(III)-EDDS where the photoactivity is higher at pH 6.0. Four kinds of photoproducts were identified in this work. This type of complexes could be formed in the natural aquatic environment due to the presence of carboxylic acids and iron. Thus, such complexes could influence the fate of inorganic and organic pollutants existing in the natural environment. This work could help us to fully understand the photoreaction processes concerning Fe(III)/Pyr complex and its potential for the degradation of pollutants in the natural surface and atmospheric water under solar irradiation.

The main conclusion of this thesis is that iron-organic acids complexes represent a class of species which can play a very important role in the environment for the transformation and as a consequence the fate of organic matter in aquatic compartments. We demonstrated that these complexes are photochemically (under solar light) in a large range of pH and in different physico-chemical properties of the aqueous solution.





## **VIII**

## **APPENDIX**



## **VIII-1-List of tables**

<b>Table II-C-1.</b>	<b>EDDS complex stability constants. Calculated using source values and given at 0 M ionic strength as overall formation constant <math>\beta</math></b>
<b>Table II-D-1</b>	<b>Physical-chemical properties of some pesticides (Tomlin, 1997; Mackay et al., 1997)</b>
<b>Table II-D-2.</b>	<b>Seven degradation products of Atrazine (Saltmiras and Lemley, 2002)</b>
<b>Table III-C-1.</b>	<b>The photonic flux at 365, 334, 313 and 296 nm</b>
<b>Table IV-A-1.</b>	<b>Molecular structures and acidity constants of ethylenediamine-disuccinic acid (EDDS) (25 °C, 0.1 M KNO<sub>3</sub>). (Vandevivere et al., 2001)</b>
<b>Table V-A-1</b>	<b>Quantum yields of disappearance of 2, 4-D and generation of Fe(II) as a function of the irradiation wavelength (at pH 3.0)</b>
<b>Table V-A-2</b>	<b>Effect of oxygen on the quantum yields of 2, 4-D disappearance and of Fe(II) generation. pH = 3.0. (<math>\lambda_{irr}</math> = 365nm)</b>
<b>Table V-A-3</b>	<b>Quantum yields of generation of Fe(II) as a function of pH at 365nm</b>
<b>Table V-A-4</b>	<b>Quantum yields of disappearance of 2, 4-D as a function of pH</b>
<b>Table V-B-1</b>	<b>Adsorption data of 2, 4-D on goethite with different time in suspension at pH 4.0</b>
<b>Table V-B-2</b>	<b>Adsorption data of 2, 4-D on goethite at different pH in suspension</b>
<b>Table VI-B-1</b>	<b>Kinetics analysis of the photodegradation of atrazine</b>

## **VIII-2-List of Figures**

- Figure II-A-1:** Ferric iron species present in aqueous solution at different pH and at a concentration of 20 mg L<sup>-1</sup>, calculated with equilibrium constants from (Flynn C. M. Jr. 1984), T = 20 °C.
- Figure II-A-2:** Speciation of Fe(III) in seawater as a function of pH (Millero et al., 1995)
- Figure II-A-3:** Quantum yields from literature. a) (Braun A. M., Maurette M. T. and Oliveros E. 1991) is for the reaction in Eq. (41) and (42). b) (David F., David P.G. 1976) and c) (Faust B. and Hoigné J., 1990) are for the reaction in Eq. (39)
- Figure II-B-1:** Scheme of the proposed pathway of hydroxyl radical generation when aqueous ozone interacts with surface hydroxyl group of FeOOH in water.
- Figure II-C-1:** Chemical structure of the different stereoisomers of EDDS.
- Figure II-C-2:** The mechanism of photochemical redox cycling of iron in the aqueous solution. Fe(II)-L and Fe(III)-L represent Fe(II) and Fe(III) complexed with Ligand. (Abida, 2005)
- Figure II-C-3:** Reaction scheme for the photolysis of Fe(III)-polycarboxylate complexes
- Figure II-D-1:** Chemical structure of Atrazine
- Figure II-D-2:** Advanced oxidation technologies
- Figure II-D-3:** Anodic Fenton treatment apparatus. (Saltmiras and Lemley, 2002)
- Figure II-D-4:** Proposed degradation pathways for the AFT of atrazine (Saltmiras and Lemley, 2002).

- Figure II-D-5.** Chemical Structures of 2, 4-D
- Figure II-D-6.** pathway for degradation of 2, 4-D by the Fe(II)/UV/H<sub>2</sub>O<sub>2</sub> (Carla et al., 2006)
- Figure III-C-1.** Monochromatic irradiation device
- Figure III-C-2.** Emission spectra of tube Philips, TLD 15W/05.
- Figure III-C-3** Home-made photoreactor with four tubes (Philips TLD 15W / 05)
- Figure III-D-4.** Calibration curve of Fe(II) concentration
- figure III-D-5** Visible absorption spectrum of the ferrous complex of ferrozine
- Figure III-D-6** Calibration curves of total iron
- Figure III-D-7.** Measurements of the absorbance as a function of the composition of the complex  $n=C_L/C_M$
- Figure IV-A-1.** UV-Visible absorption spectra of an aqueous solution with 0.3 mmol L<sup>-1</sup> of Fe(III) (different time after the preparation)
- Figure IV-A-2** pH effect on the distribution of Fe(III) species in aqueous solutions(Wang, 2008).
- Figure IV-A-3.** The UV-visible spectra of EDDS ([EDDS]=1 mol L<sup>-1</sup>)
- Figure IV-A-4.** UV-Visible absorption spectra of EDDS as function of pH. ([EDDS] = 0.3 mmol L<sup>-1</sup>)
- Figures IV-A-5.** The distribution diagram of EDDS aqueous solution as a function of pH values range from 0 to 14, calculated with equilibrium constants from (Vandevivere et al., 2001), 25 °C.
- Figure IV-A-6.** (a) the UV-Visible absorption spectra of mixtures of EDDS and Fe(III) in aqueous solutions; (b) the evolution of the absorbance at 340 nm as a function of the EDDS concentration.
- Figure IV-A-7.** Stability of the Fe(III)-EDDS complexes

- Figure IV-A-8. ([Fe(III)/EDDS]= 2 m mol L<sup>-1</sup>/2 m mol L<sup>-1</sup>) as a function of time, in the dark and at room temperature.
- Figure IV-A-9. Stability of the Fe(III)-EDDS complex ([Fe(III)/EDDS]= 0.3 m mol L<sup>-1</sup>/0.3 m mol L<sup>-1</sup>) as a function of time, in the dark and at room temperature
- Figure IV-A-9. UV-Visible absorption spectra of Fe-EDDS complex solution as function of pH. [Fe(III)]/[EDDS] = 0.3 mmol L<sup>-1</sup>/0.3 mmol L<sup>-1</sup> (a) UV-Visible spectra of Fe(III)-EDDS complex; (b) Absorbance at 340 nm
- Figure IV-A-10. Variation of UV-visible spectra of Fe(III)-EDDS complex ([Fe(III)/EDDS] = 0.1mmol L<sup>-1</sup>/0.1 mmol L<sup>-1</sup>) under irradiation (365 nm)
- Figure IV-B-1. Comparison of <sup>•</sup>OH formation under different conditions for an aqueous solution with C<sub>Fe(III)</sub> = 10 μmol L<sup>-1</sup>, C<sub>EDDS</sub> = 300 μmol L<sup>-1</sup>. Initial pH of the aqueous solution was 3.0.
- Figure IV-B-2. Effect of the initial pH value on the total <sup>•</sup>OH concentration for an aqueous solution with C<sub>Fe(III)</sub> = 300 μmol L<sup>-1</sup>, C<sub>EDDS</sub> = 300 μmol L<sup>-1</sup>.
- Figure IV-B-3. Effect of the EDDS concentration on the <sup>•</sup>OH formation under irradiation with C<sub>Fe(III)</sub> = 100 μmol L<sup>-1</sup> (Initial pH of the aqueous solution was 3.0).
- Figure IV-B-4. Effect of the Fe(III) concentration on the <sup>•</sup>OH formation under irradiation with C<sub>EDDS</sub> = 300 μmol L<sup>-1</sup>. (Initial pH of the aqueous solution was 3.0).
- Figure IV-B-5. Photochemical cycle Fe(III)/Fe(II) in the presence of organic pollutant (Poulain et al, 2003).
- Figure V-A-1. 2, 4-Dichlorophenoxyacetic acid (2, 4-D)
- Figure V-A-2. UV-visible spectra of 2, 4-D at different concentrations
- Figure V-A-3. Molar absorption coefficients at 284 nm.

- Figure V-A-4.** UV-visible spectra of 2, 4-D as the function of pH ranged from 1.5 to 5.0 ( $[2, 4-D] = 3.6 \times 10^{-5} \text{ mol L}^{-1}$ )
- Figure V-A-5.** pKa of 2, 4-D ( $[2, 4-D] = 3.6 \times 10^{-5} \text{ mol L}^{-1}$ )
- Figure V-A-6** UV-Visible absorption spectra of aqueous solution 3 min after the preparation with  $0.3 \text{ mmol L}^{-1}$  of Fe(III) and  $0.1 \text{ mmol L}^{-1}$  of 2, 4-D
- Figure V-A-7** Kinetics of 2, 4-D photodegradation as a function of Fe-EDDS concentration (Initial pH = 3.0;  $[2, 4-D]_0 = 0.1 \text{ mmol L}^{-1}$ )
- Figure V-A-8** Evolution of HPLC spectrum of reaction solution with  $0.3 \text{ mmol L}^{-1}$  Fe(III) and  $0.1 \text{ mmol L}^{-1}$  2, 4-D at pH = 3.0
- Figure V-A-9** Photoproduction concentration of 2, 4-DCP in solutions with different concentration of Fe-EDDS under irradiation (Initial pH = 3.0;  $[2, 4-D]_0 = 0.1 \text{ mmol L}^{-1}$ )
- Figure V-A-10** Photogeneration of Fe(II) as a function of Fe(III)-EDDS concentration in solutions ( Initial pH = 3.0;  $[2,4-D]_0 = 0.1 \text{ mmol L}^{-1}$ ).
- Figure V-A-11** Impact of oxygen on 2, 4-D photodegradation in the presence of Fe(III)-EDDS.
- Figure V-A-12** Impact of oxygen on 2, 4-DCP formation
- Figure V-A-13** Photogeneration of Fe(II) as function of oxygen in solutions with an initial pH = 3.0.  $[\text{Fe(III)-EDDS}]_0 = 0.3 \text{ mmol L}^{-1}$ ,  $[2,4-D]_0 = 0.1 \text{ mmol L}^{-1}$ .
- Figure V-A-14** Influence of pH on the photodegradation of 2, 4-D in the presence of Fe(III)-EDDS complex.  $[\text{Fe(III)-EDDS}]_0 = 0.1 \text{ mmol L}^{-1}$ ,  $[2,4-D]_0 = 0.1 \text{ mmol L}^{-1}$ .
- Figure V-A-15** Influence of pH on the photogeneration of Fe(II) in the presence of Fe-EDDS complex.  $[\text{Fe(III)-EDDS}]_0 = 0.1 \text{ mmol L}^{-1}$ ,  $[2,4-D]_0 = 0.1 \text{ mmol L}^{-1}$ .



Figure V-A-16	Influence of isopropanol on the photodegradation of 2, 4-D in presence of Fe-EDDS complex at pH 3.0. $[2, 4-D]_0 = 0.1 \text{ mmol L}^{-1}$ .
Figure V-A-17	Influence of isopropanol on the photogeneration of 2, 4-DCP in presence of Fe-EDDS complex at pH 3.0. $[\text{Fe(III)-EDDS}] = 0.3 \text{ mmol L}^{-1}$ , $[2,4-D]_0 = 0.1 \text{ mmol L}^{-1}$ .
Figure V-A-18	UV-visible spectrum of the Fe(III)-EDDS and 2, 4-D solutions as a function of irradiation time.
F Figure V-B-1	Adsorption of 2, 4-D on goethite with different time in suspension at pH 4.0
Figure V-B-2	Adsorption of 2, 4-D on goethite at different pH in suspensions
Figure V-B-3	Photodegradation efficiency of 2, 4-D in suspension at pH 4.0 under irradiation
Figure V-B-4	Results of 2, 4-DCP photoreduction in suspension at pH 4.0 under irradiation
Figure V-B-5	Influence of pH on the photodegradation of 2, 4-D in the presence of goethite
Figure V-B-6	Influence of pH on the photoproduction of 2, 4-DCP in suspension of goethite ( $[\text{Goethite}] = 0.2 \text{ g L}^{-1}$ , $[2, 4-D] = 0.1 \text{ mmol L}^{-1}$ )
Figure V-B-7	Influence of isopropanol on the photodegradation of 2, 4-D in suspension of goethite at pH 4.0 ( $[\text{goethite}] = 0.2 \text{ g L}^{-1}$ , $[2, 4-D]_0 = 0.1 \text{ mmol L}^{-1}$ )
Figure V-B-8	Influence of isopropanol on the photoproduction of 2, 4-DCP in suspension of goethite at pH 4.0 ( $[\text{goethite}] = 0.2 \text{ g L}^{-1}$ , $[2, 4-D]_0 = 0.1 \text{ mmol L}^{-1}$ )
Figure V-B-9	Comparison of 2, 4-D and 2, 4-DCP on photodegradation ( initial concentration: $[2, 4-D] = 0.1 \text{ mmol L}^{-1}$ , $[2,$

	4-DCP] = 0.1 mmol L <sup>-1</sup> , [goethite] = 0.2 g L <sup>-1</sup> )
Figure V-B-10	Influence of [EDDS] on 2, 4-D photodegradation in the suspension of goethite. ([goethite]=0.2 g L <sup>-1</sup> , [2,4-D] <sub>0</sub> =0.1 mmol L <sup>-1</sup> , initial pH=6.0)
Figure V-B-11	Influence of [EDDS] on photoproduction of 2, 4-DCP in the suspension of goethite. ([goethite]=0.2 g L <sup>-1</sup> , [2,4-D] <sub>0</sub> =0.1 mmol L <sup>-1</sup> , initial pH=6.0)
Figure V-B-12	Influence of goethite concentration on 2, 4-D photodegradation. ([EDDS]=0.5 mmol L <sup>-1</sup> , [2,4-D] <sub>0</sub> =0.1 mmol L <sup>-1</sup> , initial pH=6.0)
Figure V-B-13	Influence of goethite concentration on photoproduction of 2, 4-DCP in the suspension. ([EDDS]=0.5 mmol L <sup>-1</sup> , [2,4-D] <sub>0</sub> =0.1 mmol L <sup>-1</sup> , initial pH=6.0)
Figure V-B-14	Influence of initial pH on photodegradation of 2, 4-D in the suspension of goethite. ([goethite] = 0.2 g L <sup>-1</sup> , [EDDS] = 1.0 mmol L <sup>-1</sup> , [2, 4-D] <sub>0</sub> = 0.1 mmol L <sup>-1</sup> )
Figure V-B-15	Influence of initial pH on photoproduction of 2, 4-DCP in the suspension of goethite. ([goethite] = 0.2 g L <sup>-1</sup> , [EDDS] = 1.0 mmol L <sup>-1</sup> , [2,4-D] <sub>0</sub> = 0.1 mmol L <sup>-1</sup> )
Figure VI-A-1	Chemical formula of atrazine
Figure VI-A-2	UV-visible spectra of atrazine at different concentrations
Figure VI-A-3.	UV-Visible absorption spectra of aqueous solution 3 min after the preparation with 0.3 mmol L <sup>-1</sup> of Fe(III) and 10 mg L <sup>-1</sup> of atrazine
Figure VI-A-4	Photodegradation of atrazine in the Fe(III)-EDDS systems, (a) with different Fe(III) concentrations and (b) with different EDDS concentrations. pH = 3.0.
Figure VI-A-5	Influence of ratio of Fe(III)/EDDS on the photogeneration of Fe(II) in aqueous solution.

- Figure VI-A-6** Influence of initial pH on photodegradation of atrazine in the Fe(III)-EDDS systems. [Fe(III)-EDDS] = 0.3 mmol L<sup>-1</sup> ; [atrazine] = 10 mg L<sup>-1</sup>
- Figure VI-A-7** Influence of initial pH on photoproduction of Fe(II) in the Fe(III)-EDDS systems. [Fe(III)-EDDS] = 0.3 mmol L<sup>-1</sup>; [atrazine] = 10 mg L<sup>-1</sup>.
- Figure VI-A-8** Influence of initial concentration of atrazine on photodegradation efficiency. [Fe(III)-EDDS] = 0.3 mmol L<sup>-1</sup>
- Figure VI-A-9** Influence of initial concentration of atrazine on photoproduction of Fe(II) in the Fe(III)-EDDS system. [Fe(III)-EDDS] = 0.3 mmol L<sup>-1</sup>
- Figure VI-B-1.** Photodegradation of atrazine under different conditions at pH 3.0
- Figure VI-B-2.** Photodegradation of atrazine in the Fe(III)-Pyr systems, (a) at different pH values; (b) with different Fe(III) concentrations; (c) with different Pyr concentrations; (d) with different atrazine concentrations.
- Figure VI-B-3.** Kinetics analysis of atrazine degradation and Fe(II) formation.
- Figure VI-B-4** LC-MS spectra of the atrazine degradation in Fe(III)-Pyr systems after 4h of irradiation:[Atrazine]=10 mg mL<sup>-1</sup>, [Fe(III)/Pyr] = 10μM/30μM, pH=3.0.
- Figure VI-B-5.** Proposed photodegradation mechanism

## **VIII**

### **REFERENCES**



## **VIII-REFERENCES**

Abumaizar, R., Khan, L. I. Laboratory investigation of heavy metal removal by soil washing. J. Air Waste Manag. Assoc. 1996, (46) 765-768.

Acero J L, Stemmler K, Von Gunten U. Degradation kinetics of atrazine and its degradation products with ozone and OH radicals: a predictive tool for drinking water. Environ Sci Technol 2000, (34) 591-597.

Albanis, T. A., Pomonis, P. J., Sdoukos, A. Th. 1. Seasonal fluctuations of organochlorine and triazines pesticides in the aquatic system of Ionnina basin. Sci. Total Environ. 1986, (58) 243-253.

Alexander M. Biodegradation and bioremediation. San Diego CA: Academic Press, Inc., 1994.

Amarante Junior, O. P., Brito, N. M., Santos, T. C. R., Nunes, G. S., Ribeiro, M.L. Determination of 2, 4-dichlorophenoxyacetic acid and its major transformation product in soil samples by liquid chromatographic analysis. Talanta, 2003, (60) 115-121.

Amonette J. E., Workman D. J., Kennedy D. W., Fruchter J. S. and Gorby Y. A. Dechlorination of carbon tetrachloride by Fe(II) associated with goethite. Environ. Sci. Technol. 2000, 34(21) 4606-4613.

Arakaki T, Miyake T, Hirakawa T, Sakugawa H: pH dependent photoformation of hydroxyl radical and absorbance of aqueous-phase N(III) ( $\text{HNO}_2$  and  $\text{NO}_2^-$ ). Environ. Sci. Technol., 1999 (33) 2561–2565.

Arienzo M. Oxidizing 2, 4, 6-trinitrotoluene with pyrite- $\text{H}_2\text{O}_2$  suspensions, Chemosphere, 1999, (39) 1629–1638.

Arnold S M, Hickey W J, Harris R F. Degradation of atrazine by Fenton's reagent: condition optimization and product quantification. Environ Sci Technol 1995, (29) 2083-2089.

Arnold S M, Hickey W J, Harris R F, Talaat R E. Integrated chemical and biological remediation of atrazine-contaminated aqueous wastes. In: Ballantine LG, McFarland J E, Hackett D S, editors. Triazine herbicides: risk assessment. Washington,

DC: ACS Symposium Series American Chemical Society. 1998, 177-188.

Arslan-Alaton I. and Gurses F. Photo-Fenton and photo-Fenton-like oxidation of Procaine Penicillin G formulation effluent. *J. Photochem. Photobio. A: Chem.*, 2004, (165) 165-175.

Aston, L. S. and Seiber, J. N. Fate of summertime airborne organophosphate pesticide residues in the Sierra Nevada mountains. *J. Environ. Qual.* 1997, (26) 1483-1492.

Audus, L. J. The biological detoxification of 2, 4-dichlorophenoxyacetic acid in soil. *Plant and Soil.* 1949, (2) 31–36.

Ballesteros M. C., Rueda E. H., Blesa M. A. The influence of iron (II) and (III) on the kinetics of goethite dissolution by EDTA. *J. Colloid Interf. Sci.* 1998, 201(1), 13–19.

Balmer M E. and Sulzberger B. Atrazine degradation in irradiated iron/oxalate systems: effect of pH and oxalate. *Environ Sci Technol* 1999, (33) 2418–2424.

Barb W. G., Baxendale J. H., George P., Hargrave K. R. Reactions of ferrous and ferric ions with hydrogen peroxide. *Trans. Faraday Soc.*, 1951a, (47) 462-500.

Barb W. G., Baxendale J. H., George P., Hargrave K. R. Reactions of ferrous and ferric ions with hydrogen peroxide. Part II. The ferric ion reaction. *Trans. Faraday Soc.*, 1951b, (47) 591-616.

Bauer R., Waldner G., Fallmann H., Hager S., Klare M., Krutzler T., Malato S., Maletzky P. The photo-Fenton reaction and the TiO<sub>2</sub>/UV process for wastewater treatment – novel developments. *Catal. Today*, 1999, (53) 131-144.

Bidleman, T. F. and Leonard, R. Aerial transport of pesticides over the northern Indian ocean and adjacent seas. *Atmos. Environ.* 1982, (16) 1099-1107.

Bielski B. H., Cabelli D. E., Arudi R. L., Ross A. B. Reactivity of HO<sub>2</sub>/O<sub>2</sub> radicals in aqueous solution. *J. Phys. Chem. Ref. Data*, 1985, (14) 1041-1100.

Bier E. L., Singh J., Li Z. M., Comfort S. D., Shea P. J. Remediating hexahydro-1, 3, 5-trinitro-1, 2, 5-triazine-contaminated water and soil by Fenton oxidation, *Environ. Toxicol. Chem.* 1999, (18) 1078–1084.

Bigham J. M., Fitzpatrick R. W., Schulze D.G. in: J.B. Dixon, D. G. Schulze

(Eds.), Soil Mineralogy with Environmental Applications, in: SSSA Book Series, Soil Sci. Soc. Am., Madison, WI, 2002, (7) 323-366.

Bishop D. F., Stern G., Fleischmann M., Marshall L. S. Hydrogen peroxide catalytic oxidation of refractory organics in municipal waste waters. Ind. Eng. Chem. Process Des. & Dev., 1968, (7) 110-117.

Blanchard P. E. and Donald W. W. Herbicide contamination of groundwater beneath claypan soils in north-central Missouri. J Environ Qual 1997, (26)1612–1621.

Bossmann S. H., Oliveros E., Gob S., Siegwart S., Dahlen E. P., Payawan L. Jr., Straub M., Worner M., Braun A.M. New evidence against hydroxyl radicals as reactive intermediates in the thermal and photochemically enhanced Fenton reactions, J. Phys Chem., 1998, (102) 5542-5550.

Bozzi A., Yuranova T., Lais P., Kiwi J. Degradation of industrial waste waters on Fe/C-fabrics. Optimization of the solution parameters during reactor operation. Water Res., 2005, (39) 1441-1450.

Braun A.M., Maurette M.-T., Oliveros E. Photochemical technology. Wiley, Chichester. 1991.

Brillas E., Calpe J. C., Cabot P. L. Degradation of the herbicide 2, 4-Dichlorophenoxyacetic acid by ozonation catalyzed with  $\text{Fe}^{2+}$  and UV light, Appl. Catal. B: Environ., 2003 (46) 381-391.

Bucheli-Witschel and M., Egli, T. Environmental fate and microbial degradation of aminopolycarboxylic acids. FEMS Microbiol. Rev. 2001, (25) 69-106.

Buerge I. J. and Hug S. J. Influence of mineral surfaces on Chromium(VI) reduction by Iron(II). Environ. Sci. Technol. 1999, 33(23) 4285–4291.

Bukur D. B., Lang X., Rossin J. A., Zimmerman W. H., Rosynek M. P., Yeh E. B., Li C. Activation studies with a promoted precipitated iron Fischer-Tropsch catalyst. Ind. Eng. Chem. Res. 1989, (28) 1130-1140.

Burge W D. Anaerobic decomposition of DDT in soil. Acceleration by volatile compounds of alfalfa. J Agric Food Chem 1971, (19) 375–378.

Buxton G. U., Greenstock C. L., Helman W. P., Ross A. B. Critical review of rate constants for reactions of hydrated electrons, hydrogen atoms and hydroxyl



radicals ( $\text{OH}^\bullet/\text{O}^\bullet$ ) in aqueous solution. *J. Phys. Chem. Ref. Data*, 1988, (17) 513-886.

Byrne R. H., Kump, L. R., Cantrell, K. J. The influence of temperature and pH on trace metal speciation in seawater. *Mar. Chem.*, 1988, (25) 163-181.

Cai, Z., Wang, D., Ma, W. T. Gas chromatography/ion trap mass spectrometry applied for the analysis of triazine herbicides in environmental waters by an isotope dilution technique. *Analytica Chimica Acta*. 2004, (503) 263-270.

Calvert J. G., Pitts J. N., J. Photochemistry, John Wiley & Sons, New York, 1966, p. 783.

Carla B., Christiane A.R., Rodnei B. Oxidation of pesticides by in situ electrogenerated hydrogen peroxide: study for the degradation of 2,4-dichlorophenoxyacetic acid. *Journal of Hazardous Materials*. 2006, B137, 856-864.

Chan, C. H., Bruce, G., Karrison, B. Wet deposition of organochlorine pesticides and polychlorinated biphenyls to the Great lakes. *J. Great Lakes Res.* 1994, 20 (3) 546-550.

Charlet L., Bosbach D., Peretyashko T. Natural attenuation of TCE, As, Hg linked to the heterogeneous oxidation of Fe(II): an AFM study. *Chem. Geol.* 2002, 190(1-4) 303-319.

Charretour, C., Kerbaol, N., Peron, J. J. Contribution to the analysis of triazines in water by gas chromatography and ion trap tandem mass spectroscopy. *Analisis* 1996, (24) 336-343.

Chebby A. and Carlier P. Carboxylic acids in the troposphere, occurrence sources and sinks: a review. *Atmos. Environ.* 1996, 30 (24) 4233-4249.

Chen R. and Pignatello J. J. Role of quinone intermediates as electron shuttles in Fenton and photoassisted Fenton oxidations of aromatic compounds. *Environ. Sci. Technol.*, 1997, (31) 2399–2406.

Chevreuril, M., Chesteriko., A., Letolle, R., Garnier, L. Atmospheric pollution and fallout by PCBs and organochlorine pesticides (Ile de France). *Water, Air, Soil Pollution*. 1989, (43) 73-83.

Chevreuril, M., Gargouma, M., Teil, M. J., Chesteriko., A., Occurrence of

organochlorines (PCBs, pesticides) and herbicides (triazines, phenylureas) in the atmosphere and in the fallout from urban and rural stations of the Paris area. *Sci. Total Environ.* 1996, (182) 25-37.

Chung K H, Ro K S, Roy D. Fate the enhancement of atrazine biotransformation in anaerobic wetland sediment. *Water Res* 1996, 30(2) 341–346.

Ciesla P., Kocot P., Mytych P., Stasicka Z. Homogeneous photocatalysis by transition metal complexes in the environment. *J. Mol. Catal.* 2004, (A224) 17-33.

Coburn, J. A., Ripley, B. D., Chau, S. Y. Analysis of pesticides residues by chemical derivatization. II. N-methylcarbamates in natural waters and soils. *J. Assoc. Offic. Anal. Chem.* 1976, 59 (1) 1988-1996.

Commission of the European Communities. Implementation of the Community Strategy for Endocrine Disrupters. COM 262. Commission of the European Communities, Brussels 2001.

Cooper G. D. and DeGraff B. A. On the photochemistry of the ferrioxalate system. *J. Phys. Chem.*, 1971, (75) 2897-2902.

Cornell R. M., Schwertmann U. The iron oxides: structure, properties, reactions, occurrence and uses, VCH Publ., D-69451 Weinheim, Germany, 1996.

Cornell R. M., Schwertmann U. The Iron Oxides, New York, Roe B A, Lemley A T. Treatment of two insecticides in an electrochemical Fenton system. *J Environ Sci Health B.* 1996, (32) 261-281.

Cornell R. M. and Schwertmann U. The Iron Oxides. VCH Verlag, Weinheim. 2003.

Cunningham K. M., Goldberg M. C., Weiner E. R. Mechanisms for aqueous photolysis of adsorbed benzoate, oxalate, and succinate on iron oxyhydroxide (goethite) surfaces. *Environ. Sci. Technol.*, 1988, 22 (9) 1090-1097.

David F. and David P.G. Photoredox chemistry of iron(3) chloride and iron(3) perchlorate in aqueous media. A comparative study. *J. Phys. Chem.*, 1976, (80) 579-583.

Davison W. Iron and manganese in lakes. *Earth Sci. Rev.*, 1993, (34)119-163.

De Laat J., Truong Le G., Legube B. A comparative study of the effects of

chloride, sulfate and nitrate ions on the rates of decomposition of  $\text{H}_2\text{O}_2$  and organic compounds by  $\text{Fe(II)/H}_2\text{O}_2$  and  $\text{Fe(III)/H}_2\text{O}_2$ . *Chemosphere*, 2004, (55) 715-723.

Deng N. S., Wu F., Luo F., Xiao M. Ferric citrate-induced photodegradation of dyes in aqueous solutions *Chemosphere*, 1998, (36) 3101-3112.

Di Corcia, A. and Marchetti, M. Method development for monitoring pesticides in environmental water: liquid-solid extraction followed by liquid chromatography. *Environ. Sci. Technol.* 1992, (26) 66-74.

Dorfler U, Freicht E A, Scheunert I. S-Triazine residues in groundwater. *Chemosphere*. 1997, (35) 99–106.

Dorfman L. M., Taub I. A., Bühler, R. E. Pulse radiolysis studies. I. Transient spectra and reaction-rate constants in irradiated aqueous solutions of benzene. *J. Chem. Phys.*, 1962, (36) 3051-3061.

Durand, G. and Barcelo, D. Conformation of chlorotriazine pesticides, their degradation products and organophosphorous pesticides in soil samples using gas chromatographymass spectrometry with electron impact and positive- and negative-ion chemical ionization. *Anal. Chim. Acta.* 1991, (243) 259-271.

Dzombak D. A. and Morel F. M. M. Surface Complexation Modeling: Hydrrous Ferric Oxide, Wiley, New York, 1990.

Emmenegger L, King D W, Sigg L, Sulzberger B. Oxidation kinetics of  $\text{Fe(II)}$  in a eutrophic Swiss lake, *Environ. Sci. Technol.*, 1998, (32) 2990-2996.

Eriksson, G., Jensen, S., Kylin, H., Strachan, W. The pine needle as a monitor of atmospheric pollution. *Nature* 1989, (341) 42-44.

Esplugas S. and Ollis D. F. Economic aspects of integrated (chemical biological) processes for water treatment. *J. Adv. Oxid. Technol.*, 1997, (1) 197-202.

Fallmann H., Krutzler T., Bauer R., Malato S., Blanco J. Detoxification of pesticide containing effluents by solar driven Fenton process. *Z. Phys. Chemie*, 1999, (213) 67-74.

Faust B. C. and Hoigné J. Photolysis of hydroxy-complexes as sources of  $\bullet\text{OH}$  radicals in clouds, fog and rain. *Atmos. Environ.*, 1990, (24A) 79-89.

Faust B. C. and Allen J. M. Aqueous-phase photochemical formation of

hydroxyl radical in authentic cloudwaters and fogwaters. *Environ. Sci. Technol.*, 1993, (27), 1221-1224.

Faust B. C. A review of the photochemical redox reactions of iron(III) species in atmospheric, oceanic, and surface waters: influences on geochemical cycles and oxidant formation. In: Helz G. R., Zepp R. G., Crosby D. G. (Editors), *Aquatic and Surface Photochemistry*, CRC Press, Boca Raton, FL, 1994, 3-37.

Fenton H. J. H. Oxidation of tartaric acid in presence of iron. *J. Chem Soc.*, 1894, (65) 899-910.

Ferrando, M. D., Alarcon, V., Fernandez-Casalderray, A., Gamon, M., Andreu-Moliner, E. Persistence of some pesticides in the environment. *Bull. Environ. Contam. Toxicol.* 1992, (48) 747-755.

Flynn C. M. Jr. Hydrolysis of inorganic iron(III) salts. *Chem. Rev.*, 1984, (84) 31- 41.

Foster, R. K. and McKercher, R. B. Laboratory incubation studies of chlorophenoxyacetic acids in chernozemic soils. *Soil Biology & Biochemistry* 1973, (5) 333–337.

Gao H.Z. and Zepp R. G., Factors Influencing Photoreactions of Dissolved Organic Matter in a Coastal River of the Southeastern United States. *Environ. Sci. Technol.*, 1998, (32) 2940-2946.

Garbisu, C. and Alkorta, I. Phytoextraction: a cost-effective plant based technology for the removal of metals from the environment. *Biores. Technol.* 2001, (77) 229-236.

Garcia, G. B., Konjuh, C., Duffard, R. O. Evangelista de Duffard A. M. Dopamine-beta-hydroxylase immunohistochemical study in the locus coeruleus of neonate rats exposed to 2, 4-dichlorophenoxyacetic acid through mother's milk. *Drug Chem. Toxicol.*, 2006, 29(4) 435-442.

Gallard H., De Laat J., Legube B. Spectrophotometric study of the formation of iron(III)–hydroperoxy complexes in homogeneous aqueous solution. *Water Res.*, 1999, (33) 2929-2936.

Garmouma M, Blanchard M, Chesterikoff A, Ansart P, Chevreuil M. Seasonal

transport of herbicides (triazine and phenylureas) in small stream draining an agricultural basin-Melarchez (France). *Water Res.*, 1997, (31) 1489-1503.

Gernjak W., Krutzler T., Glaser A., Malato S., Cáceres J., Bauer R., Fernandez-Alba A.R. Photo-Fenton treatment of water containing natural phenolic pollutants. *Chemosphere*, 2003, (50) 71-78.

Gernjak W., Maldonado M. I., Malato S., Cáceres J., Krutzler T., Glaser A., Bauer R. Pilot-Plant Treatment of Olive Mill Wastewater (OMW) by Solar TiO<sub>2</sub> Photocatalysis and Solar Photo-Fenton. *Sol. Energy*, 2004, (77) 567-572.

Getenga, Z. M., Madadi, V., Wandiga, S. O. Studies on biodegradation of 2, 4-D and metribuzin in soil under controlled conditions. *Bulletin of Environmental Contamination and Toxicology*. 2004, (72) 504-513.

Gish T J, Gimenez D, Rawls W J. Impact of roots on ground-water. *Qual Plant Soil*. 1998, (200) 47-54.

Gledhill M. and Van den Berg, C. M. G. Determination of complexation of iron (III) with natural organic complexing ligands in seawater using cathodic stripping voltammetry. *Mar. Chem.*, 1994, (47) 41-54.

Glotfelty D. E., Taylor A. W. Turner, B. J., Zoller W. H. Volatilisation of surface-applied pesticides from fallow soil. *J. Agric. Food Chem*. 1984, (32) 638-683.

Glotfelty D. E., Leech M. M., Jersey J., Taylor A. W. Volatilization and wind erosion of soil surface applied atrazine, simazine, alachlor, and toxaphene. *J. Agric. Food Chem*. 1989, (37) 546-551.

Gob S., Oliveros E., Bossmann S. H., Braun A. M., Nascimento C. A. O., Guardani R. Optimal experimental design and artificial neural networks applied to the photochemically enhanced Fenton reaction. *Water Sci. Technol.*, 2001, 44(5) 339-345.

Goodfellow M., Brown A.M., Cai J., Chun J., Collins M.D. *Amycolatopsis iaponicum* sp. nov., an actinomycete producing (S, S)-N,N'-ethylenediaminedisuccinic acid, *System. Appl. Microbiol.* 1997, (20) 78-84.

Graedel, T. E., Mandich, M. L., Weschler, C. J. Kinetic model studies of atmospheric droplet chemistry. Homogeneous transition metal chemistry in raindrops.

J. Geophys. Res., 1986, (91) 5205-5221.

Grčman, H., Vodnik, D., Velikonja-Bolta, S., Lestan, D. Ethylenediamine disuccinate as a new chelate for environmentally safe enhanced lead phytoextraction.

J. Environ. Qual. 2003, (32) 500-506.

Grover, R. The adsorptive behaviour of acid and ester forms of 2, 4-D on soils. Weed Research 1973, (13) 51-58.

Guzzella L, Depaolis A, Bartone C, Pozzoni F, Giuliano G. Migration of pesticide-residues from agricultural soil to groundwater. Int J Environ Anal Chem 1996, (65) 261-275.

Haag W. R. and Yao C. D. Rate Constant for Reaction of Hydroxyl Radicals with Several Drinking Water Contaminants. Environ. Sci. Technol., 1992, (26) 1005-1013.

Haber F. and Weiss J. The catalytic decomposition of hydrogen peroxide by iron salts. Proc. Roy. Soc. 1934, (147) 332-351.

Haenel, H. D. and Siebers, J. Lindane volatilization under field conditions- Estimation from residue disappearance and concentration measurements in air. Agric. Forest Meteorol. 1994, (76) 237-257.

Hansel C. M., Benner S. G., Fendorf S. Competing Fe(II)-induced mineralization pathways of ferrihydrite. Environ. Sci. Technol. 2005, 39(18) 7147-7153.

Haragushi, K., Kitamura, E., Yamashita, T., Kido, A. Simultaneous determination of trace pesticides in urban air. Atmos. Environ. 1994, 28(7), 1319-1325.

Haragushi, K., Kitamura, E., Yamashita, T., Kido, A. Simultaneous determination of trace pesticides in urban precipitation. Atmos. Environ. 1995, 29(2) 247-253.

Hatchard C. G. and Parker C. A. A sensitive chemical actinometer II. Potassium ferrioxalate as a standard chemical actinometer. Proc. Roy. Soc., 1956, (A235) 518-536.

Hauser, L., Tandy, S., Schulin, R., Nowack, B. Column extraction of heavy

metals from soils using the biodegradable chelating agent EDDS. Environ. Sci. Technol. 2005, (39) 6819-6824.

Hawker P. N. and Twigg M. V. Iron: inorganic and coordination chemistry. In: King, P. B. (Ed.). Encyclopedia of Inorganic Chemistry. Wiley, Chichester, 1994, 1698-1725.

Hayes K. F., Roe A. L., Brown, Jr., G. E., Hodgson K. O., Leckie J. O., Parks G. A. In situ X-ray adsorption study of surface complexes: selenium oxyanions on  $\alpha$ -FeOOH. Science. 1987, (238) 783-786.

Hayes T B, Collins A, Lee M, Mendoza M, Noriega N, Stuart A A, Vonk A. Hermaphroditic, demasculinized frogs after exposure to the herbicide atrazine at low ecologically relevant dose. PANS 2002, 99(8) 5476-5480.

Henze M., Harremoes P., La Cour Jansen J., Arvin E. Wastewater Treatment: Biological and Chemical Processes. 3<sup>rd</sup> Ed. Springer-Verlag, Berlin, 2000.

Herranz T., Rojas S., Pérez-Alonso F. J., Ojeda M., Terreros P., Fierro J. L. G. Carbon oxides hydrogenation over silica-supported iron-based catalysts. Influence of the preparation method. Applied Catalysis A: General 2006, (308) 19-30.

Herrera F., Pulgarin C., Nadtochenko V., Kiwi J. Accelerated photooxidation of concentrated p-coumaric acid in homogeneous solution. Mechanistic studies, intermediates and precursors formed in the dark. Appl. Catal. B: Environ., 1998, (17) 141-156.

Herrmann, J. M., Disdier, J., Pichat, P., Malato, S., Blanco, J. TiO<sub>2</sub>-based solar photocatalytic detoxification of water containing organic pollutants. Case studies of 2,4- dichlorophenoxyacetic acid (2, 4-D) and benzofuran. Appl. Catal. B: Environ. 1998, (17) 15-23.

Herwig, U., Klumpp, E., Schwuger, H. D., Schwuger, M. J. Physicochemical interactions between atrazine and clay minerals. Applied Clay Science. 2001, (18) 211-222.

Hiemstra T., De Wit J. C. M., Van Riemsdijk W. H. Multisite proton adsorption modeling at the solid/solution interface of (hydr)oxides: A new approach. II. Application to various important (hydr)oxides. J. Colloid Interface Sci. 1989, (133)

105-117.

Hiemstra T., Van Riemsdijk W. H. A surface structural approach to ion adsorption: The charge distribution (CD) model. *Journal of Colloid and Interface Science*, 1996, (179) 488-508.

Hincapié M., Maldonado M.I., Oller I., Gernjak W., Sánchez-Pérez J. A., Ballesteros M. M., Malato S. Solar photocatalytic degradation and detoxification of EU priority substances. *Catal. Today*, 2005, (101) 203-210.

Hochella M. F. and White A. F. in: M. F. Hochella, A. F. White (Eds.), *Mineral–Water Interface Geochemistry*, in: *Reviews in Mineralogy*, Miner. Soc. Am., Washington, DC, 1990, (23) 1-15.

Hua J., Wei K., Zheng Q., Lin X. Influence of calcination temperature on the structure and catalytic performance of Au/iron oxide catalysts for water-gas shift reaction, *Appl. Catal. A: Gen.* 2004, (259) 121-130.

Huston P. L. and Pignatello J. J. Degradation of selected pesticide active ingredients and commercial formulations in water by the photo-assisted Fenton reaction. *Water Res.*, 1999, (33) 1238-1246.

Huysen S. and Hawkins G. W. Ferrous ion catalyzed oxidations of 2-propanol with peroxyacetic acid. *J. Org. Chem.*, 1983, (48) 1705-1708.

Joseph J. M., Varghese R., Aravindakumar C. T. Photoproduction of hydroxyl radicals from Fe(III)-hydroxy complex: a quantitative assessment. *J. Photochem. Photobiol. A: Chem.*, 2001, (146) 67-73

Kavitha V. and Palanivelu K. The role of ferrous ion in Fenton and photo-Fenton processes for the degradation of phenol. *Chemosphere*, 2004, (55) 1235-1243.

Kauffmann, C., Shoseyov, O., Shpigel, E., Bayer, E. A., Lamed, R., Shoham, Mandelbaum, R. T. Novel methodology for enzymatic removal of atrazine from water by CBD-fusion protein immobilized on cellulose. *Environ Sci Technol.* 2000, (34) 1292-1296.

Kearney P C, Kaufman D D, Alexander M. Biochemistry of herbicide decomposition in soil. In *Book: Soil Biochemistry*. Vol. 1, New York, NY: Marcel



Dekker, 1967.

Khan M. A. and Watts J. R. Mineral-catalyzed peroxidation of tetrachlorethylene, *Water Air Soil Pollut.* 1996, (88) 247-260.

King D. W., Aldrich R. A., Charnecki S. E., Photochemical redox cycling of iron in NaCl solutions. *Mar. Chem.*, 1993, (44) 105-120.

Kiwi J., Lopez A., Nadtochenko V. Mechanism and kinetics of the OH radical intervention during Fenton oxidation in the presence of a significant amount of radical scavenger (Cl<sup>-</sup>). *Environ. Sci. Technol.*, 2000, (34) 2162-2168.

Kl oppel, H. and K ordel, W. Pesticide volatilization and exposure of terrestrial ecosystems. *Chemosphere* 1997, 35 (6) 1271-1289.

Klausen J., Trober S. P., Haderlein S. B., Schwarzenbach R. P. Reduction of substituted nitrobenzenes by Fe(II) in aqueous mineral suspensions. *Environ. Sci. Technol.* 1995, 29(9) 2396-2404.

Klupinski T. P., Chin Y. P., Traina S. J. Abiotic degradation of pentachloronitrobenzene by Fe(II): reactions on goethite and iron oxide nanoparticles. *Environ. Sci. Technol.* 2004, 38(16) 4353-4360.

Kochany J. and Bolton J.R. Mechanism of photodegradation of aqueous organic pollutants. 2. Measurement of the primary rate constants for reaction of •OH radicals with benzene and some halobenzenes using an EPR spin-trapping method following the photolysis of H<sub>2</sub>O<sub>2</sub>. *Environ Sci Technol.*, 1992 (26) 262–265.

Kookana R S, Baskaran S, Naidu R. Pesticide fate and behavior in Australian soils in relation to contamination and management of soil and water-a review. *Austr J Soil Res* 1998, (36) 715-764.

Kos, B. and Lestan, D. Influence of biodegradable (S S-EDDS) and non-degradable (EDTA) chelate and hydrogel modified soil water sorption capacity on Pb phytoextraction and leaching. *Plant Soil* 2003, (253) 403-411.

Kos, B. and Lestan, D. Chelator induced phytoextraction and in situ soil washing of Cu. *Environ. Pollut.* 2004a, (132) 333-339.

Kos, B. and Lestan, D. Soil washing of Pb, Zn and Cd using biodegradable chelator and permeable barriers and induced phytoextraction by *Cannabis sativa*.

Plant Soil. 2004b, (263) 43-51.

Kremer M. L. Nature of intermediates in the catalytic decomposition of hydrogen peroxide by ferric ions. Trans. Faraday Soc., 1962, (58) 702-707.

Kremer M. L. and Stein G. The catalytic decomposition of hydrogen peroxide by ferric perchlorate. Trans. Faraday Soc., 1959, (55) 959-973.

Kremer M. L. and Stein G. Kinetics of the  $\text{Fe}^{3+}$  ion- $\text{H}_2\text{O}_2$  reaction: steady state and terminal-state analysis. Int. J. Chem. Kinet., 1977, (9) 179-184.

Krutzler T., Fallmann H., Maletzky P., Bauer R., Malato S., Blanco J. Solar driven degradation of 4-chlorophenol. Catal. Today, 1999, (54) 321-327.

Kuma K., Nakabayashi S., Suzuki Y., Kudo I., Matsunaga K. Photo-reduction of  $\text{Fe}(\text{B})$  by dissolved organic substances and existence of  $\text{Fe}(\text{B})$  in seawater during spring blooms. Mar. Chem., 1992, (37) 15-27.

Kung, K.H. and McBride, M.B. Electron transfer processes between hydroquinone and iron oxides. Clay. Clay. Miner. 1988, (36) 303-309.

Kurbus T., Marechal A. M., Vončina D. B. Comparison of  $\text{H}_2\text{O}_2/\text{UV}$ ,  $\text{H}_2\text{O}_2/\text{O}_3$  and  $\text{H}_2\text{O}_2/\text{Fe}^{2+}$  processes for the decolorisation of vinylsulphone reactive dyes, Dyes Pigments. 2003, (58) 245-252.

Lambropoulou, D. A., Sakkas, V. A., Hela, D. G., Albanis, T. A. Application of solid-phase microextraction in the monitoring of priority pesticides in the Kalamas River (N. W. Greece). J. Chromatography A. 2002, (963) 107-116.

Langlais B., Reckhow D. A., Brink D. R. Ozone in Water Treatment: Application and Engineering, Lewis Publishers, Chelsea, Michigan, 1991.

Legrini O., Oliveros E. and Braun A. M. Photochemical Processes for Water Treatment. Chem. Rev., 1993, (93) 671-698.

Lente G. and Fábíán I., A Simple Test to confirm the Ligand Substitution Reactions of the Hydrolytic Iron(III) Dimer. React. Kinet. Catal. Lett., 2001 (73) 117-125.

Li, H., Lee, L.S., Schulze, D. G., Guest, C. A. Role of soil manganese in the oxidation of aromatic amines. Environ. Sci. Technol. 2003, (37) 2686-2693.

Liger E., Charlet L., Van Cappellen P. Surface catalysis of uranium(VI)

reduction by iron(II). *Geochim. Cosmochim. Acta* 1999, 63 (19-20) 2939-2955.

Lipczynska-Kochany E. Novel Method for a Photoanalytic Degradation of 4-Nitrophenol in Homogenous Aqueous Solution. *Environ. Technol.*, 1991, (12) 87-92.

Lipczynska-Kochany E. Degradation of Nitrobenzene and Nitrophenols by Means of AOP's in Homogenous Phase: Photolysis in the Presence of Hydrogenperoxide versus the Fenton Reaction. *Chemosphere*, 1992, (24) 1369-1380.

Lipczynska-Kochany E. Sprah G., Harms S. Influence of some groundwater and surface waters constituents on the degradation of 4-chlorophenol by the Fenton reaction. *Chemosphere*, 1995, (30) 9-20.

Liu X. L., Wu F., Deng N. S. Photoproduction of hydroxyl radicals in aqueous solution with algae under high pressure mercury lamp. *Environ. Sci. Technol.*, 2004 (38) 296–299.

Lu M. C., Chen J. N., Chang C. P. Oxidation of Dichlorvos with hydrogen peroxide using ferrous ion as catalyst, *J. Hazard. Mater.* 1999, (65) 277-288.

Lu M. C. Oxidation of chlorophenols with hydrogen peroxide in the presence of goethite, *Chemosphere* 2000, (40) 125-130.

Lunar L., Sicilia D., Rubio S., Dolores P. B., Nickel U. Identification of metol degradation products under Fenton's reagent treatment using liquid chromatography–mass spectrometry, *Water Res.* 2000, 34 (13) 3400-3412.

Luo, C., Shen, Z., Lia, X. Enhanced phytoextraction of Cu, Pb, Zn and Cd with EDTA and EDDS. *Chemosphere* 2005, (59) 1-11.

Maciel R., Sant'Anna G. L., Dezotti M. Phenol removal from high salinity effluents using Fenton's reagent and photo-Fenton reactions. *Chemosphere*, 2004, (57), 711-719.

Maithreepala R. A. and Doong R. A. Synergistic effect of copper ion on the reductive dechlorination of carbon tetrachloride by surface-bound Fe(II) associated with goethite. *Environ. Sci. Technol.* 2004, 38(1) 260-268.

Malato S., Blanco J., Vidal A., Richter C. Photocatalysis with solar energy at a pilot-plant scale: an overview. *Appl. Catal. B: Environ.*, 2002, (37) 1-15.

Malato S., Blanco J., Vidal A., Alarcón D., Maldonado M. I., Cáceres J., Gernjak W. Applied studies in solar photocatalytic detoxification: an overview. *Sol. Energy*, 2003, (75) 329-336.

Maletzky P., Bauer R., Lahnsteiner J., Pouresmael B. Immobilisation of iron ions on nafion(R) and its applicability to the photo-Fenton method. *Chemosphere*, 1999, (38) 2315-2325.

Maloney, E. K. and Waxman, D. J. trans-Activation of PPARalpha and PPARgamma by structurally diverse environmental chemicals. *Toxicol. Appl. Pharmacol.*, 1999, 161(2) 209-218.

Martell, A. E., Smith, R. M., Motekaitis, R. J. NIST Critically Selected Stability Constants of Metal Complexes V6.0. NIST, Gaithersburg, USA. 2001.

Martínez F., Calleja G., Melero J. A., Molina R. Heterogeneous photo-Fenton degradation of phenolic aqueous solutions over iron-containing SBA-15 catalyst. *Appl. Catal. B: Environ.*, 2005, (60) 185-194.

Martley, E., Gulson, B. L., Pfeifer, H.-R. Metal concentrations in soils around the copper smelter and surrounding industrial complex of Port Kembla, NSW, Australia. *Sci. Total Environ.* 2004, (325) 113-127.

Masse L, Patni N K, Jui P Y, Clegg B S. Groundwater quality under conventional and no-tillage-II atrazine, deethylatrazine and metolachlor. *J Environ Qual* 1998, (27) 877-883.

McCarey, C. A., MacLachlan, J., Brookes, B. I. Adsorbent tube evaluation for the preconcentration of volatile organic compounds in air for analysis by gas chromatographymass spectroscopy. *Analyst* 1994, (119) 897-902.

McBride, M.B. Adsorption and oxidation of phenolic compounds by iron and manganese oxides. *Soil Sci. Soc. Am. J.* 1987, (751) 1466-1472.

McConnell, L. L., LeNoir, J. S., Datta, S., Seiber, J. N. Wet deposition of current-use pesticides in the Sierra Nevada mountain range, California, USA. *Environ. Toxicol. Chem.* 1998, (17) 1908-1916.

Mcknight D. M., Kimball B. A., Bencala K. E., Iron photoreduction and oxidation in an acidic mountain stream. *Science*, 1988, (240) 637-640.

Meers, E., Ruttens, A., Hopgood, M. J., Samson, D., Tack, F. M. G. Comparison of EDTA and EDDS as potential soil amendments for enhanced phytoextraction of heavy metals. *Chemosphere*. 2005, (58) 1011-1022.

Mellouki A. and Mu Y. J. On the atmospheric degradation of pyruvic acid in the gas phase. *J. Photochem. Photobiol. A: Chem.*, 2003, (157) 295-300.

Millero F. J., Sotolongo S., Izaguirre M. The kinetics of oxidation of Fe(II) in seawater. *Geochim. Cosmochim. Acta*, 1987, (51) 793-801.

Millero F. J. and Sotolongo S. The oxidation of Fe(II) with H<sub>2</sub>O<sub>2</sub> in seawater. *Geochim. Cosmochim. Acta*, 1989, (53) 1867-1873.

Millero F. J., Yao W. S., Aicher J. The speciation of Fe(II) and Fe(III) in natural waters. *Mar. Chem.*, 1995, (50) 21-39.

Millet, M., Wortham, H., Sanusi, A., Mirabel, Ph. A multiresidue method for determination of trace levels pesticides in air and water. *Arch. Environ. Contam. Toxicol.* 1996, (31) 543-556.

Millet, M., Wortham, H., Sanusi, A., Mirabel, Ph. Atmospheric contamination by pesticides: Determination in the liquid, gaseous and particulate phases. *Environ. Sci. Pollut. Res.* 1997, 4 (3) 172-180.

Milne, C. J., Kinniburgh, D. G., Van Riemsdijk, W. H., Tipping, E. Generic NICA-Donnan model parameters for metal-ion binding by humic substances. *Environ. Sci. Technol.* 2003, (37) 958-971.

Modestov, A. D. and Lev, O. Photocatalytical oxidation of 2, 4-dichlorophenoxyacetic acid with titania photocatalyst. Comparison of supported and suspended TiO<sub>2</sub>. *J. Photochem. Photobiol. A: Chem.* 1998, (112) 261-270.

Moffett J. W. and Zika R. G. Reaction kinetics of hydrogen peroxide with copper in seawater: Implications for its existence in the marine environment. *Mar. Chem.* 1983, (13) 239-251.

Moffett J. W. and Zika R. G. Reaction kinetics of hydrogen peroxide with copper and iron in seawater. *Environ. Sci. Technol.*, 1987, (21) 804-810.

Moore C. A., Farmer C. T., Zika R. G. Influence of the Orinoco River on hydrogen peroxide distribution and production in the eastern Caribbean. *J. Geophys.*

Res. 1993, (98) 2289-2298.

Muller, T. S., Sun, Z., Kumar, G., Itoh, K., Murabayashi, M. The combination of photocatalysis and ozonolysis as a new approach for cleaning 2, 4-dichloroacetic acid polluted water. *Chemosphere* 1998, (36) 2043-2055.

Nash, R. G. Volatilization and dissipation of acidic herbicides from soil under controlled conditions. *Chemosphere* 1989, 18 (11) 2373-2963.

Neal J. A. and Rose N. J. Stereospecific ligands and their complexes. I. A cobalt(III) complex of ethylenediaminedisuccinic acid, *Inorg. Chem.* 1968, (7) 2405-2412.

Nelieu S, Kerhoas L, Einhorn J. Degradation of atrazine into ammeline by combined ozone/hydrogen peroxide treatment in water. *Environ Sci Technol* 2000, (34) 430-437.

Nishikiori T., Okuyama A., Naganawa H., Takita T., Hamada M., Takeuchi T., Aoyagi T., Umezawa H. Production by actinomycetes of (S, S)-N, N'-Ethylenediamine-disuccinic acid, an inhibitor of phospholipase C, *J. Antibiot.* 1994, (37) 426-427.

Nogueira R. F. P., Trovó A. G., Modé D. F. Solar photodegradation of dichloroacetic acid and 2, 4-dichlorophenol using an enhanced photo-Fenton process. *Chemosphere*, 2002, (48) 385-391.

Oehme, M. Further evidence of long-range air transport of some organic polychlorinated aromates and pesticides: North America and Eurasia to the Arctic. *Ambio* 1991, (20) 293-297.

Oliveros E., Legrini O., Hohl M., Müller T., Braun A. M. Industrial waste water treatment: large scale development of a light-enhanced Fenton reaction. *Chem. Eng. Proc.*, 1997, (36) 397-405.

Ononye A. I., McIntosh A. R., Bolton J. R. Mechanism of the photochemistry of p-benzoquinone in aqueous solutions. 1. Spin trapping and flash photolysis electron paramagnetic resonance studies. *J. Phys. Chem.*, 1986, (90) 6266-6270.

Orama, M., Hyvonen, H., Saarinen, H., Aksela, R. Complexation of [S, S] and mixed stereoisomers of N, N'-ethylenediaminedisuccinic acid (EDDS) with Fe(III),

Cu(II), Zn(II) and Mn (II) ions in aqueous solution. *J. Chem. Soc. Dalton Trans.* 2002, (24)4644-4648.

Ozdemir O. and Dunlop D. J. Intermediate magnetite formation during dehydration of goethite. *Earth Planet. Sci. Lett.* 2000, (177)59-67.

Pan X.M., Schuchmann M.N., Von Sonntag C. Oxidation of benzene by the OH radical A product and pulse radiolysis study in oxygenated aqueous solution. *J. Chem. Soc., Perkin Trans.* 1993 (2) 289-297.

Paterlini W. C. and Nogueira R. F. P. Multivariate analysis of photo-Fenton degradation of the herbicides tebuthiuron, diuron and 2, 4-D. *Chemosphere*, 2005, (58) 1107-1116.

Payne, N. J., Thompson, D. J. Off target glyphosate deposits from aerial silvicultural applications under various meteorological conditions. *Pestic. Sci.*, 1992, 53-59.

Pecher K., Haderlein S. B., Schwarzenbach R. P. Reduction of polyhalogenated methanes by surface-bound Fe(II) in aqueous suspensions of iron oxides. *Environ. Sci. Technol.* 2002, 36(8)1734-1741.

Pedersen H. D., Postma D., Jakobsen R., Larsen O. Fast transformation of iron oxyhydroxides by the catalytic action of aqueous Fe(II). *Geochim. Cosmochim. Acta* 2005, 69(16) 3967-3977.

Pera-Titus M., García-Molina V., Banos M. A., Giménez J., Esplugas S. Degradation of chlorophenols by means of advanced oxidation processes: a general review. *Appl. Catal. B: Environ.*, 2004, (47)219-256.

Perez M., Torrades F., Garcia-Hortal J. A., Domenech X., Peral J. Removal of organic contaminations in paper pulp treatment effluents under Fenton and photo-Fenton condition, *Appl. Catal. B Environ.* 2002, (36)63–74.

Pérez-Estrada L., Maldonado M. I., Gernjak W., Agüera A., Fernández-Alba A.R., Ballesteros M. M., Malato S. Decomposition of diclofenac by solar driven photocatalysis at pilot-plant scale. *Catal. Today*, 2005, (101)219-226.

Peters, R. W. Chelate extraction of heavy metals from contaminated soils. *J. Hazard. Mater.* 1999, (66)151-210.

Piccolo, A., Conte, P., Scheunert, I., Paci, M. Atrazine interactions with soil humic substances of different molecular structure. *J. Environ. Qual.* 1998, (27) 1324-1333.

Piera, E., Calpe, J. C., Brillas, E., Domenech, X., Peral, J. 2, 4-Dichlorophenoxyacetic acid degradation by catalyzed ozonation:  $\text{TiO}_2/\text{UVA}/\text{O}_3$  and  $\text{Fe(II)}/\text{UVA}/\text{O}_3$  systems. *Appl. Catal. B: Environ.* 2000, (27)169-177.

Pignatello J. J. Dark and Photoassisted  $\text{Fe}^{3+}$ -Catalyzed Degradation of Chlorophenoxy Herbicides by Hydrogen Peroxide. *Environ. Sci. Technol.*, 1992, (26) 944-951.

Pignatello J. J., Liu D., Huston P. Evidence for an additional oxidant in the Photoassisted Fenton reaction. *Env. Sci. Technol.*, 1999, (33)1832-1839.

Pignatello J. J., Oliveros E., Mackay A. Advanced oxidation processes for organic contaminant destruction based on the Fenton reaction and related chemistry, *Crit. Rev. Env. Sci. Technol.* 36 (2006) 1-84.

Pizzigallo, M. D. R., Ruggiero, P., Crecchio, C., Mininni, R. Manganese and iron oxides as reactants for oxidation of chlorophenols. *Soil Sci. Soc. Am. J.* 1995, (59)444-452.

Pizzigallo, M. D. R., Ruggiero, P., Crecchio, C., Mascolo, G. Oxidation of chloroanilines at metal oxide surfaces. *J. Agr. Food Chem.* 1998, (46)2049-2054.

Poulain L., Mailhot G., Wong-Wah-Chung P., Bolte M. Photodegradation of chlortoluron: Role of iron(III) aquacomplexes. *J. Photochem. Photobiol. A: Chem.* 2003, 159 (1) 81-88.

Pozdnyakov, I. P., Glebov, E. M., Plyusnin, V. F., Grivin, V. P., Ivanov, Y. V., Vorobyev, D. Y., Bazhin, N. M. Mechanism of  $\text{Fe(OH)}^{2+}$  (aq) photolysis in aqueous solution. *Pure Appl. Chem.*, 2000, (72)2187-2197.

Prado, A. G. S. and Airoidi, C. Toxic effect caused on microflora of soil by pesticide picloram application. *J. Environ. Monit.*, 2001, (3)394-397.

Pratap K and Lemley A T. Electrochemical peroxide treatment of aqueous herbicide solutions. *J Agric Food Chem* 1994, (42)209-215.

Provendier H., Petit C., Estournes C., Libs S., Kiennemann A. Stabilisation of



active nickel catalysts in partial oxidation of methane to synthesis gas by iron addition. *Appl. Catal. A: Gen.* 1999, (180)163-173.

Richartz, H., Reischl, E., Trautner, F., Hutzinger, O. Nitrated phenols in fog. *Atmos. Environ.* 1990, A24 (12) 3067-3071.

Roberts, T. R., Hutson, D. H., Lee, P. W., Nicholls, P. H., Plimmer, J. R. (Eds.) *Metabolic Pathways of Agrochemical Part 1: Herbicides and Plant Growth Regulators.* The Royal Society of Chemistry, Cambridge, UK, 1998, 66-74.

Romo-Kroger, C. M., Morales, J. R., Dinator, M. I., Llona, F., Eaton, L. C. Heavy metals in the atmosphere coming from a copper smelter in Chile. *Atmos. Environ.* 1994, (28)705-711.

Rue E. L. and Bruland K. W., Complexation of iron(III) by natural organic ligands in the central North Pacific as determined by a new competitive equilibration/adsorptive cathodic stripping voltammetric method. *Mar. Chem.*, 1995 (50) 117-138.

Ruppert G., Bauer R., Heisler G. The Photo-Fenton Reaction – an Effective Photochemical Wastewater Treatment Process. *J. Photochem. Photobiol. A: Chem.*, 1993, (73)75-78.

Safarzadeh-Amiri A., Bolton J. R., Carter S. R. Ferrioxalate-mediated solar degradation of organic contaminants in water. *Sol. Energy*, 1996a, (56)439-444.

Safarzadeh-Amiri A., Bolton J. R., Cater S. R. The use of iron in Advanced Oxidation Processes. *J. Adv. Oxid. Techn.*, 1996b, (1)18-26.

Sagawe G., Lehnard A., Lubber M., Rochendorf G. and Bahnemann D. The insulated solar Fenton hybrid process: fundamental investigations. *Helv. Chim. Acta*, 2001, (84)3742-3759.

Saltmiras D. A. and Lemley A. T. Atrazine degradation by anodic Fenton treatment, *Water Research*. 2002, (36) 5113–5119

Sanusi, A., Millet, M., Wortham, H., Mirabel, Ph. A multiresidue for determination of trace levels of pesticides in atmosphere. *Analisis* 1997, (25) 302-308.

Sarria V., Kenfack S., Guillod O., Pulgarin C. An innovative coupled

solar-biological system at field pilot scale for the treatment of biorecalcitrant pollutants. *J. Photoch. Photobio.* 2003, (A159)89-99.

Sarria V., Parra S., Adler N., Péringer P., Benitez N., Pulgarin, C. Recent developments in the coupling of photoassisted and aerobic biological processes for the treatment of biorecalcitrant compounds. *Catal. Today*, 2002, (76)301-315.

Sarria V., Deront M., Péringer P., Pulgarín C. Degradation of biorecalcitrant dye precursor present in industrial wastewater by a new integrated iron(III) photoassisted-biological treatment. *Appl. Catal. B: Environ.*, 2003, (40)231-246.

Schowaneck, D., Feijtel, T. C. J., Perkins, C. M., Hartman, F. A., Federle, T. W., Larson, R. J. Biodegradation of [S, S], [R, R] and mixed stereoisomers of ethylene diamine disuccinic acid (EDDS), a transition metal chelator. *Chemosphere* 1997, (34) 2375-2391

Schowaneck D. and Verstraete W. Phosphonate utilization by bacterial cultures and enrichments from environmental samples, *Appl. Environ. Microbiol.* 1989, (56) 895-903.

Schwertmann U. and Cornell R. M. *Iron Oxides in the Laboratory: Preparation and Characterization*. Wiley-VCH, Weinheim, Germany, 1991.

Scott J. P. and Ollis D. F. Integration of chemical and biological oxidation processes for water treatment: Review and recommendations. *Environ. Prog.*, 1995, (14)88-103.

Seiber, J. N., Wilson, B. W., McChesnay, M. M. Air and fog deposition residues in four organophosphates insecticides used on Dormant Orchards in the San Joaquin valley, California. *Environ. Sci. Technol.* 1993, (27)2236-2243.

Senseman S A, Lavy T L, Daniel T C. Monitoring groundwater for pesticides at selected mixing/loading sites in Arkansas. *Environ Sci Technol* 1997, (31)283-288.

Shwertmann U and Cornell R M. *Iron Oxides in the Laboratory: Preparation and Characterization* (2nd ed.), Wiley-VCH, Weinheim 2000, 13–14

Sidderamappa R, Sethunathan N. Persistence of gamma-BHC and beta-BHC in Indian rice soils under flooded conditions. *Pestic Sci.* 1975, (6)395-403.

Sigg L., Johnson C. A., Kuhn A. Redox conditions and alkalinity generation in a

seasonally anoxic lake. Mar. Chem. 1991, (36) 9-26.

Sigman, M. E., Buchanan, A. C. Application of advanced oxidation process technologies to extremely high TOC containing aqueous solutions, J. Adv. Oxid. Technol. 1997, (2)415-423.

Smith, A. E., Aubin, A. J. Metabolites of [ $^{14}\text{C}$ ]-2, 4-dichlorophenoxyacetic acid in Saskatchewan soils. Journal of Agricultural and Food Chemistry 1991, (39)2019-2021.

Sorensen M. and Frimmel F. H. Photochemical degradation of hydrophilic xenobiotics in the UV/H<sub>2</sub>O<sub>2</sub> process: influence of nitrate on the degradation rate of EDTA, 2-amino-1-naphthalensulfonate, diphenyl-4-sulfonate and 4, 4-diamino-stilbene-2, 2-disulfonate, Water Res. 1997, (31)2885-2891

Soulas, G. Evidence for the existence of different physiological groups in the microbial community responsible for 2, 4-D mineralization in soil. Soil Biology & Biochemistry 1993, (25)443-449.

Spitzer R. H., Manning F. S., Philbrook W. O. Mixed-control reaction kinetics in the gaseous reduction of hematite. Trans. Metall. Soc. AIME. 1966, (236)726-742.

Sposito G. Surface Chemistry of Natural Particles. Oxford University Press, New York. 2004.

Stafford U., Gray K. A., Kamat P. V. Radiolytic and TiO<sub>2</sub>-assisted photocatalytic degradation of 4-chlorophenol. J. Phys. Chem. 1994, (98) 6343–6349.

Steinnes, E., Allen, R. O., Petersen, H. M., Rambæk, J. P., Varskog, P. Evidence of large scale heavy-metal contamination of natural surface soils in Norway from long-range atmospheric transport. Sci. Total Environ. 1997, (205)255-266.

Stone, A.T. Reductive dissolution of manganese(III/IV) oxides by substituted phenols. Environ. Sci. Technol. 1987, (21)979-988.

Stookey L. L. Ferrozine-A New Spectrophotometric Reagent for Iron. Analytical Chemistry, 1970, 42(7) , 779-781

Strathmann T. J. and Stone A. T. Mineral surface catalysis of reactions between Fe-II and oxime carbamate pesticides. Geochim. Cosmochim. Acta 2003, 67(15), 2775-2791.

Struthers J K, Jayachandran K, Moorman T B. Biodegradation of atrazine by *Agrobacterium radiobacter* J14a and use of this strain in Bioremediation of contaminated soil. *Appl Environ Microbiol* 1998, (64)3368-3375.

Stumm W. *Chemistry of the Solid-Water Interface*, Wiley, New York, 1992.

Stumm W. and Sulzberger B. The cycling of iron in natural environments—considerations based on laboratory studies of heterogeneous redox processes. *Geochim. Cosmochim. Acta* 1992, 56(8)3233-3257.

Sulzberger B., Schnoor J. L., Giovanoli R., Hering J. G., Zobrist J., Biogeochemistry of iron in an acidic lake. *Aquat. Sci.* 1990, (52) 57-74.

Sulzberger B., Laubscher H., Karametaxas G. Photoredox reactions at the surface of iron(III)(hydr-)oxides. In: Helz G. R., Zepp R. G. and Crosby, D. G. (Eds.) *Aquatic and surface photochemistry*. Lewis Publishers, Boca Raton, 1994, 53-74.

Sun Y. and Pignatello J. J. Chemical treatment of pesticide wastes. Evaluation of Fe(III) chelates for catalytic hydrogen peroxide oxidation of 2, 4-D at circumneutral pH. *J. Agric. Food Chem.*, 1992, (40)322-327.

Sun, Y. and Pignatello J. J. Activation of hydrogen peroxide by iron(III) chelates for abiotic degradation of herbicides and insecticides in water. *J. Agric. Food Chem.*, 1993a, (41)308-312.

Sun Y. and Pignatello J. J. Photochemical reactions involved in the total mineralization of 2, 4-D by  $\text{Fe}^{3+}/\text{H}_2\text{O}_2/\text{UV}$ . *Environ. Sci. Technol.*, 1993b, (27) 304-310.

Sun, Y. and Pignatello, J. J. Evidence for a surface dual holeradical mechanism in the  $\text{TiO}_2$  photocatalytic oxidation of 2, 4-dichlorophenoxyacetic acid. *Environ. Sci. Technol.* 1995, (29)2065-2072.

Sychev A. Y. and Isaak V. G. Iron compounds and the mechanisms of the homogeneous catalysis of the activation of  $\text{O}_2$  and  $\text{H}_2\text{O}_2$  and of the oxidation of organic substrates. *Russ. Chem. Rev.*, 1995, (64)1105-1129.

Talbot R. W., Dibb J. E., Lefer B. L., Scheuer E., Bradshaw J. D., Sandholm S. T., Smyth S., Blake D. R., Blake N. J., Sachse G. W., Collins Jr., Gergory G. L. Large-scale distributions of tropospheric nitric, formic, and acetic acids over the

western pacific basin during wintertime, J. Geophys. Res., 1997, (102) 28303-28313,.

Tanaka K., Luesaiwong W., Hisanaga T. Photocatalytic degradation of mono-, di- and trinitrophenol in aqueous TiO<sub>2</sub> suspension, J. Mol. Catal. A Chem. 1997, (122) 67-74.

Tandy, S., Bossart, K., Mueller, R., Ritschel, J., Hauser, L., Schulin, R., Nowack, B. Extraction of heavy metals from soils using biodegradable chelating agents. Environ. Sci. Technol. 2004, (38) 937-944.

Tandy S., Ammann A., Schulin R., Nowack B. Biodegradation and speciation of residual S S-ethylenediaminedisuccinic acid (EDDS) in soil solution left after soil washing Environmental Pollution 2006, (142) 191-199

Thayalakumaran, T., Robinson, B., Vogeler, I., Scotter, D., Clothier, B., Percival, H. Plant uptake and leaching of copper during EDTA enhanced phytoremediation of repacked and undisturbed soil. Plant Soil 2003, (254) 415-423.

Thill, D. Growth regulator herbicides. In: Herbicide action course. West Lafayette: Purdue University. 2003, 267-291.

Thurman E. M. in Organic Geochemistry of Natural Waters, ed. Martinus Nijhoff / W. Junk, Dordrecht, 1985, 497-502.

Thurman, E. M., Goolsby, D. A., Myer, M. T., Mills, M. S., Pomes, M. L., Kolpin, D. W. A reconnaissance study of herbicides and their metabolites in surface water of the Midwestern United States using immunoassay and gas chromatography/mass spectrometry. Environ. Sci. Technol. 1992, (26) 2440-2447.

Tomlin C. Pesticide Manual, 10th Edition, Crop Protection Publication, Reprint 1995, British Crop Protection Council, The Royal Society of Chemistry. 1994.

Tomlin, C. D. S. (Ed.), The Pesticide Manual, 11th ed. British Crop Protection Council, Farnham, Surrey, UK, 1997, 1606.

Tong, S. T. Y., Lam, K. C., Home sweet home? A case study of household dust contamination in Hong Kong. Sci. Total Environ. 2000, (256) 115-123.

Torrades F., Pérez M., Mansilla H. D. and Peral J. Experimental design of Fenton and photo-Fenton reactions for the treatment of cellulose bleaching effluents. Chemosphere, 2003, (53) 1211-1220.

Trojanowicz M., Drzewicz P., Pańta P., Gluszewski W., Nalece- Jawecki G., Sawicki J., Radiolytic degradation and toxicity changes in  $\gamma$ -irradiated solutions of 2, 4-dichlorophenol, *Radiat. Phys. Chem.* 2002, (65) 357–366.

US Environmental Protection Agency. National survey of pesticides in drinking water wells, phase I report. US EPA Report 570/9-90-015, USEPA Office of Water. Office of Pesticides and Toxic Substances, US Gov. Print. Office, Washington, DC, 1990.

Van Benschoten, J. E., Matsumoto, M. R., Young, W. H. Evaluation and analysis of soil washing for seven lead-contaminated soils. *J. Environ. Eng.* 1997, (123) 217-224.

Vandevivere, P., Hammes, F., Verstraete, W., Feijtel, W., Schowanek, D. Metal decontamination of soil, sediment and sewage sludge by means of transition metal chelate [S, S]-EDDS. *J. Environ. Eng.* 2001a, (127) 802-811.

Vandevivere, P., Saveyn, H., Verstraete, W., Feijtel, W., Schowanek, D. Biodegradation of metal-[S, S]-EDDS complexes. *Environ. Sci. Technol.* 2001b, (35) 1765-1770.

Varghese R., Mohan H., Manoj P., Manoj V. M., Aravind U. K., Vandana K., Aravindakumar C. T. Reactions of hydrated electrons with trazine derivatives in aqueous medium, *J. Agric. Food Chem.* 2006, (54) 8171–8176.

Venugopal A. and Scurrrell M.S. Low temperature reductive pretreatment of Au/Fe<sub>2</sub>O<sub>3</sub> catalysts, TPR/TPO studies and behaviour in the water-gas shift reaction *Appl. Catal. A: Gen.* 2004, 258(2) 241-249.

Vikesland P. J. and Valentine R. L. Iron oxide surfacecatalyzed oxidation of ferrous iron by monochloramine: implications of oxide type and carbonate on reactivity. *Environ. Sci. Technol.* 2002a, 36(3) 512-519.

Vikesland P. J. and Valentine R. L. Modeling the kinetics of ferrous iron oxidation by monochloramine. *Environ. Sci. Technol.* 2002b, 36(4) 662-668.

Voelker B. M., Morel F., Sulzberger B. Iron redox cycling in surface waters: Effects of humic substances and light. *Environ. Sci. Technol.* 1997, (31) 1004-1011.

Voelker B M. and Sedlak D L. Iron reduction by photoproduct superoxide in

seawater. *Mar. Chem.*, 1995, (50) 93-102.

Von Gunten U. Ozonation of drinking water: Part I. Oxidation kinetics and product formation. *Water Research*. 2003, (37)1443-1467

Von Sonntag C., Dowideit P., Fang X., Mertens R., Pan X., Schuchmann M. N., Schuchmann H.-P. The fate of peroxy radicals in aqueous solution. *Water Sci. Technol.*, 1997, 35(4)9-15.

Watts R. J., Udell M. D., Rauch P. A., Leung S. W. Treatment of pentachlorophenol (PCP) contaminated soils using Fenton's reagent, *Hazard. Waste Hazard. Mater.* 1990, (7) 335-345.

Walling C. Fenton's reagent revisited. *Acc Chem Res* 1975, (8)125-132.

Wang L., Zhang C., Wu F., Deng N. Glebov E. M., Bazhin N. M. Determination of hydroxyl and peroxy radicals from photolysis of Fe(III)-pyruvate complexes in homogeneous aqueous solution. *React. Kinet. Catal. Lett.* 2006, (89) 183-192.

Wang L. Photodegradation of organic pollutants induced by Fe(III)- Carboxylate complexes in aqueous solutions. Ph. D Thesis, UNIVERSITE BLAISE PASCAL, These en cotutelle avec l'Université de Wuhan (Chine), 2008, 24.

Wang Y. J., Zhou D. M., Sun R. J., Cang L., Hao X. Z. Cosorption of zinc and glyphosate on two soils with different characteristics, *J. Hazard. Mater.* 2006, (137) 76-82.

Wang Y. J., Zhou D. M., Sun R. J., Ji D. A., Zhu H. W., Wang S. Q. Zinc adsorption on goethite as affected by glyphosate, *Journal of Hazardous Materials* 2008, (151) 179-184.

Watanabe, T. Determination of the concentration of pesticides in atmosphere at high altitudes after aerial application. *Bull. Environ. Contam. Toxicol.* 1998, (60) 669-676.

Wehrli B., Sulzberger B. and Stumm W. Redox processes catalyzed by hydrous oxide surfaces. *Chem. Geol.* 1989, (78) 167-179.

Wehrli B. and Stumm W. Vanadyl in natural-waters adsorption and hydrolysis promote oxygenation. *Geochim. Cosmochim. Acta.* 1989, 53(1) 69-77.

Wells M. L., Mayer L. M., Donard O. F. X., de Souza M. M., Ackleson S. The

photolysis of colloidal iron in the oceans. *Nature*, 1991, (353) 248-250.

Wells M. L., Mayer L. M., Guillard R. R. L. A chemical method for estimating the availability of iron to phytoplankton in seawater. *Mar. Chem.*, 1991, (33) 23-40.

Wells M. L. and Mayer L. M. The photoconversion of colloidal iron oxyhydroxides in seawater. *Deep-Sea Res.* 1991, (38) 1379-1395.

Wells M. L., Price N. M., Bruland K. W. Iron chemistry in seawater and its relationship to phytoplankton: a workshop report. *Mar. Chem.*, 1995, (48) 157-182.

Wenzel, W. W., Unterbrunner, R., Sommer, P., Sacco, P. Chelate-assisted phytoextraction using canola (*Brassica napus* L.) in outdoors pot and lysimeter experiments. *Plant Soil* 2003, (249) 83-96.

Weschler C. J., Mandich M. L., Graedel T. E. Speciation, Photosensitivity, and Reactions of Transition Metal Ions in Atmospheric Droplets, *J. Geophys. Res.*, 1986, 91(D4) 5189-5204.

Wilson, R. D., Geronimo, J., Armbruster, J. A. 2, 4-D dissipation in field soils after applications of 2, 4-D dimethylamine salt and 2, 4-D 2-ethylhexyl ester. *Environmental Toxicology and Contamination* 1997, (16) 1239-1246.

Wu F., Deng N. S., Zuo Y. Discoloration of dye solutions induced by solar photolysis of ferrioxalate in aqueous solutions. *Chemosphere*, 1999, (39) 2079-2085.

Wu F. and Deng N. S. Photochemistry of hydrolytic iron (III) species and photoinduced degradation of organic compounds. A minireview. *Chemosphere*, 2000, (41) 1137-1147.

Wu J., Hsu F., Cunningham S. D. Chelate-assisted Pb phytoextraction: Pb availability, uptake, and translocation constraints. *Environ. Sci. Technol.* 1999, (33) 1898-1904.

Wu L. H., Luo Y. M., Xing X. R., Christie P. EDTA-enhanced phytoremediation of heavy metal contaminated soil with Indian mustard and associated potential leaching risk. *Agric.Ecosyst.Environ.* 2004, (102) 307-318.

Young L Y and Haggblom M M. The anaerobic microbiology and biodegradation of aeromatic compounds. In: Kamely D, Chakrabarty A, Omenn GS, editors. *Book: Biotechnology and Biodegradation*. Gulf Publishing Company, 1990.



Zepp R. G., Hoigné J., Bader H. Nitrate-induced photooxidation of trace organic chemicals in water. *Environ. Sci. Technol.*, 1987, (21) 443-450.

Zepp R. G., Faust B. C., Hoigné J. Hydroxyl radical formation in aqueous reactions (pH 3-8) of iron(II) with hydrogen peroxide: The photo-Fenton reaction. *Environ. Sci. Technol.*, 1992, (26) 313-319.

Zhang, C. L., Xu, J. M., Yao, B. The response of soil microbial biomass to organic amendments and fertilizers under atrazine stress. *Acta Pedologica Sinica* (in Chinese). 2004, (41) 323-326.

Zhang Y., Charlet L. and Schindler P. W. Adsorption of protons, Fe(II) and Al(III) on lepidocrocite ( $\gamma$ -FeOOH). *Colloids Surf.* 1992, 63(3-4) 259-268.

Zika R. G., Saltzman E. S. and Cooper W. J. Hydrogen peroxide concentrations in the Peru upwelling Area. *Mar. Chem.* 1985a, (17) 265-275.

Zika R. G., Moffett J. W., Pestane R. G., Cooper W. J., Saltzman E. S. Spatial and temporal variations of hydrogen peroxide in Gulf of Mexico waters. *Geochim. Cosmochim.* 1985b, (Acta 49) 1173-1184.

Zinder B., Furrer G., Stumm W. The coordination chemistry of weathering. II. Dissociation of Fe(III) oxides, *Geochim. Cosmochim. Acta.* 1986, (50) 1861-1869.

Zuo Y. and Hoigné J. Formation of hydrogen peroxide and depletion of oxalic acid in atmospheric water by photolysis of iron(III)-oxalato complexes. *Environ. Sci. Technol.*, 1992, (26) 1014-1022.

Zuo Y. G., Zhan J., Wu T.X. Effects of Monochromatic UV-visible light and sunlight on Fe(III)-catalyzed oxidation of dissolved sulfur dioxide. *J. Atmos. Chem.* 2005, (50) 195-210.

